

Regulation of Autophagy in Mammalian Cells by Stress-activated Signaling Pathways

DISSERTATION

ZUR ERLANGUNG DES AKADEMISCHEN GRADES DES DOKTORS
DER NATURWISSENSCHAFTEN (DR. RER. NAT.)
DER CHEMISCHEN FALKULTÄT
DER TECHNISCHEN UNIVERSITÄT DORTMUND

VORGELEGT VON

JAKIA AMIN , MSc

AUS BANGLADESH

DORTMUND, GERMANY 2013

1. Gutachter: Prof. Dr. J.G. Hengstler
2. Gutachter: Prof. Dr. Frank Wehner

Table of contents

List of Figures	vii
List of Tables	xi
List of Abbreviations	xii
Abstract	xiv

1.0 Introduction

1.1	Autophagy	1
1.1.1	Induction and characteristics of autophagy	2
1.1.2	Molecular mechanism of autophagy	4
1.1.2.1	Phagophore formation	4
1.1.2.1.1	ULK complex	4
1.1.2.1.2	Class III phosphatidylinositol 3-kinase complex	5
1.1.2.2	Phagophore elongation and autophagosome formation	6
1.1.2.2.1	Atg5–Atg12 conjugation	6
1.1.2.2.2	LC3 processing	7
1.1.2.3	Selective autophagy: cargo for degradation	8
1.1.2.4	Maturation of autophagosome and its fusion with lysosome	9
1.1.2.4.1	The role of the cytoskeleton	9
1.1.2.4.2	The role of lysosomal composition in autophagic maturation	10
1.1.2.3	Physiological roles of autophagy	11
1.1.2.4	Regulation of autophagy by signaling pathways	14
1.2	p38 Mitogen activated protein kinases	15
1.2.1	Induction and regulation of p38 MAPK activity	16
1.2.2	Biological consequences of p38 MAPK activation	18
1.2.3	p38 MAPK and its potential role in autophagy	19

1.3	Oncogene-induced senescence	20
1.3.1	Features of senescent cells	20
1.3.2	Role of senescence on tumorigenesis	22
1.3.3	The MCF-7/NeuT Cell system as a model of oncogene-induced senescence	23
	Aim of the work	24
		25
2.0	Materials and Methods	
2.1	Materials	25
2.1.1	Cell Lines	25
2.1.1.1	MCF7/NeuT	25
2.1.1.2	Human embryonic kidney 293 (HEK)	26
2.1.1.3	HeLa	26
2.1.2	Antibodies	26
2.1.2.1	Primary antibodies	26
2.1.2.2	Secondary antibodies	27
2.1.3	Media for cell culture	28
2.1.4	Inhibitors	28
2.1.5	Chemical reagents and Kits	28
2.1.6	Buffer and Solution	30
2.1.7	Technical equipment	31
2.1.8	Consumables	32
2.2	Methods	33
2.2.1	Cell Culture	33
2.2.2	Gene expression	33
2.2.2.1	Isolation of RNA	34
2.2.2.2	Quantitative RNA yield	35

2.2.2.3	cDNA synthesis	36
2.2.2.4	Quantitative reverse transcription polymerase chain reaction (qRT-PCR)	38
2.2.3	Protein analysis	41
2.2.3.1	Total protein extraction	42
2.2.3.2	Protein quantification assay	42
2.2.3.3	SDS electrophoresis and western blot	44
2.2.3.3.1	Gel preparation	44
2.2.3.3.2	SDS gel electrophoresis	46
2.2.3.3.3	Membrane transfer	48
2.2.3.3.	Antibody incubation and membrane detection	49
2.2.4	Immunofluorescence	52
2.2.4.1	Immunofluorescence assay for LC3 and Tubulin staining	53
2.2.4.2	Immunofluorescence assay for BrdU staining	54
3.0	Result	55
3.1	Oncogene ERBB2/HER2 (NeuT) expression leads to premature senescence in MCF-7 Cells	55
3.1.1	Expression of oncogenic ERBB2/NeuT in MCF-7 cells	55
3.1.2	Oncogene ERBB2/NeuT-induced senescence is accompanied by alterations in cell morphology in MCF7 cells	56
3.1.3	ERBB2/NeuT overexpression Induces growth arrest in MCF-7 cells.....	57
3.2	ERBB2/NeuT oncogene-induced activation of signaling pathways in senescent cells	59
3.2.1	Activation of the RAF-MEK-ERK cascade by the ERBB2/NeuT oncogene	59
3.2.2	Activation of the PI3K/AKT pathway during NeuT- induced senescence	62
3.2.3	p38 is activated during NeuT-induced premature senescence	64

3.2.4	JNK signaling pathway is not activated during senescence.....	65
3.3	Autophagy in oncogene-induced senescence cells	66
3.4	Autophagy maturation is impaired in senescent cells	69
3.5	Senescence-associated blockade of the autophagic flux is triggered by the p38-MAPK pathway	72
3.6	The MEK1/2-ERK1/2 signaling pathway is involved in initial induction of autophagy upon NeuT induction	76
3.7	Mechanism underlying P38-mediated block of autophagy maturation	78
3.7.1	Cytoskeleton-mediated transport of autophagosomes (delivery of autophagosomes to lysosomes) is impaired in senescent cells via p38	78
3.7.1.1	Regulation of microtubule- associated protein activity by p38	78
3.7.1.2	Regulation of dynein light chain 1 (DYNLL1) expression by p38 ...	83
3.7.2	Regulation of acidification and composition of lysosomes by p38..	85
3.7.2.1	Down-regulation of Cathepsin D expression by p38 in senescent cells	85
3.7.2.2	The p38/MAPK pathway mediates down-regulation of the vacuolar ATPase	86
3.8	Attenuation of p38 by SB in senescence rescues the microtubule network and restores the autophagy flux in a time-dependent manner	88
3.9	p38 regulates the autophagy flux by a similar mechanism in other cell lines upon different Kinds of stress	93
3.10	Biological consequences of the blockade in the autophagy flux ...	102
4.0	Discussion	104
4.1	Role of p38 in autophagy in oncogene induced senescence cells .	104
4.2	A proposed model for regulation of autophagy by p38	105
4.3	Mechanism of late block of autophagy by p38	106

4.4	Mechanism of early induction of autophagy by p38	108
4.4	Does p38 regulate autophagy in other stress/pathological conditions by a similar mechanism?	109
4.5	Biological consequences of impaired autophagy	110
4.6	Role of Autophagy in senescence	111
5.0	Literature	116

List of Figures

Figure 1:	Macroautophagy, microautophagy, and chaperone-mediated autophagy	2
Figure 2:	Overview of macroautophagy	3
Figure 3:	Phosphorylational regulation of ULK1/2 complexes by mTORC1 in response to nutrient levels.....	4
Figure 4:	Two conjugation pathways.....	6
Figure 5:	Schematic diagram of autophagosome formation in mammalian cells	8
Figure 6:	Autophagosome–lysosome fusion and degradation of intra-autophagosomal contents	10
Figure 7:	Physiological signals and diseases related to autophagy ...	12
Figure 8:	The p38 MAPK pathway	17
Figure 9:	Features of cellular senescence.....	21
Figure 10:	MCF7/NeuT cell transfection constructs	25
Figure 11:	InnuPREP RNA Mini Kit flow chart for total RNA isolation in MCF7/NeuT and MCF7/EGFP cells	34
Figure 12:	Nanodrop measurement	35
Figure 13:	Principle of cDNA synthesis	36
Figure 14:	Real time PCR.....	39
Figure 15:	Principle of the BCA assay for protein quantification	43
Figure 16:	Mini-PROTEAN Tetra cell casting frame and casting stand	44
Figure 17:	Mini-PROTEAN Tetra cell Running chamber	47
Figure 18:	Semi dry membrane transfer	48
Figure 19:	Schematic diagram of direct and indirect immunofluorescence	52
Figure 20:	ERBB2 (NeuT) protein expression in MCF7/NeuT cells.....	56
Figure 21:	Morphological changes during NeuT oncogene induction	57

Figure 22: Decreased BrdU-staining in 3 days dox-treated MCF-7/NeuT cells confirms cell cycle arrest upon senescence.....	58
Figure 23: Activation of Raf-1/c-Raf upon NeuT expression.....	60
Figure 24: Phosphorylation of MEK1/2 in MCF-7/NeuT cells	61
Figure 25: Activation of ERK1/2 during NeuT oncogene-induced senescence	62
Figure 26: Activation of the AKT pathway in MCF-7/NeuT cells	63
Figure 27: Phosphorylation of mTOR in MCF-7/NeuT cells	64
Figure 28: Activation of the p38 signaling pathway upon NeuT expression	65
Figure 29: Phosphorylation of JNK pathway in MCF-7/NeuT cells	66
Figure 30: Increased levels of autophagosomes in senescent cells	68
Figure 31: Inhibition of autophagy by 3-MA treatment	69
Figure 32: LC3-II turnover assay reveals a biphasic behavior of autophagy	70
Figure 33: Impairment of autophagy maturation in senescence	71
Figure 34: Impaired autophagic flux is mediated by the p38 signaling pathway in senescence	73
Figure 35: p38 signaling pathway mediates blockade of autophagy in oncogene-induced senescence	74
Figure 36: Detection of LC3-puncta by confocal microscopy	75
Figure 37: Inhibition of ERK signaling pathway has no effect on autophagy maturation in senescence	77
Figure 38: Destabilization of microtubules in senescent cells through phosphorylation of MAP4 and dephosphorylation of oncoprotein18	79
Figure 39: Destabilization of microtubules in senescence cells via p38 signaling pathway	80
Figure 40: Disruption of the microtubule network in senescent MCF-7/NeuT cells via p38	82

Figure 41:	Down regulation of the dynein motor protein subunit DYNLL1 in senescence.....	83
Figure 42:	Down regulation of dynein motor protein subunit DYNLL1 by p38 signaling pathway	84
Figure 43:	Down regulation of Cathepsin D in senescent cells via p38 signaling pathway	86
Figure 44:	p38 activation down regulated the vacuolar ATPase subunit ATP6V0A2	87
Figure 45:	Vacuolization in MCF-7/NeuT senescent cells is abolished by treatment with the SB inhibitor	88
Figure 46:	Effect of time-dependent SB inhibition of p38/MAPK pathway on LC3-II (autophagosomes) and p62 accumulation	89
Figure 47:	The p38 pathway negatively regulates autophagy and SB inhibitor restores autophagic flux	90
Figure 48:	Effect of SB inhibition of p38/MAPK pathway on MAP4 phosphorylation and Op18 dephosphorylation	91
Figure 49:	SB inhibition of p38/MAPK pathway recued the tubulin formation	92
Figure 50:	Activation of p38 signaling pathway and autophagosome formation by Anisomycin	94
Figure 51:	Autophagy is impaired by sustained activation of p38 signaling pathway	94
Figure 52:	Sustained activation of p38 signaling pathway mediates blockade of autophagy	95
Figure 53:	Subcellular localization of LC3 puncta	96
Figure 54:	Destabilization of microtubules in Anisomycin treated MCF-7 cells	97
Figure 55:	Disassembly of the microtubule network in MCF-7 cells via p38	98

Figure 56	Down regulation of dynein motor protein subunit DYNLL1 by sustained activation of the p38 signaling pathway	99
Figure 57:	Autophagy maturation is impaired in HEK and HeLa cells by sustained activation of the p38 signaling pathway.....	100
Figure 58:	p38-MAPK-triggered autophagy flux blockade occurs via disruption of microbule network	101
Figure 59:	PARP cleavage in Senescence cells	102
Figure 60:	PARP cleavage in Anisomycin treated cells	103
Figure 61:	Proposed model for the role of p38 in autophagy	105
Figure 62:	Mechanism by which p38 leads to a blocked autophagic flux	107
Figure 63:	Possible mechanism by which p38 may induce autophagy ...	109

List of Tables

Table 1:	Composition of the reaction mixture for cDNA synthesis	37
Table 2:	Program for the thermo cycler for cDNA synthesis	38
Table 3:	Composition of the TaqMan Mastermix for gene expression analysis	40
Table 4:	Thermal cycling conditions for TaqMan analysis of gene expression	40
Table 5:	Components of the western blot SDS-gels (10% gel)	45
Table 6:	Parameters for antibodies detection for western blot.....	50
Table7:	Parameters for antibodies detection for immunofluorescence	54
Table 8:	p38 as positive regulator of autophagy.....	104
Table 9:	p38 as a negative regulator of autophagy.....	105

List of Abbreviations

APS	Ammonium per Sulfate
BCA	Bicinchoninic acid
BSA	Bovine Serum Albumin
cDNA	Complementary DNA
cm ²	Square Centimetres
Ct	Cycle Threshold
d	Day
DAPI	4',6-Diamidino-2-phenylindol
DMEM	Dulbecco's Modified Eagle Medium
Dox	Doxycycline
DTT	Dithiothreitol
EDTA	Ethylene diamine tetra acetic acid
ERBB2, HER2, Neu	Epidermal Growth factor Receptor 2
ERK	Extracellular Signal-regulated Kinases
FCS	Fetal Calf Serum
FRET	Fluorescence Resonance Energy Transfer
g	Gram
X g	Gravitational Force
h	Hour
HEK	Human embryonic kidney
HRP	Horseradish peroxidase
kDa	Kilo dalton
l	Litre
mA	Milliampere
MAPK	Mitogen Activated Protein Kinases
MCF-7/NeuT	Human Breast carcinoma Cell line transfected with rat-homolog NeuT
mg	Milligram

List of Abbreviations

min	Minute
mRNA	Messenger Ribonucleic Acid
NaCl	Sodium chloride
nM	nanomolar
NP-40	Nonident P-40
PARP	poly (ADP-ribose) polymerase
PBS	Phosphate buffered saline
PCR	Polymerase chain Reaction
PI3K	Phosphatidylinositide 3-kinases
PVDF	Polyvinylidene fluoride
qRT-PCR	PCR quantitative real time polymerase chain reaction
Raf	Ras-activator factor
Ras	Oncogene discovered in rat sarcoma
RIPA	Radiimmunoprecipitation assay
RNA	Ribonucleic acid
rpm	Rounds per minute
RT	Room temperature
s	Second
SDS	Sodium dodecyl sulfate
SDS-PAGE	PAGE sodium dodecyl sulfate poly acrylamide gel electrophoresis
TBS	Tris buffered saline
TBS-T	Ttris buffered saline - Tween
TEMED	Tetramethylethylenediamine
TET	Tetracycline
UBC	Ubiquitin C
v	Volt
v/v	Volume per volume

Abstract

Autophagy is an intracellular bulk degradation process of cytoplasmic proteins and organelles aimed to preserve cellular homeostasis. It involves the formation of double-membrane structures, called autophagosomes that transport their cargo to the lysosomes where it becomes degraded. The molecular mechanisms underlying induction of autophagy, biogenesis, trafficking and turnover of autophagosomes have been extensively studied. However, the regulation of these steps by signaling pathways that adjust the autophagy flux to different cellular stress situations is still poorly understood. The aim of this work was to investigate the regulation of autophagy upon particular stress conditions in a time-dependent manner. We particularly focused on the control of autophagy by p38. For this purpose we applied a MCF-7/NeuT cell model of oncogene-induced senescence (OIS). In this model, doxycycline-inducible expression of an oncogenic variant of ERBB2 (NeuT) in the breast cancer cell line MCF-7 leads to premature senescence, a process that was shown to be accompanied by aberrant accumulation of autophagic vesicles. We found that autophagy becomes initially induced but that its maturation is later impaired upon oncogenic stress. In addition we identified p38/MAPK as the signaling pathway mediating the block of autophagic flux. This was evidenced by the fact that pharmacological inhibition of p38 by the small molecule compound SB203580 can restore the autophagic flux. This result was confirmed in time-dependent rescue experiments with SB203580. Furthermore, mechanisms by which p38 mediates the autophagic flux blockade were identified. These involved post-translational modifications of the microtubule-associated proteins MAP4 and OP18/STMN1, as well as down regulation of a particular dynein motor protein subunit DYNLL1, which all together provoke microtubule disruption and defective autophagosome transport to the lysosome. The biphasic behaviour of autophagy upon stress (early induction, late block) was confirmed in several cell lines exposed to a different stress-stimulus (anisomycin). Here we could show that also p38/MAPK is involved in these effects in a dual way, with an early induction of initial steps of autophagy and a later block of maturation. In addition, the p38-mediated block of the autophagic maturation was shown to occur via the same mechanism described above.

In conclusion, this work revealed new aspects of the control of autophagy by p38 signaling, mainly that the duration and intensity of p38 activation are key determinants of the autophagic flux rate. Low or transitory stress conditions that moderately activate p38 stimulate the autophagic flux. In contrast, more permanent and intensive stress that causes a strong activation of p38 blocks the autophagic flux.

Zusammenfassung

Autophagie ist ein intrazellulärer Prozess zum Abbau cytosolischer Proteine und Organellen, denen als Hauptrolle die Aufrechterhaltung der zellulären Homöostase zugeschrieben wird. Bei diesem Vorgang werden Doppelmembran-Strukturen gebildet, Autophagosomen, welche ihr eingeschlossenes Material dem lysosomalen Abbau zuführen. Die molekularen Mechanismen, welche Initiation der Autophagie, Biogenese, Transport und Abbau von Autophagosomen zugrunde liegen, sind weitgehend untersucht. Wie Signaltransduktionswege der Zelle diese Schritte regulieren, um den Autophagiefluss an verschiedenen Stress-Bedingungen anzupassen, ist allerdings ungenügend verstanden. Ziel dieser Arbeit war, die zeitabhängige Regulation der Autophagie unter verschiedenen Stressbedingungen zu untersuchen. Der Schwerpunkt lag in der Erforschung der Steuerung durch P38. Zu diesem Zweck wurde ein Zellmodell der Onkogen-vermittelten Seneszenz, das MCF-7/NeuT Zellsystem, verwendet. In diesem Modell führt die Doxyzyklin-abhängige Expression einer onkogenen Variante von ERBB2 (NeuT) in der Brustkrebszelllinie MCF-7 zu einer verfrühten Seneszenz, ein Zustand der eine dramatische Akkumulation von autophagischen Vakuolen aufweist. Im Rahmen dieser Dissertation wurde gezeigt, dass unter onkogenem Stress die Autophagie zunächst induziert, jedoch in einer späteren Phase blockiert wird. Darüber hinaus konnte durch pharmakologische Inhibition von p38 mit dem *small molecule* SB203580 gezeigt werden, dass der p38/MAPK Signalweg die Blockade des Autophagieflusses vermittelt. Des Weiteren wurden Mechanismen aufgeklärt, die für den p38-vermittelten Autophagie-Block verantwortlich sind. Dabei konnten post-translationale Modifikationen der Mikrotubuli-assoziierten Proteine MAP4 und OP18/STMN1, sowie die Herunterregulierung der Dynein Untereinheit DYNLL1 mit P38 in Verbindung gebracht werden. Diese Ereignisse führen zu einer Destabilisierung des Zytoskeletts und einem gestörten Autophagosom-Transport. Das biphasische Verhalten der Autophagie unter Stress-Bedingungen (frühe Induktion, späte Blockade) wurde in verschiedenen Zelllinien unter einem anderen Stress- Stimulus (Anisomycin) bestätigt. Hier konnte die Rolle von p38, sowohl in Induktion als auch in Blockade der Maturation, nachgewiesen werden.

Die Beteiligung des Zytoskeletts in der Blockade der Maturation der Autophagie durch p38 wurde ebenfalls im Anisomycin Zellmodell gezeigt. Zusammengefasst, konnte diese Arbeit neue Aspekte in der Regulation der Autophagie durch p38 identifizieren. Die Stärke und Dauer der p38 Aktivierung bestimmt den Autophagiefluss, wobei moderate, transiente Stress-Stimuli die Autophagie anregen und intensive, anhaltende Stress-Stimuli die Autophagie blockieren.

CHAPTER ONE
INTRODUCTION

1.0 Introduction

1.1 Autophagy

Autophagy is the bulk degradation of proteins and organelles, a process essential for cellular maintenance and cell viability (Ohsumi, 2001; Reggiori & Klionsky, 2002; Thumm, 2002; Yoshimori, 2004). It is an evolutionarily conserved mechanism, observed in a variety of organisms ranging from yeast and plants to animals, including humans. Several genes that are critical for autophagy, called autophagy related genes (Atg), have been best characterized in yeast (Klionsky et al., 2003). In mammals, autophagy has been observed in many tissues and has been shown to be essential for differentiation and development as well as for cellular maintenance. In addition, autophagy has been shown to have significant associations with neurodegenerative diseases, cardiomyopathies, cancer, programmed cell death, and bacterial and viral infections (Baehrecke, 2003; Bursch, 2001; Dorn et al., 2002; Edinger & Thompson, 2003; Eskelinen et al., 2003; Larsen & Sulzer, 2002; Liebert et al., 2002; Nishino et al., 2000; Perlmutter, 2002; Tolkovsky et al., 2002).

There are three defined types of autophagy that have been discovered: macro-autophagy, micro-autophagy and chaperone-mediated autophagy, all of which promote proteolytic degradation of cytosolic components at the lysosome. Macro-autophagy delivers cytoplasmic cargo to the lysosome through the intermediary of a double membrane-bound vesicle, referred to as an autophagosome, that fuses with the lysosome to form an autolysosome. In micro-autophagy, by contrast, cytosolic components are directly taken up by the lysosome itself through invagination of the lysosomal membrane. Both macro- and micro-autophagy are able to engulf large structures through both selective and non-selective mechanisms. In chaperone-mediated autophagy (CMA), targeted proteins are translocated across the lysosomal membrane in a complex with chaperone proteins (such as Hsc-70) that are recognized by lysosomal-associated membrane protein 2A (LAMP-2A), resulting in their unfolding and degradation (Saftig et al., 2008).

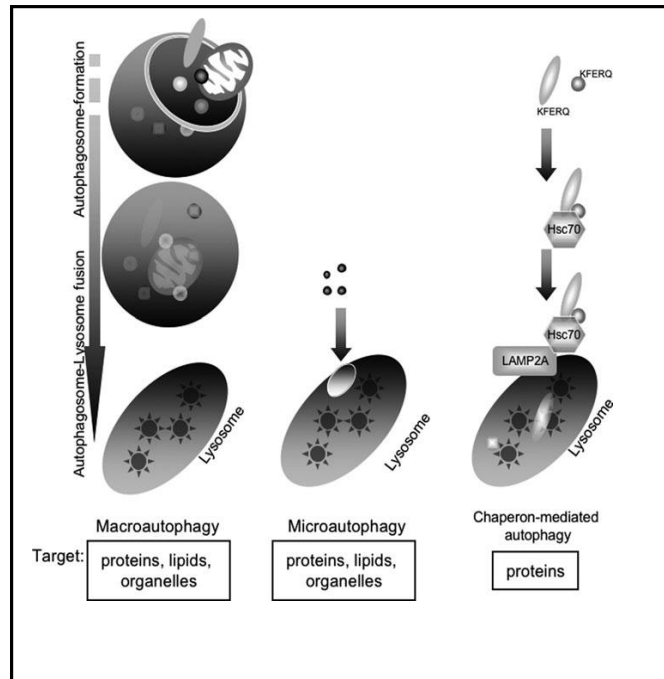


Figure 1: Macroautophagy, microautophagy, and chaperone-mediated autophagy (adapted from Tanida,2001)

1.1.1 Induction and characteristics of autophagy

Stress stimuli, such as nutrient deprivation often result in the activation of autophagy (Klionsky, 1999; Kim et al., 2000; Emr, 2009). Upon induction of autophagy, a flat membrane cistern known as the isolation membrane or phagophore, appears and wraps around a portion of cytosol and/or organelles (Klionsky et al.,2007). These membranes are formed at either the peri-vacuolar, pre-autophagosomal structure (PAS) in yeast or throughout the cytoplasm in higher organisms (Suzuki et al., 2001;Noda et al., 2002). Sealing of the edges of the phagophore results in a unique double membrane vesicle called the autophagosome that is devoid of any lysosomal enzymes. Once formed, autophagosomes undergo a series of maturation processes, during which the autophagosomes are delivered to the endosomal lumen, forming unique structures called the amphisomes (Berg et al.,1998). The amphisomes eventually form autophagolysosomes, upon fusion with lysosomes that are loaded with various acidic hydrolases, specialized for rapid and effective degradation of the delivered cargo. The pH of the autophagosomes is similar to that of the surrounding cytoplasm, but upon

fusion with the endosomes and/or lysosomes, the luminal pH drops due to the presence of membrane spanning proton pumps, which in turn results in increased lysosomal enzyme (cathepsin) activity (Dunn, 1990). Unlike in mammalian cells, however, yeast autophagosomes do not seem to fuse with late endosomes. Instead, both autophagosomes and endosomes fuse with the vacuole, the yeast equivalent of the lysosome, where their contents are degraded and recycled (Scott & Klionsky, 1998; Hanaoka et al., 2002).

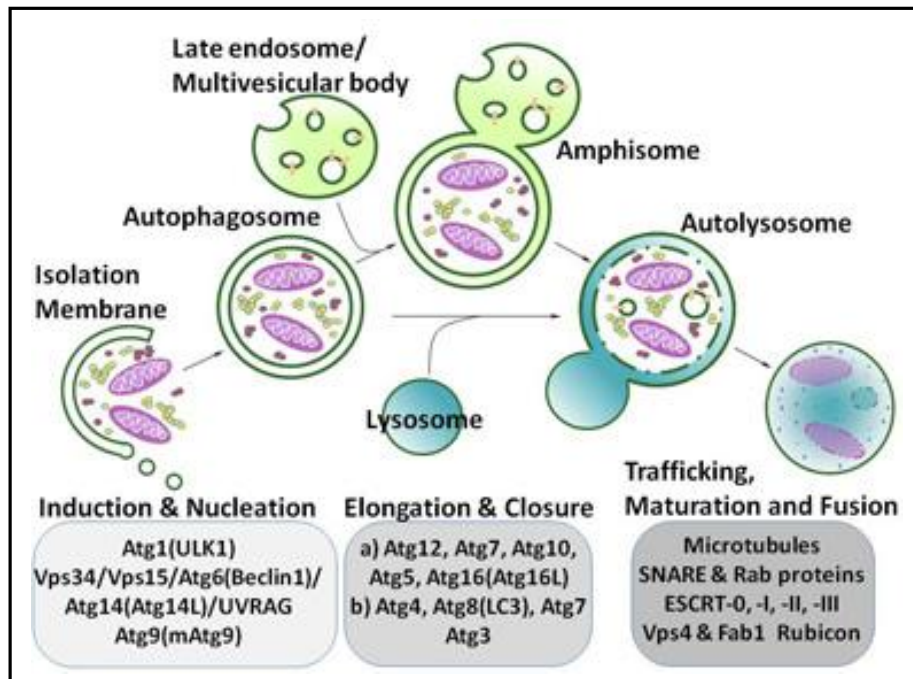


Figure 2: Overview of macroautophagy. Upon induction of autophagy, a membrane of unknown origin forms the initial phagophore or isolation membrane. The phagophore expands, forms the double membrane autophagosome. The autophagosome later fuses with endosomes and lysosomes to have its internal contents degraded.

(<http://www.mssm.edu/research/labs/yue-laboratory>)

1.1.2 Molecular mechanism of autophagy

1.1.2.1 Phagophore formation

1.1.2.1.1 ULK complex

Autophagosome initiation in yeast is centrally controlled by the Atg1:Atg13:Atg17 complex. In mammals, the induction of autophagy requires the unc-51-like kinase (ULK; ATG1 in yeast), which exists in a large complex with mATG13 and FIP200 that is regulated by mammalian target of rapamycin (mTOR) (Ganley et al., 2009). Although it bears no structural homology to the yeast counterpart, FIP200 has been proposed to be a functional orthologue of yeast ATG17 during autophagosome induction and is important for the stability and phosphorylation of ULK1 (Hara & Mizushima, 2009).

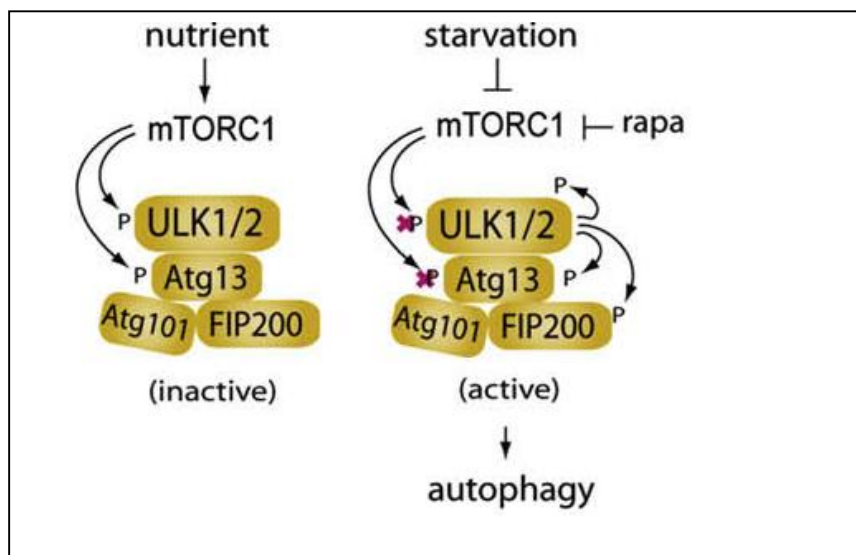


Figure 3. Phosphorylation regulation of ULK1/2 complexes by mTORC1 in response to nutrient levels. mTORC1 phosphorylates ULK1/2 and Atg13 and inhibits the kinase activity of ULK1/2 under high nutrient conditions. Under starvation, mTORC1 phosphorylation of ULK complex is suppressed releasing ULK from mTORC1 inhibition, which subsequently induces ULK to phosphorylate Atg13, FIP200 and itself (adapted from Jung et al., 2009).

Under nutrient rich conditions, the ULK complex interacts with mTORC1 and remains inactivated by mTORC1-mediated phosphorylation of ULK1 and ULK2. Upon nutrient deprivation, mTORC1 dissociates from the complex causing dephosphorylation and activation of ULK1 and ULK2, which can then phosphorylate and activate mATG13 and FIP200, leading to subsequent localization of the activated ULK complex to the phagophore (Jung et al., 2009). Atg101, is a protein conserved in various eukaryotes, is important for the stability and basal phosphorylation of Atg13 and ULK1 (Hosokawa et al., 2009; al., 2009; Mercer et al., 2009). However, the substrates of the ULK complex and how it regulates the autophagic machinery are not entirely known.

1.1.2.1.2 Class III phosphatidylinositol 3 kinase (PI3K) complex

A Class III phosphatidylinositol 3-kinase (PI3K) complex is necessary for the formation of phosphatidylinositol 3-phosphate (PI3P), which is essential for the early stages of nucleation of the phagophore. The PI3K core complex consists of the PI3K protein Vps34, beclin1 (Atg6 in yeast) and its regulatory protein kinase p150 or hVps15 (Simonsen et al., 2009). Though the exact mechanism is not yet clear, it is evident that the core complex localizes to the phagophore and facilitates recruitment of subsequent ATGs. Recent studies have identified various binding partners of beclin1, including ultraviolet (UV) radiation resistance-associated gene (UVRAG) (C. Liang et al., 2007; Itakura et al., 2008), ATG14L/Barkor (Zhong et al., 2009; Matsunaga et al., 2009), Ambra1 (Kang et al., 2011) which all positively regulate beclin1 activity and regulate different steps of autophagosome formation and maturation. Moreover, another molecule named Rubicon (RUN domain and cysteine-rich domain containing, Beclin1-interacting protein) has been uncovered as a negative regulator of beclin1 (Zhong et al., 2009), which binds to the UVRAG–beclin complex and regulates late stages of autophagy, more specifically, the late endosomal and lysosomal maturation process.

1.1.2.2 Phagophore elongation and autophagosome formation

There are two ubiquitin-like systems that are key to autophagy (Mizushima, 2007; Kirkin et al., 2009), acting at the Atg5–Atg12 conjugation step and at the LC3 processing step, decorate the phagophore surface resulting in the formation of autophagosomes.

1.1.2.2.1 Atg5–Atg12 conjugation

Atg12, a small hydrophilic protein of 186 amino acids, can covalently link to a unique target protein, Atg5 (Mizushima et al., 1998). The mode of conjugation of Atg12 and Atg5 is quite similar to that of ubiquitination. Atg12 is first activated in an ATP-dependent manner by Atg7 (it functions as an ubiquitin-activating enzyme, E1), leading

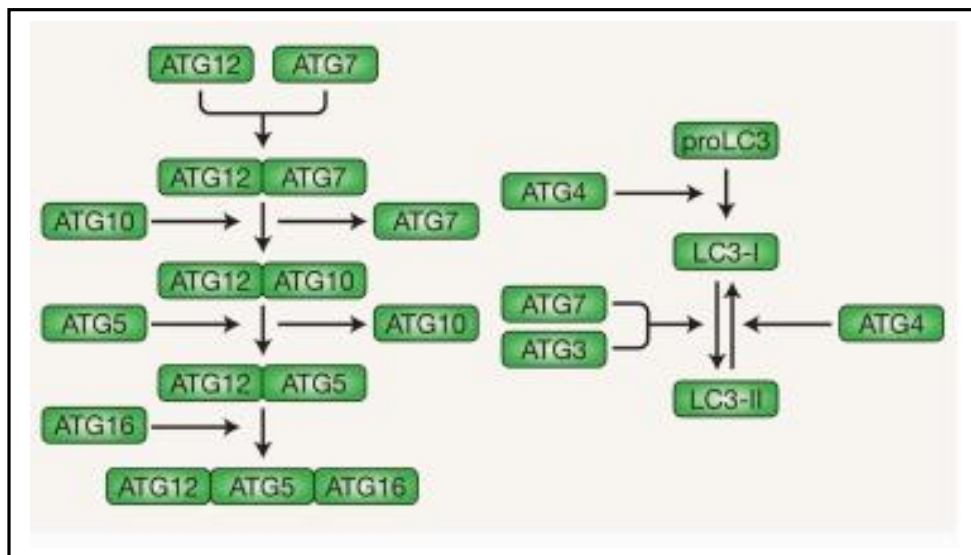


Figure 4. Two conjugation pathways. Atg5 and Atg12 interact with one another through a series of activation and conjugation reactions resulting in the formation of a multimeric Atg12-Atg5-Atg16 complex that clusters on the surface of the isolation membrane, enabling it to expand and grow into an autophagosome. Similarly, the other conjugation pathway involves LC3/Atg8 and plays an equally important role in autophagic vesicle formation (adapted from Rosenfeldt 2009).

to the formation of a thioester bond between the C-terminal glycine in Atg12 and a cysteine residue in Atg7 (Tanida et al., 2001). Atg12 is then transferred to Atg10, an E2-like ubiquitin carrier protein that potentiates covalent linkage of Atg12 to lysine 130 of Atg5 and Atg7 is released. Conjugated Atg5–Atg12 complexes in pairs with Atg16L dimers form a multimeric Atg5–Atg12–Atg16L complex that associates with the extending phagophore. Once the autophagosome is formed, Atg5–Atg12–Atg16L dissociates from the membrane, making conjugated Atg5–Atg12 a relatively poor marker of autophagy (Barth et al., 2010).

1.1.2.2.2 LC3 processing

The second ubiquitin-like system involved in auto-phagosome formation is the processing of microtubule-associated protein light chain 3 (LC3), which is encoded by the mammalian homologue of Atg8. LC3 targets to the autophagosomal membranes in an Atg5-dependent manner and remains attached even after Atg12–Atg5 dissociates. Thus LC3 is the only credible marker of the autophagosome in mammalian cells (Barth et al., 2010). LC3 is expressed in most cell types as a full-length cytosolic protein that, upon induction of autophagy, is proteolytically cleaved by Atg4, a cysteine protease, to generate LC3-I. The carboxyterminal glycine exposed by Atg4-dependent cleavage is then activated in an ATP-dependent manner by the E1-like Atg7. Activated LC3-I is then transferred to Atg3, a different E2-like carrier protein before phosphatidylethanolamine (PE) is conjugated to the carboxyl glycine to generate processed LC3-II. Recruitment and integration of LC3-II into the growing phagophore is dependent on Atg5–Atg12 and LC3-II is found on both the internal and external surfaces of the autophagosome, where it plays a role in both hemifusion of membranes and in selecting cargo for degradation. The relative amount of membrane-bound LC3-II reflects the abundance of autophagosomes, so the induction and inhibition of autophagy can be monitored through measuring total and free LC3-II levels by means of immunoassay (Kabeya et al., 2000).

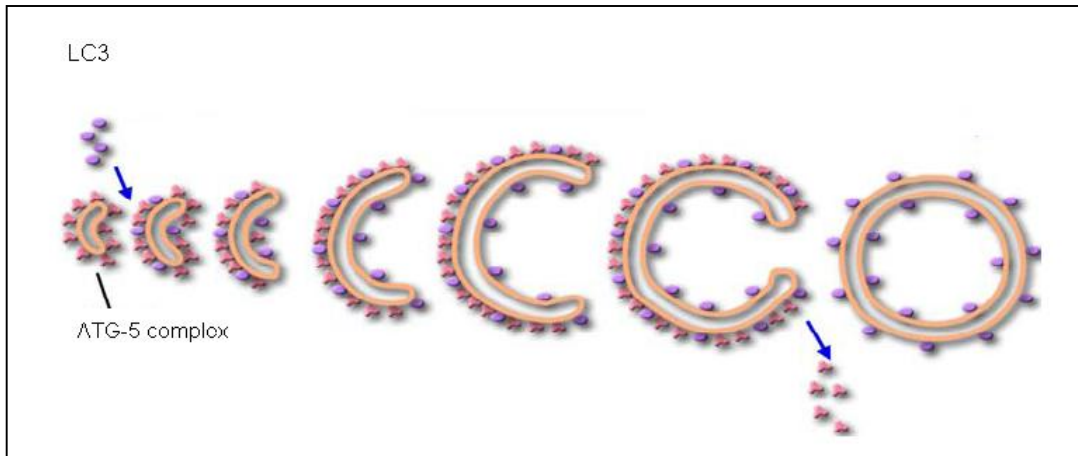


Figure 5. Schematic diagram of autophagosome formation in mammalian cells. A protein complex, which includes Atg5, Atg12, and Atg16L, is associated with the membranes of small cisternae, recruits LC3-II to the membranes, and initiates elongation of the membranes. The membranes grow into the isolation membrane and eventually mature into autophagosomes. The Apg5 complex leaves the membrane just before or after membrane fusion, while LC3 remains (adapted from Yoshimori, 2005)

1.1.2.3 Selective autophagy: cargo for degradation

Several studies have been shown that the growing phagophore membrane can interact selectively with protein aggregates and organelles. It is proposed that LC3-II, acting as a 'receptor' at the phagophore, interacts with 'adaptor' molecules on the target (eg protein aggregates, mitochondria) to promote their selective uptake and degradation. The best-characterized molecule in this regard is p62/SQSTM1, a multi-functional adaptor molecule that promotes turnover of polyubiquitinated protein aggregates. Mutation of p62/SQSTM1 is linked to Paget's disease, arthritis and nerve injury (Ralston, 2008). Other molecules, such as NBR1, function similarly to p62/SQSTM1 in promoting turnover of ubiquitinated proteins, while in yeast, Uth1p and Atg32 have been identified as proteins that promote selective uptake of mitochondria, a process known as mitophagy (Kirkin et al., 2009; Kim et al., 2007).

1.1.2.4 Maturation of autophagosome and its fusion with lysosome

When the autophagosome completes fusion of the expanding ends of the phagophore membrane, the next step towards maturation to form the 'autolysosome' (Mizushima, 2007). This aspect of the process is relatively understudied but requires the small G protein Rab7 in its GTP-bound state (Gutierrez et al., 2004; Jäger et al., 2004), two beclin-1 binding protein Rubicon and UVRAG and also mammalian orthologs of SNARE protein family members and the NSF protein for autophagosome maturation.

1.1.2.4.1 The role of the cytoskeleton

The cytoskeleton plays a role in autophagosome biogenesis and trafficking. Autophagosomes utilize microtubule tracks on their way to lysosomes. Among their other functions, microtubules serve as roadways for membrane traffic. Destabilization of microtubules by either vinblastine or nocodazole blocks the maturation of autophagosomes, whereas their stabilization by taxol increases the fusion between autophagic vacuoles and lysosomes (Høyvik et al., 1991; Aplin et al., 1992; Yu et al., 1986). Several studies have confirmed the role of microtubules in the fusion with the acidic compartment (Jahreiss, L. et al., 2008; Kochl R. et al., 2006; Webb J.L. 2004). Autophagosomes move bidirectionally along microtubules. Their centripetal movement is dependent on the dynein motor (Ravikumar, B et al., 2005; Kimura S. et al., 2008). Interestingly, the functional loss of dynein has been linked to certain neurodegenerative disorders. In vitro studies have demonstrated that the loss of dynein leads to an impairment of the clearance of aggregate-prone proteins by autophagy and to increased levels of LC3-II, reflecting a defect in the fusion between autophagosomes and lysosomes (Ravikumar et al., 2005). This data have recently also been confirmed using live-cell imaging analyses that revealed that dynein is required for autophagosome trafficking along microtubules and this centripetal movement discontinues once the autophagosome reaches the microtubule-organizing centre (Jahreiss et al., 2008).

1.1.2.4.2 The role of lysosomal composition in autophagic maturation

Within the lysosome, cathepsin proteases B and D are required for turnover of autophagosomes and the maturation of the autolysosome (Koike et al., 2005). Lamp-1 and Lamp-2 at the lysosome are also critical for functional autophagy, as evidenced by the inhibitory effect of targeted deletion of these proteins in mice on autolysosome maturation (Tanaka et al., 2000).

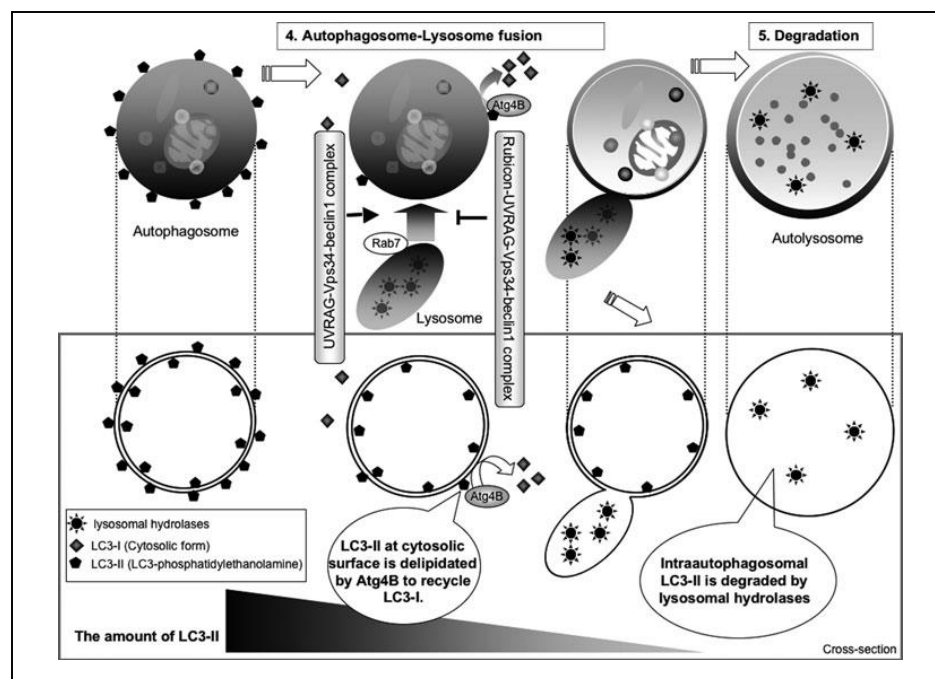


Figure 6. Autophagosome–lysosome fusion and degradation of intra-autophagosomal contents. Autophagosome–lysosome fusion is positively regulated by Rab7 and the UVRAG-Vps34-beclin1 PI3-kinase complex, whereas it is negatively regulated by the Rubicon-UVRAG-Vps34-beclin1 complex. After the formation of the autolysosome, the lysosomal hydrolases degrade the intra autophagosomal contents, including LC3-II. Therefore, the amount of LC3-II decreases during these steps. The inset shows the decrease in LC3-II (adapted from Tanida, 2011).

Although delivery of the endocytosed cargo to the lysosomes has been widely accepted, the mechanisms by which endosomal contents are transferred to lysosomes remain controversial. Lysosomes are dynamic, membrane-bound organelles found in animal cells containing acid hydrolases which are kept active with the help of several proton pumping vacuolar ATPases, found on the lysosomal and late endosomal membranes, which maintain the luminal pH at 4.6-5.0 (Mellman et al. 1986).

Numerous theories exist wherein the endosomes are thought to either (i) mature into lysosomes, the contents are transferred through numerous transient “kiss and run” contacts or (ii) a direct fusion mechanism is employed to form a endo-lysosomal compartment, or (iii) hybrid organelle (Luzio et al., 2007). Upon fusion with phagosomes, endosomes, or autophagosomes, conventional lysosomes may traffic to the plasma membrane to secrete the digested contents out of the cell.

1.1.3 Physiological roles of autophagy

Recently, increased numbers of autophagic vacuoles have been found in several human diseases including neurodegenerative diseases (e.g., Alzheimer’s, Parkinson’s, Huntington’s and Creutzfeldt-Jakob disease), cardiomyopathy (e.g., Danon disease) (Ravikumar et al., 2002; Qin et al., 2003; Webb et al., 2003; Shibata et al., 2006).

Upregulation of autophagy is also useful in eliminating pathogens following bacterial and viral infections. The pathogens infecting the host cell can be engulfed by the autophagosomes and targeted to lysosomes for degradation (Kirkegaard et al., 2004; Bélanger et al., 2006; Tallóczy et al., 2006; Yoshimori, 2006).

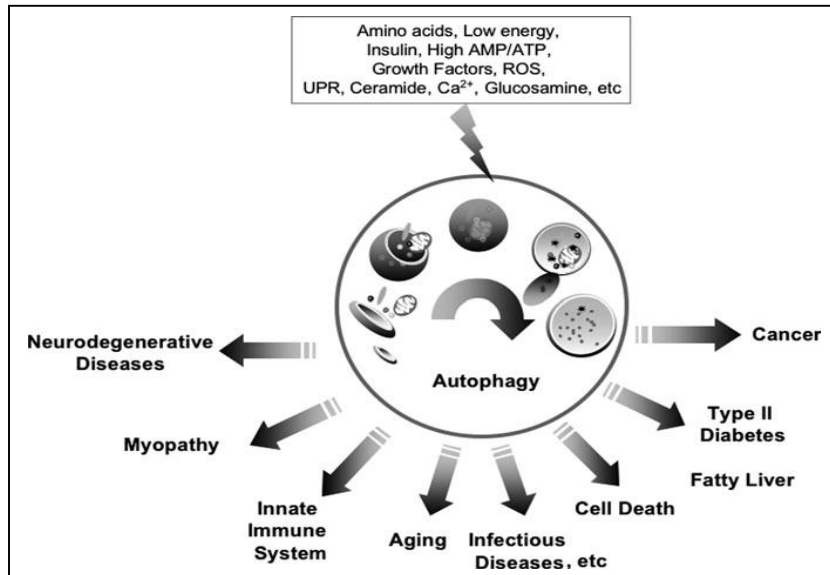


Figure 7. Physiological signals and diseases related to autophagy. Autophagy is induced by many physiological signals and is related to many diseases and processes. (adapted from Tanida, 2011).

Another important physiological role of autophagy is in tumorigenesis. Recently, a number of studies have shown important but seemingly paradoxical roles for autophagy during cancer progression which may depend on tumor type, context and stage. Autophagy clearly mediates tumor cell survival and growth during times of nutrient starvation or metabolic stress, particularly prior to angiogenesis, and autophagy facilitates tumor recurrence following chemotherapy (Lum et al., 2005; Degenhardt et al., 2010; Amaravadi et al., 2007; Karantza-Wadsworth et al., 2007). On the other hand, however, autophagy also appears to suppress tumorigenesis. This is suggested by the fact that tumor cells lose expression of autophagic proteins, as the level of beclin 1 expression was shown to be lower in malignant than in normal breast epithelial cell (Liang et al., 1999). In addition, gene transfer of beclin 1 was observed to promote autophagy in these malignant cells, leading to the loss of malignant morphologic features. In addition to beclin 1, other positive regulators of autophagy, such as UVRAG also function as tumor suppressors (Xiao et al., 2001; Liang et al., 2007) and certain

negative regulators of autophagy, such as Bcl-2 promote tumorigenesis and prevent apoptosis (Kirkin et al., 2004). Moreover, oncogenes like Akt, Ras, and ERK (Furuta et al., 2004) inhibit autophagy primarily by activating the mTOR signaling pathway. On the other hand, there is abundant evidence that tumor suppressors like p53 (Crighton et al., 2006), PTEN (Arico et al., 2001) and ARF (Pimkina et al., 2009; Reef et al., 2006) activate autophagy. All together these observations have led to the assumption that in non-transformed cells autophagy acts as a tumor suppressor mechanism by preventing accumulation of damage and thus avoiding mutations. However, once cells are transformed, autophagy promotes tumor cell survival.

The critical role of autophagy in maintaining cell viability upon shortage of external nutritional sources was first documented in yeast (Tsukada et al., 1993; Levine et al., 2004). Later, a similar cytoprotective role of autophagy-dependent production of metabolites during nutrient starvation or growth factor deprivation was also demonstrated in mammalian cells lacking essential *atg* genes (Boya et al., 2005; Degenhardt et al., 2006; Lum et al., 2005). Autophagy is also involved in removing damaged or over-activated and thereby potentially dangerous organelles (mitochondria, endoplasmatic reticulum, peroxisomes and lysosomes) as well as cytotoxic protein aggregates from the cell thereby promoting cell survival (Bernales et al., 2006; Ostefeld et al., 2008; Iwata et al., 2006). Paradoxically, autophagy has also been implicated in cell death called autophagic or type II programmed cell death (Clarke, 1990; Kroemer et al., 2005). It is not fully understood the final outcome of autophagy, but it does not depend solely on either the cell-type or the stimulus. For example, autophagy protects HeLa cervix carcinoma cells against starvation but contributes to the death of the same cells following treatment with interferon- γ (Pyo et al., 2005; Boya et al., 2005) and tunicamycin-induced autophagy enhances the survival of colon cancer cells but contributes to the killing of immortalized murine embryonic fibroblasts (Ding et al., 2007). However, the role of autophagy in this type of cell death is currently being questioned, as it may reflect cell death with autophagy rather than by autophagy.

1.1.4 Regulation of autophagy by signaling pathways

The class III PI3K, Vps34 plays an important role in mediating autophagosome formation. It directly interacts with beclin 1 and promotes the formation of the autophagosome vesicle (Kihara, A et al., 2001). Class I PI3K can negatively regulate autophagy indirectly via Akt and mTORC1. Akt phosphorylates and inhibits TSC2 (tuberous sclerosis complex-2) which leads to the activation of mTORC1 complex resulting inhibition of autophagy (Huang, J et al., 2009).

Owing to its energy sensing functions, mTOR (the mammalian target of rapamycin) is considered the master regulator of autophagy. In yeasts, TOR inhibits the association between ATG1 (ULK1 in humans) and ATG13 by hyperphosphorylating ATG13, thereby decreasing its affinity for ATG1 (Kamada, Y. et al., 2000; Kamada, Y. et al., 2010). Recent studies suggest that when nutrient is abundant, active mTORC1 inhibits autophagosome formation by associating with the ULK1-ATG13-FIP200 complex and phosphorylating ULK1 and Atg13 (Jung, C.H. et al., 2009; Kim, J. et al., 2011; Hosokawa, N. et al., 2009; Chan, E.Y. et al., 2009). Inhibition of mTORC1 by rapamycin or starvation results in dephosphorylation of ULK1 and initiation of autophagy. mTORC1 has also been shown to play a role in the termination of autophagy and lysosomal homeostasis through an unknown mechanism (Yu, L. et al., 2010).

The stress-activated AMP-dependent protein kinase (AMPK), which is activated in response to stress and low cellular ATP levels is positive regulator of autophagy via inhibition of mTORC1 (Gwinn, D.M. et al., 2008; Inoki, K. et al., 2003).

ERK has been shown to induce autophagy in response to a number of anti-tumor/cytotoxic agents, such as soyasaponins in colon cancer cells (Ellington, A.A. et al., 2006), capsaicin in breast cancer cells (Choi, C.H. et al., 2012) and cadmium in mesangial cells (Wang, S.H. et al., 2009; Yang, L.Y. et al., 2009). Inhibition of ERK was associated with a decrease in autophagy and increased cellular sensitivity to tumor necrosis factor- α (TNF) in breast cancer MCF-7 cells (Sivaprasad, U et al., 2008). ERK was shown to promote TNF-induced autophagy in mouse fibroblast L929 cells by activating p53 (Cheng, Y. et al., 2008). Activation of ERK by the transformation of human mesenchymal stem cells by H-ras (Shima, Y. et al., 2007), overexpression of

TrkA (tropomyosin-related kinase A) in glioblastoma cells (Hansen, K et al., 2007) and overexpression of mutant LRRK2 (leucine rich repeat kinase 2) in neuronal cells (Plowey, E.D. et al., 2008) was associated with an increase in autophagy. Recent studies suggest that ERK regulates the maturation of autophagic vacuoles. Activation of ERK has been associated with the formation of large cytoplasmic vacuoles (Martin, P. et al., 2006). Lindane-associated formation of large vacuoles, which reflected arrested autolysosomes, was shown to be dependent on sustained activation of ERK (Corcelle, E. et al., 2006).

JNK has been implicated in the induction of autophagy by various stimuli, including starvation (Li, C. et al., 2006), cytokine stimulation (Jia, G. et al., 2006), T-cell receptor activation (Li, C. et al., 2006), neuronal excitotoxic stimuli (Borsello, T. et al., 2003) and ER stress (ogata, M. et al., 2006). One mechanism by which JNK contributes to autophagy involves phosphorylation of the antiapoptotic protein Bcl-2 (Chen, J.L. et al., 2008; Nopparat, C., 2010). p38 is another very important signaling pathway in autophagy which has been described in next section.

1.2 p38 Mitogen activated protein kinases

Mitogen-activated protein kinases (MAPKs) are members of discrete signaling cascades that serve as focal points in response to a variety of extracellular stimuli and function to regulate fundamental cellular processes. In humans, the p38 MAPK family comprises four splice variants: p38 α , p38 β , p38 γ and p38 δ (Han et al., 1994; Jiang et al., 1996; Jiang et al., 1996; Jiang et al., 1997a). Of these, p38 α and p38 β are ubiquitously expressed, whereas the others are expressed differentially in different tissues (Kumar et al., 1997). Sequence comparisons revealed that each p38 isoform has more than ~ 60% homology, but only 40-45% homology with the other MAPKs, including c-Jun N-terminal kinases (JNKs) and extracellular signal-regulated kinases (ERKs).

1.2.1 Induction and regulation of p38 MAPK activity

p38 is activated by MAPK kinases (MKKs) in response to a wide variety of stimuli, such as UV irradiation, heat, osmotic shock, inflammatory cytokines (TNF- α & IL-1), and growth factors (CSF-1, GM-CSF, VEGF, PDGF) (Freshney et al., 1994; Lee et al., 1994; Rouse et al., 1994; Raingeaud, 1995.). This plethora of activators conveys the complexity of the p38 pathway and this is further complicated by the observation that activation of p38 α is not only dependent on stimulus, but on cell type as well. For example, insulin can stimulate p38 in 3T3-L1 adipocytes (Sweeney et al., 1999), but downregulates p38 activity in chick forebrain neuron cells (Heidenreich et al., 1996).

There are two main MAPKKs that are known to activate p38; MKK3 and MKK6 (Jiang et al., 1997a). In addition to the activation by upstream kinases, p38 can also be activated through two alternative MKK-independent mechanisms, in a cell type and stimulus-specific manner. Two mechanisms are known: (i) Phosphorylation of p38 on a novel site (Tyr 323) by the ZAP-70 tyrosine kinase (Salvador et al., 2005) and (ii) autophosphorylation *via* a physical interaction with transforming growth factor- β -activated protein kinase 1 (TAK1)-binding protein (TAB1) (Ge et al. 2002).

MKK-independent p38 activation has been reported in response to other cytokines and nitric oxide (Makeeva, Myers, & Welsh, 2006). In addition, the ZAP-70 mediated phosphorylation of p38 has been observed exclusively in T cells (Salvador et al. 2005).

The activation and subsequent activity of the p38 isoforms are conferred by a Thr-Gly-Tyr (TGY) dual phosphorylation motif in the regulatory loop between the kinase subdomains (Hanks et al., 1995). The glycine residue in the TGY motif and the length of the regulatory loop influences p38 substrate specificity and controls autophosphorylation (Jiang et al., 1997a; Jiang et al., 1997). Like all MAPKs, p38 undergoes a sequence of phosphorylation and dephosphorylation events, to act on several downstream substrates, including protein kinases or transcription factors, resulting in a wide variety of responses. MAP kinase activated protein kinase 2 (MK-2) was the first substrate identified to be activated by p38 α (Rouse et al., 1994). Active MK-2 in turn activates other substrates, like the heat shock protein 27 (HSP27),

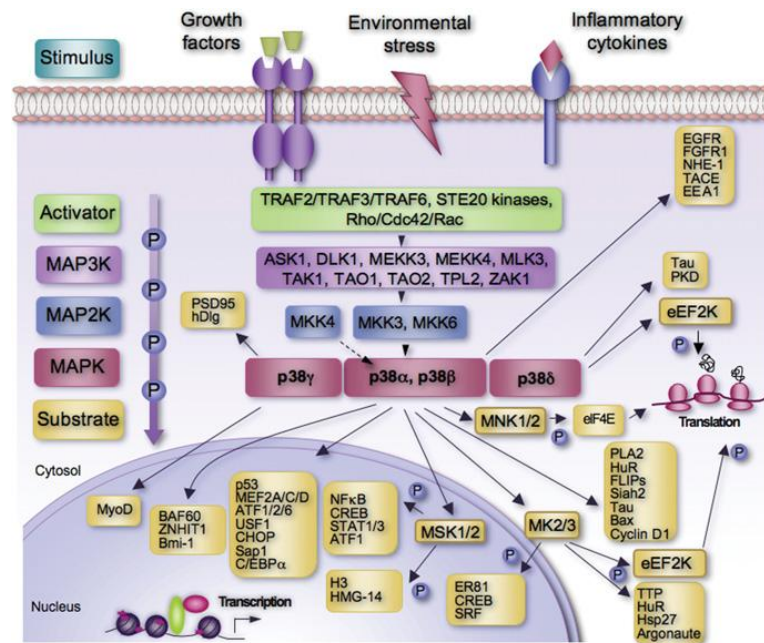


Figure 8. The p38 MAPK pathway. Different stimuli such as growth factors, inflammatory cytokines or a wide variety of environmental stresses can activate p38 MAPKs. A number of representative downstream targets, including protein kinases, cytosolic substrates, transcription factors and chromatin remodellers, are shown (adapted from Cuadrado, A., 2010).

lymphocyte lymphocyte-specific protein (LSP1), cAMP response element binding protein (CREB), activating transcription factor 1 (ATF1), serum response factor (SRF) and enzyme tyrosine hydroxylase (Stokoe et al.,1992; Tan et al., 1996; Huang et al.,1997; Thomas et al.,1997; Heidenreich et al., 1999). MK2 has been found to phosphorylate tristetraprolin (TTP), a protein that is known to destabilize mRNA hinting at a role for p38 in mRNA stability (Mahtani et al., 2001). MNK1 is another kinase substrate of p38 whose function is thought to reside in translational initiation, since MNK1 and MNK2 can phosphorylate eukaryotic initiation factor-4e (eIF-4E) (Waskiewicz et al., 1997; Fukunaga et al.,1997). Mitogen and stress-activated protein kinase-1 (MSK1) can be directly activated by p38 and ERK, and may mediate activation of CREB (Deak et al.,1998), (Pierrat et al., 1998). p38 is also thought to regulate S phase activation of histone 2B (H2B) promoter through OCA-S, a component of p38 (Zheng et al.,2003). In addition to these proteins, p38 MAPK also phosphorylates structural proteins, like keratin and stathmin (Parker et al., 1998; Feng et al., 1999).

1.2.2 Biological consequences of p38 MAPK activation

A strong link has been established between the p38 pathway and inflammation. Rheumatoid arthritis, Alzheimer's disease and inflammatory bowel disease are all postulated to be regulated in part by the p38 pathway (Johnson, 2003; Hollenbach et al., 2004). The activation of the p38 pathway plays essential roles in the production of pro inflammatory cytokines (IL-1 β , TNF- α and IL-6) (Guan et al., 1998), induction of enzymes such as COX-2 (Badger et al., 1998), expression of intracellular enzymes such as iNOS (Da Silva, Pierrat, Mary, & Lesslauer, 1997), induction of VCAM-1 and other adherent proteins along with other inflammatory related molecules. In addition, a regulatory role for p38 in the proliferation and differentiation of immune system cells such as GM-CSF, EPO, CSF and CD-40 has been established (Kummer, Rao, & Heidenreich, 1997). p38 has been implicated in cell differentiation and apoptosis for certain cell types.

There have been reports that activation of p38 led to senescence in response to telomere shortening, H₂O₂ exposure, and chronic RAS oncogene signaling (Wang et al., 2002; Haq et al., 2002; Bulavin et al., 2002). A common feature of tumor cells is a loss of senescence and p38 may be linked to tumorigenesis in certain cells. It has been reported that p38 activation may be reduced in tumors and that loss of components of the p38 pathway such as MKK3 and MKK6 resulted in increased proliferation and likelihood of tumorigenic conversion regardless of the cell line or the tumor induction agent used. p38 has been implicated in G1 and G2/M phases of the cell cycle in several reports (Yee et al., 2004; Molnár et al., 1997). G1 arrest of NIH3T3 cells caused by microinjection of Cdc42 was found to be p38 α - dependent (Wang et al., 2000). Also a link between p38 and G1 cell cycle control has been proposed through the regulation of p38 substrates HBP1 and p21 (Yee et al., 2004). p38 α is activated in mammalian cells upon M phase arrest by disruption of the spindle with nocodazole (Molnár et al., 1997). Furthermore, it has been shown that p38 α and p38 γ are required for UV-induced G2 cell cycle arrest (Wang et al., 1998).

1.2.3 p38 MAPK and its potential role in autophagy

Activation of p38 was associated with induction of autophagy by polygonatum cyrtoneum lectin (PCL) in human melanoma cells (Liu et al., 2009), MCP-1 (monocyte chemoattractant protein-1) in cardiomyoblast (Younce et al., 2010), silibinin in fibrosarcoma cells (Duan et al., 2011), bromelain in breast cancer cells (Bhui et al., 2010), oridonin in HeLa cells (Cui et al., 2007) and resveratrol in hepatocellular carcinoma cells (Liao et al., 2010). The induction of autophagy by p38 was often accompanied by an increase in Atg proteins, such as beclin 1 and Atg5 (Kim et al., 2010; Lim et al., 2010). In several studies, the tumor suppressor protein p53 was shown to be involved in the autophagy induction by p38. Phosphorylation of p53 at Ser392 by p38 enhanced its transcriptional activity causing increased expression of beclin1. ER stress-induced beclin 1 expression and induction of autophagy also correlated with increased p38 phosphorylation/activation (Lim et al., 2010).

Contrary to these observations, studies have revealed the induction of autophagy in certain types of cancer cells that are depleted of p38 MAPK activity (Comes et al. 2007; Simone 2007), suggesting that p38 negatively regulates autophagy. In line with the later reports, p38 was also shown to negatively regulate autophagy in other studies. Inhibition of p38 in colon cancer cells and myelogenous leukemic K562 cells was associated with increase in beclin 1 and induction of autophagy (Thyagarajan et al., 2010; Colosetti et al., 2009). A recent report demonstrated that p38 inhibits autophagy by competing with transmembrane protein mAtg9 for binding to p38 interacting protein (p38IP) (Webber et al., 2010).

In summary, the role of p38 in regulation of autophagy has been studied in different contexts and cell lines, leading to different observations that appear contradictory or at least don't allow a consensus.

1.3 Oncogene-induced Senescence

Senescence was identified by Hayflick and Moorhead, as a process associated with the lack of infinite replicative potential of human primary fibroblasts (Hayflick & Moorhead, 1961). Subsequent work by others demonstrated that the mechanism underlining the phenomenon was telomere attrition. This type of senescence was termed 'replicative' and was suggested to represent a failsafe mechanism preventing the expansion of aged cells (Campisi et al., 2007).

Nearly three decades ago, it was observed that normal cells are refractory to oncogene transformation (Newbold et al., 1983). In 1997 Serrano and colleagues observed that ectopic expression of the oncogene H-RASG12V in normal fibroblast induced senescence that was later shown to be telomere-independent (Serrano et al., 1997; Wei et al., 1999). Ever since, this form of senescence called 'oncogene-induced senescence' (OIS) has been displayed by a variety of oncogenes, in vitro and in vivo.

1.3.1 Features of senescent cells

Senescent cells show different features from proliferating cells (Figure-1). Cells remain viable, stop to synthesize DNA, i.e. lack 5-bromo-2'-deoxyuridine (BrdU) incorporation, do not respond to mitogenic stimuli and their morphological characteristics and function change dramatically. The transition from a growing, proliferative state to senescence involves gradual but massive changes in cell physiology and protein expression (Campisi, 2000; Sitte et al., 2000). Depending on the senescence trigger, cells can become large, flat, and multinucleated, or rather refractile. A flat cell phenotype is commonly seen in cells undergoing H-RASV12-induced senescence (Serrano et al., 1997), stress-induced senescence (Parrinello et al., 2003), or DNA damage-induced senescence (Chen et al., 2001). Cells senescing due to BRAFE600 expression or the silencing of p400, however, acquire a more spindle-shaped morphology. Melanocytes undergoing RASV12-induced senescence display extensive vacuolization as a result of

endoplasmic reticulum stress caused by the unfolded protein response (Chan et al., 2005; Michaloglou et al., 2005; Denoyelle et al., 2006).

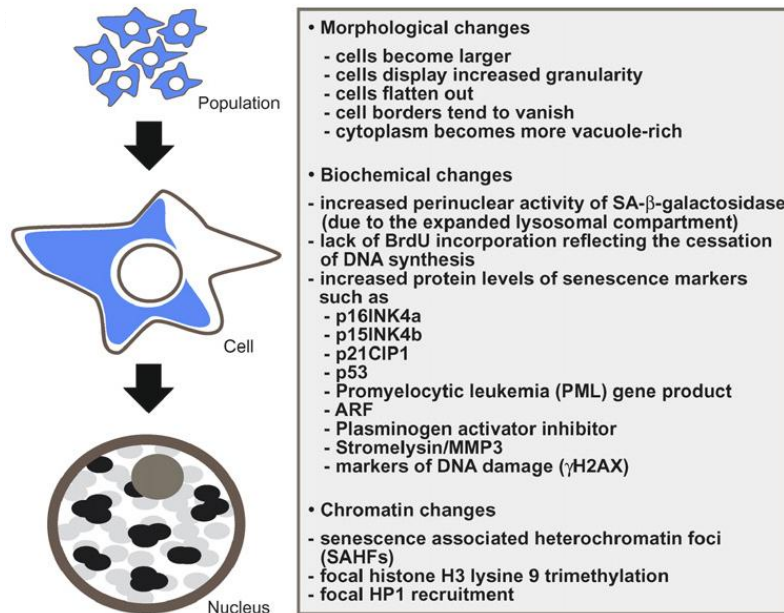


Figure 9. Features of cellular senescence. Schematic view of a senescent cell population with characteristic morphological alterations and typical biochemical markers (adapted from Schmitt, 2007).

These changes are accompanied by alterations in nuclear structure, gene expression, protein processing, and metabolism. In addition, senescent cells often down-regulate genes involved in proliferation and extracellular matrix production, and up-regulate inflammatory cytokines and other molecules known to modulate the tissue microenvironment or immune response. Consistent with the role of senescence as a barrier to malignant transformation, senescent cells activate the p53 and p16/Rb tumor suppressor pathways that are required to various degrees in different cell types to execute the program (Courtois-Cox et al., 2008). SA- β -GAL is a commonly used senescence biomarker (Dimri et al., 1995; Debacq-Chainiaux et al., 2009). Its increased activity in senescent cells derives from lysosomal β -D-galactosidase, which is encoded by the GLB1 gene.

1.3.2 Role of senescence on tumorigenesis

Tumorigenesis is a multistep process, in which a normal cell acquires mutations in a number of cancer-causing genes. By restricting cell proliferation and thereby impeding the accumulation of mutations, senescence acts as an important tumor suppression mechanism. Furthermore, senescence induced by aberrant activation of oncogenes, oxidative stress, or DNA damage prevents cells at risk of malignant transformation from proliferating. Senescence represents a physiologic response that cells must overcome in order to divide indefinitely and develop into tumors (Wright et al., 2001; Sharpless et al., 2004; Campisi, 2005; Sager, 1991).

In mouse tumor models with oncogenic Ras, senescent cells are found in premalignant lesions in lung (Collado et al., 2005), spleen (Braig et al., 2005), breast (Sarkisian et al., 2007), and pancreas (Morton et al., 2010). The observation of senescent cells has been extended to many premalignant lesions or benign tissues induced by different oncogene activation or tumor suppressor inactivation in mouse and human. Importantly, senescent cells are absent in malignant tumors, suggesting that oncogene induced senescence is a powerful tumor suppression mechanism by restricting proliferation of cells with oncogenic mutations and this senescence block must be evaded for malignancy to progress. Consistently, deletion of senescence regulators such as p53, Arf, p16, p27, SUV39H1 or PRAK abrogates senescence and causes progression of tumors to the malignant stage. These observations point to a causal link between loss of senescence and malignant transformation (Goel et al., 2009; Young et al., 2008; Bartkova et al., 2006; Michaloglou et al., 2005; Sun et al., 2007).

Besides tumor suppression, senescence can also promote tumorigenesis. Factors secreted by senescent cells can promote tumor development in vivo and malignant phenotypes such as proliferation and invasiveness in cell culture models. This effect, termed the senescence-associated secretory phenotype (SASP), has been observed with a number of cell types, including cells derived from breast (Tsai, K.K. et al., 2005),

skin (Sun, P. et al., 2007), prostate (Choi, J. et al., 2000), pancreas (Ohuchida, K. et al., 2004) and oropharyngeal mucosa (Coppe et al., 2008). SASP can also alter the microenvironment affecting the neighboring cells. SASP factors can boost up cancer progression by stimulating proliferation, inducing epithelial to mesenchymal transition (EMT) (Thiery et al., 2009; Parinello et al., 2005; Coppe et al., 2008).

Although paracrine activities of many SASP proteins can promote phenotypes associated with malignancy, the SASP is complex and thus not all components are cancer promoting. For example, senescent keratinocytes secrete the anti-angiogenic factor maspin (Nickoloff et al., 2004). In addition, each SASP factor has effects that depend on the cell and tissue context. For example, the IL-6, IL-8, and plasminogen activator inhibitor-1 (PAI-1) that are secreted by senescent fibroblasts can promote tumor suppression induced by activated oncogenes or oxidative stress (Kortlever et al., 2006; Acosta et al., 2008; Kuilman et al., 2008). However, IL-6 and IL-8 have also been shown to promote malignant tumorigenesis in cooperation with certain activated oncogenes (Sparmann and Bar-Sagi, 2004; Ancrile et al., 2007).

1.3.3 The MCF-7/NeuT cell system as a model of oncogene-induced senescence

The ERBB2/Neu proto-oncogene is a member of the EGFR family and is overexpressed in approximately 15-30% of breast carcinomas (Slamon D.J. et al., 1989). Elevated ERBB2 expression is a predictor of poor prognosis with early metastasis and short overall survival. Exploiting the tetracycline expression system, it has been previously shown that inducible hypermitogenic ERBB2 signaling results in growth arrest of MCF-7 breast carcinoma cells and activation of the cyclin-dependent kinase inhibitor, P21, is an important mediator of this cellular response (Trost et al., 2006; Spangenberg et al., 2008; Cadenas et al., 2010; Cadenas et al., 2012). This cell system is particularly advantageous to be studied as a senescence model because more than 90% cells undergo senescence after doxycycline treatment. Furthermore, it resembles other in vitro as well as in vivo senescence-associated phenotype (Cadenas et al., 2012).

Aim of the work

Autophagy is an intracellular degradation process that involves sequestering of cellular material in autophagosomes and its delivery to the lysosome. Due to the important roles of autophagy in cell survival and cell death its levels and flux must be properly regulated and adapted to cell requirements.

The aim of this work is to investigate the regulation of the autophagy flux by different signaling pathways. The stress activated pathway p38/MAPK is particularly considered since its precise role in autophagy is conflicting and thus not clarified up to date. Furthermore, the regulation of the autophagic flux will be studied in a time dependent manner during the course of exposure to a stress stimulus. For this purpose two models of cellular stress are applied: i) a model of oncogene-induced senescence, in which preliminary work had provided initial evidence for a deregulated autophagy and ii) a model of anisomycin (a protein synthesis inhibitor that activates stress-signaling cascades in the cell) induced stress. These investigations require the establishment of state of the art techniques to monitor the autophagic flux, such as detection of the turnover of the autophagosome marker LC3-II by both immunoblotting and by immunofluorescence followed by confocal microscopy.

A further purpose of this study is to identify the molecular mechanism by which the p38 signaling pathway exerts its regulation on autophagy. This involves identifying targets of p38 that are directly or indirectly involved in the autophagic process.

CHAPTER TWO
MATERIALS AND METHODS

2.1 Materials

2.1.1 Cell Lines

2.1.1.1 MCF7/NeuT

The MCF7/NeuT cell line was generated by Tatjana Trost (Trost et al., 2005) in order to study the consequences of overexpressing NeuT, an oncogenic variant of the transmembrane tyr kinase receptor ERBB2. This cell model takes advantage of the tetracycline-on (Tet-On) system, an expression module that enables tetracyclin-inducible expression of a gene of interest. For this purpose the human breast cancer cell line MCF7 was stably transfected with the pcDNA3Neo/rtTA2 plasmid that allows expression of the reverse tetracyclin-dependent transactivator (rtTA) and a second plasmid, pINSpBI-EGFP/NeuT, that contains the EGFP reporter and the NeuT gene under the control of a tetracyclin responsive element (TRE) as a bidirectional promoter. By adding doxycycline, a tetracycline derivative, to the culture medium the transactivator (rtTA) becomes active and binds the TRE whereby expression of both NeuT and the EGFP reporter gene become switched on (Trost, et al. 2005).

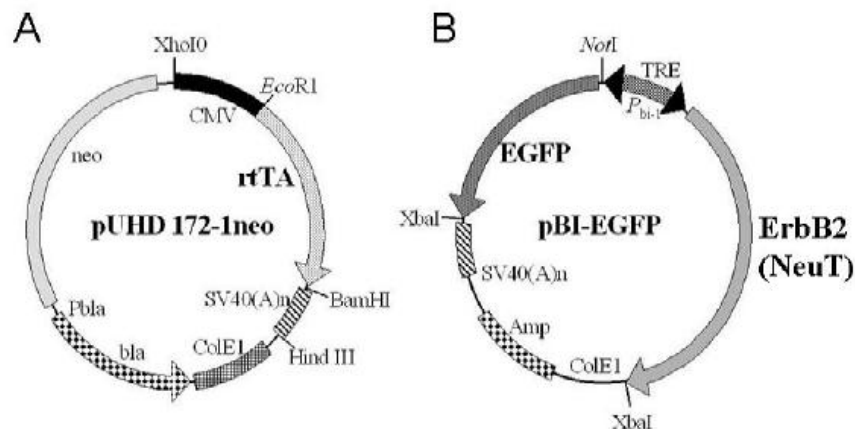


Figure 10: MCF7/NeuT cell transfection constructs

2.1.1.2 Human Embryonic Kidney 293 (HEK293)

Permanent human embryonic kidney cell line grown in tissue culture transformed with sheared adenovirus 5 DNA and was first described in 1977 (Graham et al.,1977).

2.1.1.3 HeLa

HeLa is a widely used human epithelial carcinoma cell line derived from cervical cancer cells taken from Henrietta Lacks in 1951.

2.1.2 Antibodies

2.1.2.1 Primary Antibodies

Antibody	Host	Company	Catalog No.
α -Tubulin	Rabbit	Cell Signaling	2144
β -Actin	Mouse	Sigma	A5316
BrdU	Rat	Serotec	MCA2060
Phospho Akt (Ser473)	Rabbit	Cell Signaling	9271
Total Akt	Rabbit	Cell Signaling	9272
Phospho c-Raf (Ser388)	Rabbit	Cell Signaling	9427
Phospho c-Raf (Ser259)	Rabbit	Cell Signaling	9421
Total c-Raf	Rabbit	Cell Signaling	9422
Dynein (DYNLL1)	Rabbit	Abcam	Ab104603
Phospho p44/42 MAPK (Erk1/2) (Thr202/Tyr204)	Rabbit	Cell Signaling	9101
p44/42 MAPK (Erk1/2)	Rabbit	Cell Signaling	9102
Phospho SAPK/JNK (Thr183/Tyr185)	Rabbit	Cell Signaling	9251

Total SAPK/JNK	Rabbit	Cell Signaling	9251
LC3	Rabbit	Cell Signaling	2775
Phospho MAP4 (Ser768)	Rabbit	Ab Frontier	LF-PA40702
Total MAP4	Rabbit	Abcam	Ab89650
Phospho-MEK1/2 (Ser217/221)	Rabbit	Cell Signaling	9121
Total MEK 1/2	Rabbit	Cell Signaling	9122
Phospho-MSK1 (Ser376)	Rabbit	Cell Signaling	9591
Neu	Rabbit	Santa Cruz	sc-284
Phospho p38	Rabbit	Cell Signaling	9211
Total p38	Rabbit	Cell Signaling	9212
PARP	Rabbit	Cell Signaling	9542
Phospho Stathmin (Ser16)	Rabbit	Cell Signaling	3353
Total Stathmin	Rabbit	Cell Signaling	3352
SQSTM1/p62	Rabbit	Cell Signaling	5114

2.1.2.2 Secondary Antibodies

Antibody	Company	Catalog No.
Anti-mouse IgG, HRP linked	Cell Signaling	7076
Anti-rabbit IgG, HRP linked	Cell Signaling	7074
Donkey anti rabbit IgG-cy3	Dianova	712-166-152
Donkey anti rat IgG-cy3	Dianova	712-166-150

2.1.3 Media for cell culture

Cell	medium	FCS	Antibiotic
MCF7/NeuT	DMEM high glucose	10% tetracycline free	Penicillin Streptomycin
HEK293	DMEM high glucose	10%	Penicillin Streptomycin
HeLa	DMEM high glucose	10%	Penicillin Streptomycin Gentamycin

2.1.4 Inhibitors

Inhibitor	Company	Catalog No.
Anisomycin	Sigma, Steinheim	A9789
Bafilomycin A1	Sigma, Steinheim	B1793
PD 98059	Sigma, Steinheim	P215
Phosphatase inhibitor cocktail 2	Sigma, Steinheim	P5726
Protease Inhibitor Cocktail	Sigma, Steinheim	P8340
SB 203580	Sigma, Steinheim	S8307
Vinblastine sulfate salt	Sigma, Steinheim	V1377

2.1.5 Chemical reagents and kits

Reagent/Kit	Company
Acrylamid (30%)	C. Roth, Karlsruhe
Albumin Fraction V (BSA)	C. Roth, Karlsruhe
Ammonium persulfate (APS)	Sigma, Steinheim
Anode Buffer Concentrate A	C. Roth, Karlsruhe

BCA™ Protein Assay Kit	Thermo Scientific
BrdU	Sigma, Steinheim
Bromophenol blue	C. Roth, Karlsruhe
cDNA Kit	Applied Biosystems
Cathode Buffer Concentrate K	C. Roth, Karlsruhe
DAPI	Invitrogen , Karlsruhe
DEPC Treated water	Invitrogen , Karlsruhe
DMEM, high glucose, culture media	PAN Biotech GMBH
Deoxycycline hyclate	Sigma, Steinheim
DMSO	C. Roth, Karlsruhe
DTT	C. Roth, Karlsruhe
Ethanol	Th.Geyer, Hamburg
Entellan	Merck, Darmstadt
FCS, tetracycline free	PAN Biotech GMBH
Formaldehyde	C. Roth, Karlsruhe
Glycerol	C. Roth, Karlsruhe
Glycine	C. Roth, Karlsruhe
Hydrochloric acid	C. Roth, Karlsruhe
Isopropanol	C. Roth, Karlsruhe
Methanol	Th.Geyer, Hamburg
Magic market	Invitrogen , Karlsruhe
Penicillin/Streptomycin	PAN Biotech GMBH
Rapamycin	Sigma, Steinheim
SDS-Pellets	C. Roth, Karlsruhe
Sera Plus fetal calf serum	PAN Biotech GmbH
Sodium hydroxide	C. Roth, Karlsruhe
Sodium chloride	C. Roth, Karlsruhe
Trichlorite acetic acid	Sigma, Steinheim
Tris	C. Roth, Karlsruhe
Triton X-100	C. Roth, Karlsruhe

RNase free water	QIAGEN GmbH
Sera plus	PAN Biotech GmbH
TaqMan master mix	Applied Biosystems
Tween®20	Sigma, Steinheim
Western Lightning® Plus-ECL.	Perkin-Elmer
Enhanced Chemiluminescence Substrate	
2-Propanol	Roth

2.1.6 Buffer and Solution

Anode buffer	Buffer concentrate A	20 ml
	Methanol	40 ml
	Water	140 ml
Cathode buffer	Buffer concentrate K	20 ml
	Methanol	40 ml
	Water	140 ml
Loading buffer (5 x)	Bromphenol blue	5 mg
	DTT 1 M	2.5 ml
	Glycerol	5 ml
	SDS 10 %	0.5g
	Tris-HCl 1 M	2.25 ml
Ponseau S	Ponseau S	1 g
	3 % trichloride acetic acid	500 ml
RIPA buffer	50 mM tris-Cl (pH 7.5)	50mM
	NaCl	150 mM
	NP-40	1%
	Sodium deoxycholate	0.5%
	SDS	0.1%

Running buffer (10 x)	Glycine	144.0 g
	SDS	10.0 g
	Tris base	30.3 g
Separation buffer (3 M Tris-HCl)	Tris in 100 ml water	36.34 g
	pH set to 8.8	
Stacking buffer: (0.47 M Tris-HCl)	Tris in 100 ml water	5.69 g
	pH set to 6.7	
Stripping buffer	Glycine	15 g
	SDS	1 g
	Tween 20	10 ml
	pH set to 2.2	
	bring up to 1 L with dis. water	
TBS-T	TBS	250 ml
	Tween-20	2.5 ml
	Water	250 ml
	H ₂ O replenished to 2.5L	
5 % BSA solution	TBS-T	100 ml
	BSA	5 mg
10% APS	Ammonium persulphate	0.5 g in 5ml water
10 % SDS	SDS	0.5 g in 5 ml water

2.1.7 Technical equipment

Equipment	Description, Company
Autoclave	5075 ELV, Tuttenauer
Balance	EW, Kern
Benches	HERA-Safe, Heraeus

Centrifuge	Rotina 35R, Heraeus
Centrifuge with cooling function	Biofuge fresco, Heraeus
Electrophoresis chamber	Biometra
Hood	Heraeus
Ice machine	AF 100, Scotsman
Incubators	Binder
Magnetic stirrer	IKAMAG RCT, IKA
Microscope	Eclipse TS 100, Nikon
Minishaker	MS 2, IKA
pH meter	Schott
Power Supplies	Standard Power Pack 25, Biometra Power Pack 300, BIO RAD
Precision balance	EW 150-3M, Kern
Shaker	KS 260 basic, IKA
Spectrometer	Thermoscientific
TaqMan 7500 Real-Time PCR	Applied Biosystems
Thermocycler	TGRADIENT, Biometra
Thermoshaker	HTM 130, HLC PHMT Grant-bio, Keison
Transfer chamber	Fastblot B33 / B34, Biometra
UV/Vis Spectrometer	V-530, Jasco
Waterbath	Labortechnik
Western blot Chamber	Biometra, Bio red

2.1.8 Consumables

75cm ² Cell Culture Flasks	GreinerBio
24-well Culture Plates	Corning
Cell Scrapers	Sarstedt
PVDF-Membrane Transfer Paper	Perkin-Elmer
Whatman® Paper 3MM	Schleicher & Schuell

2.2 Methods

2.2.1 Cell Culture

The MCF7/NeuT cell line was routinely cultured in high glucose Dulbecco's Modified Eagle's Medium (DMEM) containing 1% Penicillin/Streptomycin and 10% tetracycline-free fetal bovine serum. Cells were incubated at constant humidity in 37°C and 5% CO₂. MCF7/NeuT cells were seeded onto the suitable culture dishes for each experiment and kept in the incubator to attach for a minimum of 24 hours before changing the media and adding doxycycline. Cells were treated with a non-cytotoxic concentration of dox (1 µg/mL). The media was changed every 48 hours whereby dox was freshly added to the cell culture medium.

Cells were passaged before reaching confluency. For this purpose cells were washed twice with sterile 1x PBS and trypsin/EDTA mixture was added for detachment of the cells from culture flask. The cells were incubated for 5-10 minutes in trypsin/EDTA at 37 °C and the reaction was stopped by adding normal culturing medium. Next, cells were centrifuged for 5 minutes at 600 x g to remove the trypsin. After discarding the supernatant, the cells were resuspended in pre-warmed culturing medium and after counting the cells a certain volume with the desired cell number was seeded into new flasks.

2.2.2 Gene expression

The mRNA abundance of particular genes in cells and tissues can be analyzed by different types of PCR. For this purpose, the first step is to isolate RNA from the cells and to synthesize cDNA. cDNA is more stable than RNA and is suitable as a template for PCR (e.g. Real time-PCR).

2.2.2.1 Isolation of RNA

RNA isolation is a technique used to purify RNA from biologic samples. In this thesis the AnalytikJena innuPREP[®] RNA Mini Kit was applied for RNA isolation and the procedure was followed the manufacturer's protocol. Basically, after cell lysis, ribonucleases (RNAses) are rapidly denaturated to prevent degradation of the RNA. Subsequently, the RNA is bound to an affinity chromatographical column to separate it from proteins and other cell compounds. Finally the RNA is eluted from the column at high salt concentrations.

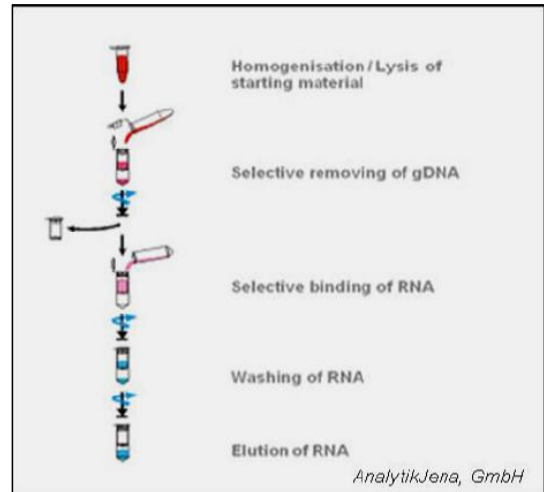


Figure 11: InnuPREP RNA Mini Kit flow chart for total RNA isolation in MCF7/NeuT.

MCF7/NeuT cells were cultured in 6 well culture plates at the specified time points needed. In order to extract total RNA, first culture media was removed from the plate and cells were washed twice with 1x PBS. Cells were then trypsinised and resuspended in media to stop the trypsinisation. The suspension was then centrifuged at 400 x g for 5 minutes and supernatant was discarded. 400 μ L of RL lysis buffer (AnalytikJena) was added to the pellet and gently mixed. The tube was then incubated for 2 minutes at room temperature and resuspended the cell pellet completely by pipetting up and down. To insure complete disruption, cells were briefly vortex before continuing on to the RNA isolation steps. Next the supernatant was placed into Spin Filter D in to a 2.0 ml receiver tube and centrifuged at 10,000 x rpm for 2 minutes in order to separate protein and genomic DNA from RNA. Care should be taken that all of the supernatant passed through the filter into the collection tube. An equal volume of 70% ethanol (approx. 400 μ L) was gently mixed into the filtrate by pipetting up and down. The mixed filtrate was then transferred to Spin Filter R and centrifuged at 10,000 x rpm for 2 minutes to bind the total RNA to the silicon filter. Filtrate was discarded. 500 μ L of washing buffer HS

was added to the spin column of Spin Filter R and centrifuged at 10,000 x rpm for 1 minutes and filtrate was discarded. Then 700 μ L of washing buffer LS was added to Spin Filter R and centrifuged for 1 minute at 10,000 x rpm and filtrate was discarded. To remove any residual ethanol from the filter, the spin filter R was centrifuged for an additional 5 minutes at 10,000 x rpm. Spin Filter R was then placed into a micro-centrifuge tube and 20 μ L of RNase-free water was added to the spin column. To elute the total RNA, the spin column was incubated for 1 minute and centrifuged at 10,000 x rpm for 2 minutes. Spin Filter R was then discarded and the total RNA sample was stored at - 80°C until needed for further experiments.

2.2.2.2 Quantitative RNA Yield

The RNA content in the samples is quantified using the Thermo Scientific NanoDrop™ 1000 Spectrophotometer. It measures the RNA concentration with high accuracy. The principle of a measurement with the NanoDrop is depicted in Fig-12. Briefly, 1.5 μ l of a sample is pipetted onto the end of a fiber optic cable (the receiving fiber). A second fiber optic cable (the sampling arm) is then brought into contact with the liquid sample. A pulsed xenon flash lamp provides the light source. A spectrometer is used to analyze the light after passing through the sample. The instrument is controlled by PC based software. When the measurement is complete, the sampling arm is opened and the sample wiped from both the upper and lower pedestals using a soft laboratory wipe.

The first step is to initialize the machine with 1.5 μ L of RNase free water. Afterwards, a blank measurement is made, also with the 1.5 μ L of RNase free water. Then the samples can be measured. To quantify the purity of the

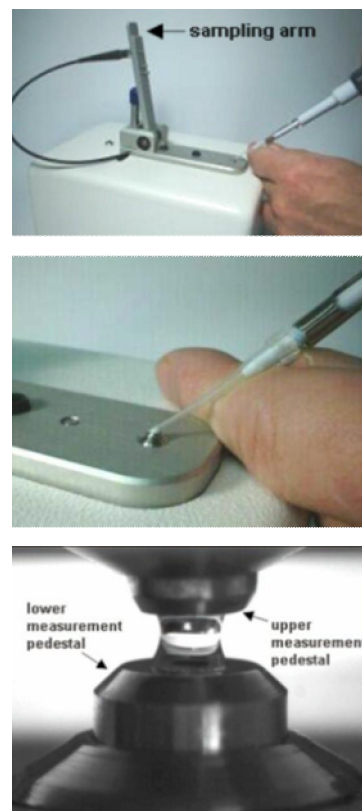


Figure 12: Nanodrop measurement (source: NanoDrop 1000 Spectrophotometer User's Manual)

RNA samples, the program gives three values. The first one is the concentration of RNA in ng/μl based on absorbance at 260 nm. The second one is 260/280, the ratio of sample absorbance at 260 and 280 nm. This ratio is used to assess the purity of DNA and RNA. A ratio of ~1.8 is generally accepted as “pure” for DNA, a ratio of ~2.0 is generally accepted as “pure” for RNA. If the ratio is appreciably lower in either case, it may indicate the presence of protein, phenol or other contaminants that absorb strongly at or near 280 nm. The third given value is 260/230; the ratio of sample absorbance at 260 and 230 nm. This is a secondary measure of nucleic acid purity. The 260/230 values for “pure” nucleic acid are often higher than the respective 260/280 values. They are commonly in the range of 1.8-2.2. If the ratio is appreciably lower, this may indicate the presence of co-purified contaminants.

2.2.2.3 cDNA synthesis

The reverse transcriptase reaction is used to make cDNA out of RNA. mRNA is copied to cDNA by the enzyme reverse transcriptase (RT). RT adds complementary nucleotide bases to the mRNA strand creating a strand of cDNA, as shown in figure in below. The transcription begins at an oligo-dT primer, a short DNA sequence made of dT that binds to the poly-A at the 3' end of all mRNAs. Afterwards the enzyme digests and displaces the mRNA and synthesizes the second cDNA strand.

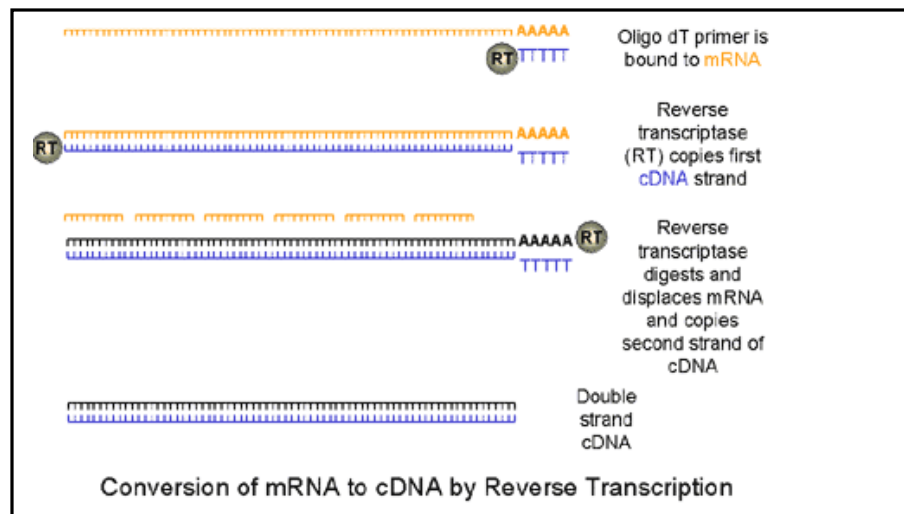


Figure 13: principle of cDNA synthesis (Source: Hunt, M., Real Time PCR)

Here, the cDNA synthesis was implemented with the High Capacity cDNA Reverse Transcription Kit from Applied Biosystems. For the reaction 500 ng of RNA are needed. From the measured concentration given by the NanoDrop in ng/ μ l it can be calculated how much volume of the cellular RNA extraction must be used. The 500 ng should be in 10 μ l, so water is added if less than 10 μ l sample are needed. The needed amount of sample and water is given into a reaction tube. Then 10 μ l of master mix was prepared for per sample containing buffer, free nucleotides as a substrate for DNA synthesis, a primer as starting point for synthesis and the reverse transcriptase. All components were mixed well and 10 μ l of this master mix were then added to every reaction tube containing 500ng of RNA to make a final volume of 20 μ l.

The reaction mixture for cDNA synthesis contained the following:

Table 1: Composition of the reaction mixture for cDNA synthesis

Compound	Volume (μl)
Master mix	
10x RT-Buffer	2
25x dNTP	0.8
Random primer	2
Reverse transcriptase	1
H ₂ O	4.2
Total volume 1	10 μl
RNA	500 ng
H ₂ O	Up to 10 ul
Total volume 2	10 μl
Final total volume	20 μl

The thermo cycler was programmed as following:

Table 2: Program for the thermo cycler for cDNA synthesis

Step	Temperature	Time
Incubation	25°C	10 min
Reverse transcription	37°C	120 min
Inactivation	85°C	5 min
	4°C	hold

Completed cDNA sample was diluted with DEPC water and stored at -20°C for long-term or at 4°C for short-term.

2.2.2.4 Quantitative reverse transcription polymerase chain reaction (qRT-PCR)

Real Time quantitative Reverse Transcription PCR (qRT-PCR) is a quantitative technique which is used to detect and simultaneously quantify the expression level of a target gene. This technique is based on the introduction of an oligonucleotide probe, called a TaqMan probe, that is constructed containing a high energy dye termed Reporter on the 5' end and a low energy molecule termed Quencher on the 3' end. While the probe is intact, the proximity of the quencher dye greatly reduces the fluorescence emitted by the reporter dye by fluorescence resonance energy transfer (FRET) through space. With the beginning of the extension phase of PCR, the polymerase enzyme starts to cleave the TaqMan probe and the distance between the

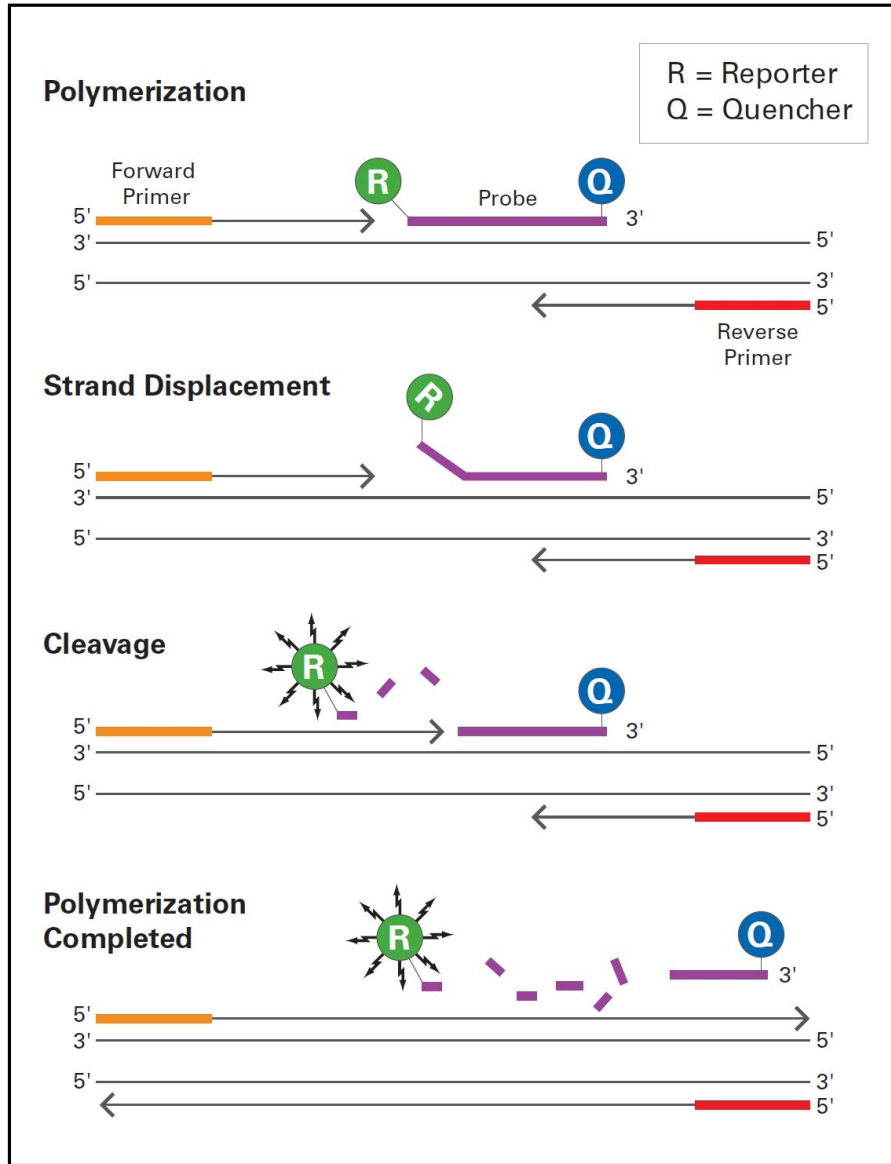


Figure 14: Real time PCR (Source: www.appliedbiosystems.com)

Reporter and the Quencher increases causing the transfer of energy to stop which results in a release of reporter dye. An automated sequence detector, equipped with specific software, is used to monitor the increasing amount of reporter fluorescent dye. During the PCR cycles, Cycle threshold (Ct) values are registered. The Threshold line is the level of detection or the point at which a reaction reaches a fluorescent intensity above background. The threshold line is set in the exponential phase of the amplification for the most accurate reading.

Here in this work, the Real time PCR assays were performed on an ABI 7500 (Applied Biosystem) using 96-well plates. The pre-reaction mixture for one sample was pipetted according to the following table:

Table 3: Composition of the TaqMan mastermix for gene expression analysis

Component	Volume (µl)
TaqMan™ Probe	1
Universal PCR Master Mix	10
H ₂ O	6.5
Final volume	17.5

The solution was vortex and 17.5 µl of reaction mixture were transferred into each well of the TaqMan™ plate. Afterwards 2.5 µl cDNA of the sample were added and mixed with the pre-reaction mixture. The plate was sealed using sealing foils and centrifuged at 400 x g for 1 minute to remove any bubbles and pull down any liquid. Plates were then analyzed in the ABI 7500 Real time PCR System.

The standard amplification conditions are specified in the following table:

Table 4: Thermal cycling conditions for TaqMan analysis of gene expression

Step	Temperature (°C)	Time
1. Heating up	50	2 min
2. Enzyme activation	95	10 min
3. Denaturation	95	15 sec
4. Annealing + Elongation	60	1 min
5. Repetition of steps 3 and 4, 40 times		

For quantifying the gene expression levels of a target gene, several quantification methods are available:

- standard curve method
- relative quantification method
- comparative threshold method (= $\Delta\Delta\text{Ct}$ method)

In this thesis, the $\Delta\Delta\text{Ct}$ method was applied for data analysis. This approach is a relative method, exhibiting a correlation between the gene expression stimulated under certain conditions and the non stimulated control cells, but not giving absolute values. In addition, the expression level of a particular target gene is normalized to the expression level of a house keeping gene, which is also measured in parallel. Furthermore, also the gene expression of control (= untreated) cells has to be analyzed.

The data is analyzed according to the following calculation steps:

1. $\Delta\text{Ct1} = \text{Ct}_{\text{target gene}} - \text{Ct}_{\text{house keeper}}$
2. $\Delta\text{Ct2} = \text{Ct}_{\text{target gene control samples}} - \text{Ct}_{\text{house keeper control samples}}$
3. $\Delta\text{Ct} = \Delta\text{Ct1} - \Delta\text{Ct2}$
4. Calculation of $2^{-\Delta\Delta\text{Ct}}$

Finally, the $2^{-\Delta\Delta\text{Ct}}$ is diagrammed in a histogram, showing the fluorescence intensity or degree of gene expression for every experimental condition.

2.2.3 Protein analysis

Protein extracts can be effectively obtained from cultured cells and tissues. In order to detect a particular protein in a complex sample such as cell and tissue lysates the protein samples must be first separated by gel electrophoresis (SDS-PAGE) and transferred to a membrane by westernblot. Detection takes place by using an antibody that specifically recognizes the target protein. To ensure an equal loading of the samples to analyze by SDS-PAGE and immunoblotting, the protein concentration on the extracts is determined by the BCA Protein assay.

2.2.3.1 Total protein extraction

Here in this thesis, the common cell lysis reagent radio immunoprecipitation assay (RIPA) buffer was applied to extract proteins from cell lysates. Cells were grown to 80% confluency in culture flask. Prior to extraction, 1 μ L of Protease Inhibitor (Invitrogen) and 1 μ L of Phosphatase Inhibitor (Invitrogen) were added for 1 mL of RIPA buffer and mixed gently. RIPA buffer combines ionic and non-ionic detergents like SDS and NP-40 to break up the cell membrane and release soluble components. Protease and phosphatase inhibitor cocktails were added to stabilize the released proteins and prevent them from degradation. On ice, RIPA lysis buffer was added directly onto the cells and left to incubate for a few minutes. Using a cell scraper, cells were scraped from the culture flask and pipetted into micro-centrifuge tubes. Lysate was then left on ice for 30 minutes and hardly vortex every 10 minutes for 3 times. Following incubation, cell lysates were centrifuged at 13,000 x rpm for 15 minutes at 4°C. The supernatant containing total protein was then collected and transferred to a new microcentrifuge tube. Total protein lysates were then stored at -80°C.

2.2.3.2 Protein quantification assay

The BCA assay is a bioanalytical technique based on bicinchoninic acid for colorimetric detection and quantification of total protein. It is the most popular method and basically consists of two reaction steps:

First, the so called Biuret reaction takes place: In an alkaline environment, protein amino acid side chains chelate copper and reduce the Cu^{2+} ions to Cu^+ . In this step a light blue complex is formed.

The second step involved in the assay is the highly sensitive and selective colorimetric detection of the resulting cuprous cation (Cu^{1+}) using a unique reagent containing bicinchoninic acid (BCA). This occurs by the chelation of two molecules of BCA with one cuprous ion, resulting in a purple color product. The BCA/copper complex is water-

soluble and exhibits a strong linear absorbance at 562 nm. The amount of Cu^{2+} reduced is proportional to the amount of protein existing in the solution. The purple color can be measured at any wavelength between 550 nm and 570 nm with minimal (less than 10%) loss of signal.

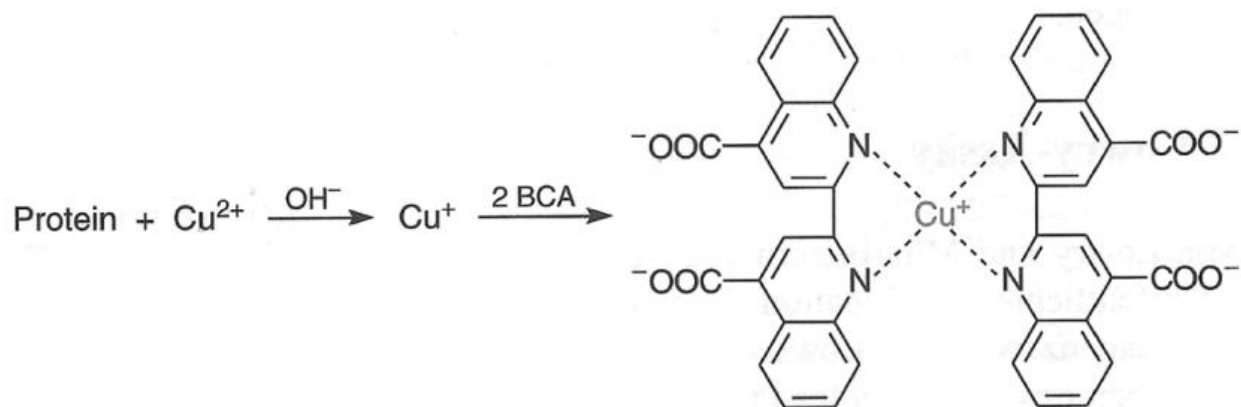


Figure 15: Principle of the BCA assay for protein quantification (Lottspeich and Zorbas, 1998)

Protein quantification of all protein samples was determined by using the BCA™ Protein Assay Kit (ThermoScientific). The samples were defrosted on ice and then diluted in water using 5 μl of sample and 795 μl of water. The working reagent comprises BCA Reagent A which contains the bicinchoninic acid and BCA Reagent B, which contains 4% cupric sulfate. For the working reagent 50 parts of BCA Reagent A were mixed with 1 part of BCA Reagent B. 200 μl of this reagent was added to each sample. In the next step the samples were incubated on a shaker at 60°C for 30 min and then incubated at room temperature for another 10 min. Afterwards each sample was transferred to a cuvette which is placed in a UV/VIS spectrophotometer (V-530, Jasco). The computer software “Spectra manager” was used to quantify the samples. Each sample was measured three times at 562nm and an average of the concentration was given by the program. This value was multiplied with 0.16 to get the concentration in the undiluted sample. For a western blot 30 μg to 50 μg of protein were routinely required.

2.2.3.3 SDS electrophoresis and western blot

The western blot is a technique for the detection of specific proteins. Thereby SDS polyacrylamide gel electrophoresis (SDS PAGE) is used to separate denatured proteins according to their molecular weight. Afterwards the proteins are transferred (blotted) to a PVDF-membrane for detecting a particular protein of interest.

2.2.3.3.1 Gel preparation

Gels were prepared using the Bio-Rad Mini-PROTEAN® Tetra Electrophoresis System (Bio-Rad), illustrated in Fig.16.

The gel was prepared with a gel cassette assembly. It contains a spacer plate, a plate with permanently bonded gel

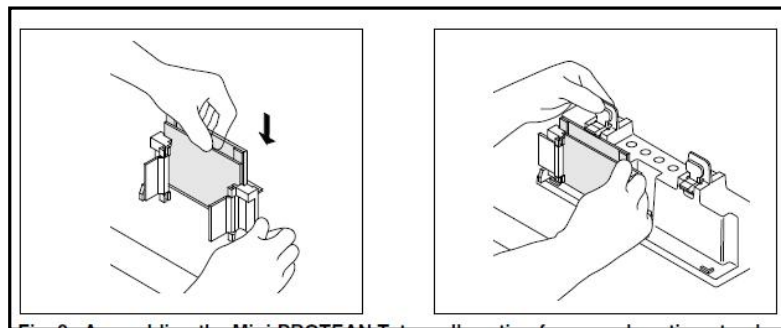


Figure 16: Mini-PROTEAN Tetra cell casting frame and casting stand (source: Mini-PROTEAN Tetra Cell Instruction Manual from Bio-Rad)

spacers and a short plate that combines with the spacer plate to form a gel cassette sandwich. They were held together by the casting frame. During gel casting this gel cassette assembly was secured by the casting stand. All glass plates were cleaned with 70% ethanol, dried and then placed into the casting frames. Gray seals were placed onto the bottom of the casting apparatus to insure no leakage.

The gel contains actually two sequential gels. The top gel is called stacking gel. It is slightly acidic (pH 6.8) and has a low acrylamide content to form a porous gel. The proteins separate poorly but form sharply defined bands. The lower gel is called separating gel. It is more basic (pH 8.8) and has a higher polyacrylamide concentration what causes the gel to have narrower pores. As a result, the proteins get concentrated into sharp bands by the stacking gel and then travel through the separating gel. There the narrower pores have a sieving effect and smaller proteins travel more easily than bigger ones. The following table shows the components of the gels.

Table 5: Components of the western blot SDS-gels (10% gel)

	Separation gel	Stacking gel
H ₂ O	3.2 ml	2.4 ml
Acrylamide	2.64 ml	0.5 ml
Separation buffer	2 ml	
Stacking buffer		0.4ml
10 % SDS	80 µl	32.5 µl
TEMED	3.2 µl	2.5 µl
10 % APS	80 µl	50 µl

Polyacrylamide gels are formed from the polymerization of two compounds, acrylamide and N,N-methylenebis-acrylamide (Bis, for short). Bis is a cross-linking agent for the gels. The gels are neutral, hydrophilic, three-dimensional networks of long hydrocarbons cross linked by methylene groups. The separation of molecules within a gel is determined by the relative size of the pores formed within the gel. The pore size of a gel is determined by two factors: the total amount of acrylamide present (designated as %T) and the amount of cross-linker (%C). As the percentage of acrylamide increases, the pore size decreases. TEMED accelerates the polymerization of acrylamide and bisacrylamide by catalyzing the formation of free radicals from Ammonium persulfate.

For gel preparation all components of the separation gel listed in Table (above) were first mixed. Since polymerization is begun as soon as the TEMED has been added, without delay the mixture was rapidly swirled and briefly vortexed. The solution was then poured into the gap between the glass plates. The glass plates were not filled completely but sufficient space was left for the stacking gel (the length of the teeth of

the comb plus 1cm). 1 mL of isopropanol was added to the top of the gel to prevent oxygen from diffusing into the gel and inhibiting polymerization. The gel was then left to polymerize for approximately 30 minutes at room temperature. After polymerization was complete, the isopropanol overlay was poured off and the top of the gel was washed several times with deionized water to remove any unpolymerized acrylamide. As much fluid as possible from the top of the gel was drained and any remaining water was removed with the edge of a paper towel.

A stacking gel was prepared according the table, mixed quickly following addition of TEMED and APS and pipetted directly onto the surface of the separation gel. A clean comb was immediately inserted into the stacking gel solution, being careful to avoid trapping air bubbles. More stacking gel solution was added to fill the spaces of the comb completely and left the gel for polymerization for 20 minutes. Polymerized gels were then stored by removing the glass plates from the casting frame, wrapping in paper towels soaked with distilled water and placing them in a plastic bag for storage at 4⁰C for up to one week.

2.2.3.3.2 SDS gel electrophoresis

Protein samples and marker were first thawed on ice. Based on the concentrations calculated from the BCA protein assay, 50 µg of the protein samples were first mixed with a required volume of water to unify the concentrations and then diluted using 5X loading buffer. Samples were vortexed and then heated at 95⁰C for 5 mins to denature the proteins. The addition of the anionic detergent sodium dodecyl sulfate (SDS) in loading buffer causes denaturation of the tertiary structure of the protein and all the proteins become negatively charged by their attachment to the SDS anions. Dithiothreitol (DTT) is usually necessary to reduce disulphide bridges in proteins before they adopt the random-coil configuration. Glycerol is added to the loading buffer to increase the density of the sample to be loaded and hence maintain the sample at the bottom of the well, restricting overflow and uneven gel loading. To enable visualization

of the migration of proteins bromophenol blue is used in the loading buffer. The dye will migrate the fastest of any component in the mixture to be separated and provide a migration front to monitor the separation progress.

The gel was then mounted in the electrophoresis apparatus and the comb was removed carefully. The wells were washed immediately with deionized water to remove any unpolymerized acrylamide by using a squirt bottle and the teeth of the stacking gel were straightened properly. 1X Tris-glycine running buffer was poured in to the inner chamber of the apparatus and checked for leaking. Any air bubbles that became trapped at the bottom of the gel between the glass plates were removed. Approximately 20 μ l of protein sample was loaded into its each well and an equal volume of 1X loading buffer was loaded to empty wells to ensure uniform electrophoresis. To

estimate the molecular weight of the separated proteins, two different protein standard markers were additionally loaded on the gel. One gel pocket was loaded with 5 μ l of Precision plus Protein standard to enable a first estimation by eye, in which part of the membrane the protein is localized. The second marker was the MagicMark™ XP Western Protein Standard, containing a mixture of proteins with repetitive units of a fusion protein forming the size variation and an IgG binding side. This marker only becomes visible by applying an enzyme linked antibody and using chemoluminescent substrate. 2.5 μ l of MagicMark™ XP standards were loaded on the gel. Finally, the loaded gel first run at 20 mA until the dye front moved out of the stacking gel. Then the

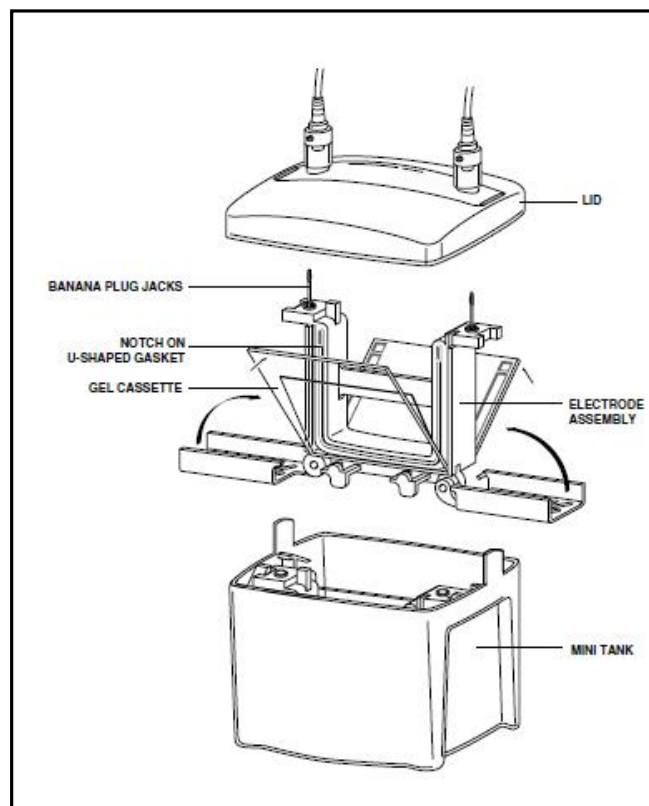


Figure 17: Mini-PROTEAN Tetra cell running chamber (source: Mini-PROTEAN Tetra Cell Instruction Manual from Bio-Rad)

gel run at 30mA and run the gel until the bromophenol blue reached the bottom of the separation gel. The power supply was then turned off and the gel was removed from the electrophoresis apparatus and placed on a paper towel. The two glass plates were opened by using a spatula and the orientation was marked by cutting off the top left corner of the gel. The gel was then placed in cathod buffer until needed for membrane transfer.

2.2.3.3.3 Membrane transfer

The proteins are first separated by SDS-PAGE and then, by applying an electric field, transferred from the gel on a polyvinylidene difluoride (PVDF) matrix or nitrocellulose membrane. In this way, a copy of the protein pattern that was originally in the polyacrylamide gel is obtained. After the transfer, the proteins are immobilized on the membrane by hydrophobic interactions and hydrogen bonds, but their immunoreactive features are preserved. This provides the opportunity to detect and identify single proteins by specific antibody reaction out of complex protein mixtures like cell lysates.

Using a semidry dry blot system from Biometra, the separated proteins were electrophoretically transferred to a PVDF membrane. 16 Whatman papers and a piece of PVDF membrane were cut to the exact size of the SDS PAGE gel and the orientation was marked by cutting the top left corner off. If the paper or the membrane is larger than the gel, there is a risk that the overhanging

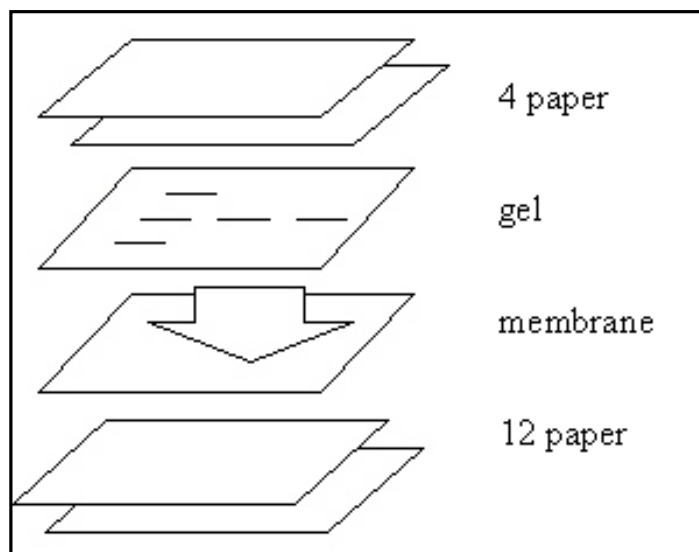


Figure 18: Semi dry membrane transfer

edges of the paper and membrane will touch, causing a short circuit that will prevent the

transfer of protein. Oils and secretions from the skin will also prevent the transfer of the proteins from the gel to membrane.

12 pieces of Whatman papers were placed in anode buffer and 4 pieces were placed in cathode buffer for several minutes before beginning the transfer to allow the papers to equilibrate to the buffer. The membrane was activated in methanol for a few seconds and then also left in anode buffer. The Fastblot® B34 (Biometra) electro-blotting apparatus was used for transferring protein samples onto the membrane. A 'paper sandwich' was then prepared as follows from bottom up: 12 Whatman papers, PVDF membrane, transfer paper, gel and 4 Whatman papers. To ensure that no bubbles were present, a large volume pipette was rolled over the 'paper sandwich'. The power pack was connected and run for approximately 40 minutes at 300 mA per/gel. Current was calculated by multiplying 5 mA into the width and length of the gel. After the transfer was complete the PVDF-membrane was washed with distilled water for 5 minutes. To verify that the proteins were successfully transferred to the membrane, Ponceau S prepared in trichloroacetic acid was used. The membrane was stained for 2 minutes with Ponceau S and then washed with distilled water to visualize the blot. Later it was washed out from the membrane with 1x TBS-T for 5-10 minutes.

2.2.3.3.4 Antibody incubation and membrane detection

The membrane was first blocked in 5% non-fat milk or 5% BSA solution in 1x TBS-T, depending on the antibody of interest, for 1 hour at room temperature. Primary antibodies were prepared in non-fat milk or BSA solution in 1x TBS-T. The final concentration depends on the individual antibody. The membrane was incubated with the primary antibody at 4°C overnight in a cold room on a level shaker. Then the membrane was washed 6 times for 5 minutes each in 1xTBS-T. The secondary antibody was prepared using non-fat milk or BSA solution in 1x TBS-T. The concentrations also varied depending on the antibody. The secondary antibodies used for western blot are labeled with horseradish peroxidase (HRP). After incubation of the

secondary antibody for 1 hour, the membrane was washed again 6 times for 5 minutes each in 1x TBS-T.

Luminol solution (Perkin Elmer) was prepared in a Petri dish using equal volumes of solution A and B (approx. 5 mL total volume). Western Lightning chemistry is based on a Chemiluminescence reaction in which the enzyme horseradish peroxidase (HRP) catalyzes light emission from the oxidation of Luminol. Because the secondary antibodies used for western blot are labeled with HRP the chemiluminescence is only detected in the protein band that has been specifically bound by the antibody complex.

Table 6: parameters for antibodies detection for western blot

Primary Antibody	incubation	Dilution	Secondary Antibody	Incubation	Dilution
α -Tubulin	1hr at RT	1:1000 in 5% BSA	Rabbit	1hr at RT	1:5000 in 5% BSA
β -Actin	30 min at RT	1:5000 in 5% BSA	Mouse	20 min at RT	1:10,000 in 5% BSA
Phospho Akt	overnight	1:1000 in 5% BSA	Rabbit	1hr at RT	1:5000 in 5% BSA
Total Akt	overnight	1:1000 in 5% BSA	Rabbit	1hr at RT	1:5000 in 5% BSA
Phospho c-Raf (S-388)	overnight	1:1000 in 5% BSA	Rabbit	1hr at RT	1:5000 in 5% BSA
Phospho c-Raf (S-259)	overnight	1:1000 in 5% BSA	Rabbit	1hr at RT	1:5000 in 5% BSA
Total c-Raf	overnight	1:1000 in 5% BSA	Rabbit	1hr at RT	1:5000 in 5% BSA
Dynein	overnight	1:500 in 5% BSA	Rabbit	1hr at RT	1:5000 in 5% BSA
Phospho p44/42	overnight	1:1000 in 5% BSA	Rabbit	1hr at RT	1:5000 in 5% BSA
p44/42 MAPK	overnight	1:1000 in 5% BSA	Rabbit	1hr at RT	1:5000 in 5% BSA
Phospho JNK	overnight	1:1000 in 5% BSA	Rabbit	1hr at RT	1:5000 in 5% BSA
Total JNK	overnight	1:1000 in	Rabbit	1hr at RT	1:5000 in

		5% BSA			5% BSA
LC3	overnight	1:1000 in 5% BSA	Rabbit	1hr at RT	1:5000 in 5% BSA
Phospho MAP4	overnight	1:500 in 5% BSA	Rabbit	1hr at RT	1:5000 in 5% BSA
Total MAP4	overnight	1:1000 in 5% BSA	Rabbit	1hr at RT	1:5000 in 5% BSA
Phospho-MEK1/2	overnight	1:1000 in 5% BSA	Rabbit	1hr at RT	1:5000 in 5% BSA
Total MEK 1/2	overnight	1:1000 in 5% BSA	Rabbit	1hr at RT	1:5000 in 5% BSA
Phospho MSK1	overnight	1:1000 in 5% BSA	Rabbit	1hr at RT	1:5000 in 5% BSA
Neu	overnight	1:2000 in 5% BSA	Rabbit	1hr at RT	1:5000 in 5% BSA
Phospho p38	overnight	1:1000 in 5% BSA	Rabbit	1hr at RT	1:5000 in 5% BSA
Total p38	overnight	1:1000 in 5% BSA	Rabbit	1hr at RT	1:5000 in 5% BSA
PARP	overnight	1:1000 in 5% BSA	Rabbit	1hr at RT	1:5000 in 5% BSA
Phospho Stathmin	overnight	1:1000 in 5% BSA	Rabbit	1hr at RT	1:5000 in 5% BSA
Total Stathmin	overnight	1:1000 in 5% BSA	Rabbit	1hr at RT	1:5000 in 5% BSA
SQSTM1/p62	overnight	1:1000 in 5% BSA	Rabbit	1hr at RT	1:5000 in 5% BSA

Addition of the Western Lightning ECL to the membrane leads to oxidative degradation of Luminal resulting in light emission at a wavelength of 428 nm. This light is captured with an image acquisition system (Fusion Fx7, Vilber Lourmat). The membrane was then placed into the Petri dish and imaged. After imaging of the membrane was completed, the membrane was washed in 1x TBS-T for 5 minutes. Membranes could be stripped of antibodies by incubation in the stripping buffer for approximately 30 minutes followed by a washing step of 5 minutes in 1x TBS-T. To ensure complete removal of antibody, the membrane was subjected a second time to the Luminol solution. If the antibody was completely stripped from the membrane, it was then washed again in 1x TBS-T and stored at 4°C in 1x TBS-T or air dried and stored at -20°C until needed.

2.2.4 Immunofluorescence

Immunofluorescence (IF) is a common laboratory technique allowing the visualization of a specific protein or antigen in cells or tissue sections by binding a specific antibody chemically conjugated with a fluorescent dye. Fluorochromes are dyes that absorb ultra-violet rays and emit visible light. This process is called fluorescence. Immunofluorescence stained samples are examined under a fluorescence microscope or confocal microscope.

The two main methods of immunofluorescent labeling are direct and indirect. In the direct method, the cells are incubated with an antibody directly conjugated to a fluorochrome. The direct method has the advantage of speed (only one incubation) and simplicity but is less sensitive than the indirect method. In the indirect method, cells are incubated with a primary non-conjugated antibody, for example, a monoclonal mouse

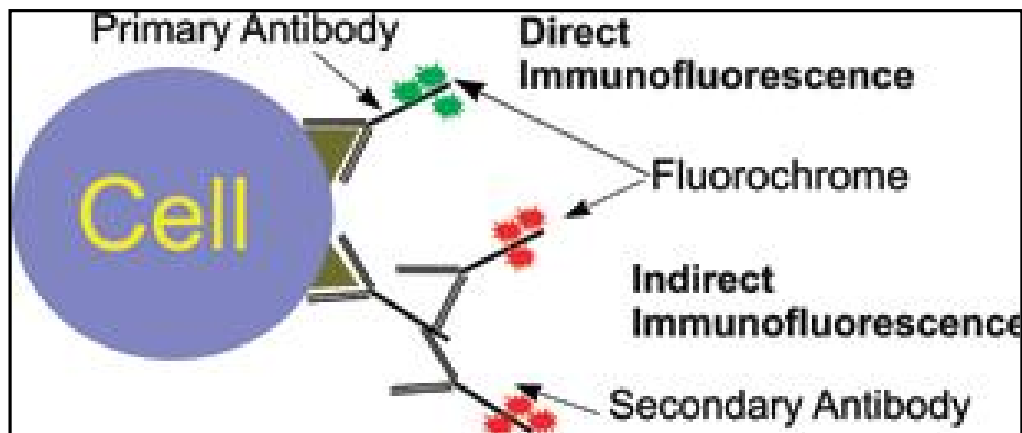


Figure 19: Schematic diagram of direct and indirect immunofluorescence.
(source: www.dako.com)

anti-human antibody. Cells are then stained with a second antibody that recognizes the primary antibody, conjugated to a fluorochrome, for example, an FITC-goat anti-mouse antibody. This protocol is more complex and time consuming than the direct protocol, but it allows more flexibility because a variety of different secondary antibodies and detection techniques can be used for a given primary antibody.

2.2.4.1 Immunofluorescence assay for LC3 and Tubulin staining

MCF7-NeuT Cells were seeded onto glass cover slips which were pre-coated by poly-L-Lysin for overnight inside the 24-well culture plates at a low density. Briefly, cells were washed twice with 1x PBS and fixed with 4% paraformaldehyde for 20 minutes at room temperature. The purpose of fixation is to denature the components of cells enough so that they are preserved without destroying cellular morphology and can be bound by antibodies. After fixation, cells were washed twice with 1x PBS for 5 minutes. Cells were then incubated with 50 mM Ammonium chloride (NH₄Cl) in 1x PBS for 10 minutes to quench the aldehyde groups, thereby diminishing autofluorescence and reduce background staining and again washed with 1x PBS for 5 minutes. For blocking, the cells were incubated with 3% BSA in 1x PBS for 90 min at room temperature. Cells were then washed with 1x PBS for 5 minutes. Incubation with the primary antibody was done over night at 4⁰C in a cold room in 0.3% BSA in PBS, 0.1% Tween 20. The concentration of antibody depended on the specific antibody of interest. Cells were then washed with 1x PBS 3 times for 5 minutes each. The secondary antibody was then diluted in a 0.3% BSA, 0.1% Tween 20 solution in 1x PBS and incubated in dark humid chamber at room temperature. After secondary incubation cells were washed with 1x PBS 3 times for 5 minutes each and a DAPI stain was then performed for 15 min at room temperature (1:20000 in 1x PBS) in dark. The fluorescence dye DAPI binds selectively to double-stranded DNA and forms blue-fluorescent complexes with A-T rich nucleic acid regions. In aqueous solution DAPI has an absorption maximum at a wavelength of 340 nm and an emission maximum at 488 nm. It is absorbed by cells quickly and the nuclei are stained with a high specificity and cytoplasmic fluorescence is not detectable. After the DAPI staining, cells were washed again in 1x PBS 2 times for 5 minutes. The cover slips were dehydrated using the graded ethanol (30%, 50%, 70%, 90% and 100% 30 seconds each) and mounted using a drop of entellan on glass slides. The slides were dried in the dark for overnight and stored in the cold room until further analysis by using a laser scanning confocal microscope (Olympus).

Table 7: parameters for antibodies detection for immunofluorescence

Primary Antibody	incubation	Dilution	Secondary Antibody	Incubation	Dilution
α -Tubulin	overnight	1:200	anti rabbit Cy3	1hr at RT	1:200
LC3	overnight	1:400	anti rabbit Cy3	1hr at RT	1:200
BrdU	1hr at RT	1:500	anti rat Cy3	1hr at RT	1:200

2.2.4.2 Immunofluorescence Assay for BrdU staining

DNA synthesis of senescence cells were measured by the incorporation of 5-bromo-2-deoxyuridine (BrdU, catalog B5002, Sigma-Aldrich) into nuclei. Briefly, following pre-culture for 24 hours in BrdU media (DMEM full medium supplemented with 150 μ g/ml BrdU) the cells were incubated in presence or absence of doxycycline (1 μ g/mL) for 3 days. The cells were washed with 1XPBS, fixed with 4% paraformaldehyde and permeabilized with 0.2%Triton-X100, followed by 10 min incubation with 2N HCl for DNA denaturation. Unspecific binding sites were blocked with 3% bovine serum albumin (BSA) in 1X PBS for 1h at room temperature, subsequently incubated with rat anti-BrdU antibody (catalog MCA2060, Serotec, oxford, UK) for 1 hour at room temperature. Detection was achieved by using a secondary donkey anti rat Cy3 antibody diluted in 0.3% BSA, 0.1% tween 20 in PBS and incubated for 1 hour at room temperature. After each antibody incubation, the slides were washed three times with 1X PBS and a DAPI stain was then performed for 15 min at room temperature (1:20000 in 1x PBS). After the DAPI staining, cells were washed again in 1x PBS 2 times for 5 minutes. The cover slips were dehydrated using the graded ethanol (30%, 50%, 70%, 90% and 100% 30 seconds each) and mounted using a drop of entellan on glass slides. The slides were dried in the dark for overnight and stored in the cold room until further analysis. Proliferation was expressed as percentage of BrdU positive nuclei, determine by counting at least 10 random regions per slide by using fluorescence microscope.

CHAPTER THREE

RESULTS

3.0 Results

3.1 Oncogene ERBB2/HER2 (NeuT) expression leads to premature senescence in MCF-7 cells

3.1.1 Expression of oncogenic ERBB2/NeuT in MCF-7 cells

The MCF-7/NeuT cell line harboring a doxycycline (dox) inducible oncogenic version of ERBB2 (NeuT) was previously generated by Trost et al. (2005) in order to understand the mechanisms involved in oncogene-induced transformation and cellular senescence. Further characterization of this cell line was performed by Spangenberg et al. (2006) and Cadenas et al. (2010, 2012).

As previously described in the methods section, expression of both the oncogene NeuT and the reporter gene EGFP are induced upon exposure of MCF-7/NeuT cells to the tetracycline derivate doxycycline. Expression of NeuT results in premature senescence, characterized by cell-cycle arrest, expression of the senescence-associated beta-galactosidase and morphological alterations. As an initial step in this work it was necessary to ensure that dox-induced expression of NeuT caused senescence in the MCF-7/NeuT cell batches that were used for characterization of the cellular signaling network and the autophagy process.

Therefore, in order to confirm the over expression of NeuT in our cell system, protein expression of NeuT was monitored by immunoblotting. Already after 6h dox treatment NeuT expression was detected and increased further in later time points after addition of doxycycline to the culture media (24h-14d). This confirmed previous data (Trost et al., 2005, Spangenberg et al., 2006, Cadenas et al., 2010, 2012).

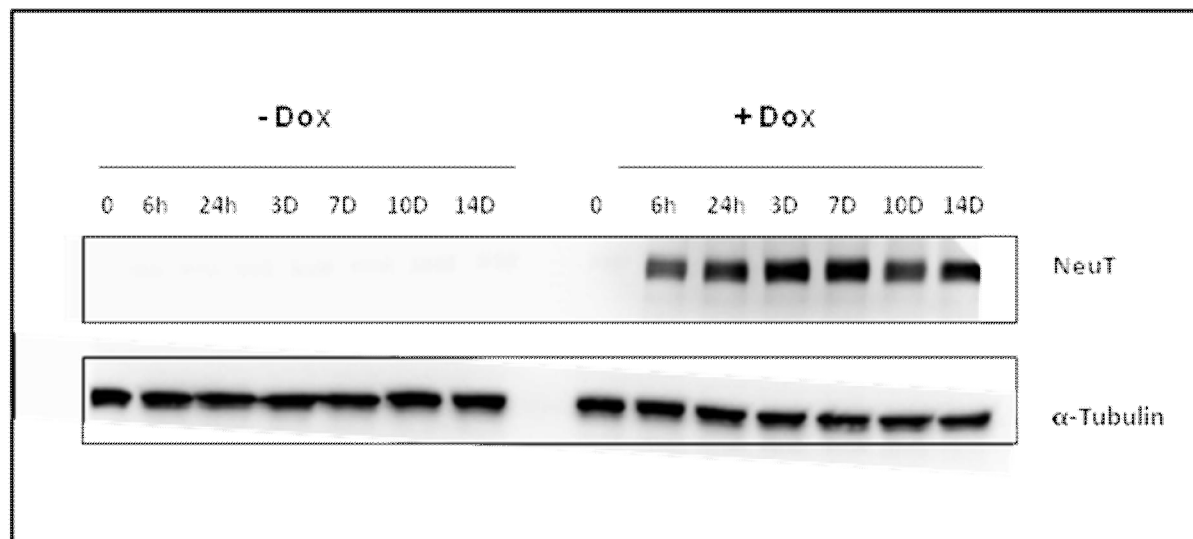


Figure 20: ERBB2 (NeuT) protein expression in MCF7/NeuT cells. Protein extracts of NeuT cells cultured in with or without doxycycline containing media for the indicated time periods were immunoblotted and probed for NeuT expression. α -Tubulin was used as loading control.

3.1.2 Oncogene ERBB2/NeuT induced senescence is accompanied by alterations in cell morphology in MCF7 cells

Upon up-regulation of NeuT expression, the MCF7/NeuT cells begin to display first shape-related alterations, such as cytoplasmic protrusions. Following this stage, prolonged dox treatment (3 days) resulted in senescence-like characteristics such as an enlarged and flattened-type morphology, a centralised nucleolus and the development of vacuole structures within the cytoplasm. These morphological alterations were only observed in EGFP-positive cells. As previously mentioned, EGFP is co-expressed with NeuT and thus serves as an indirect measure for NeuT expression.

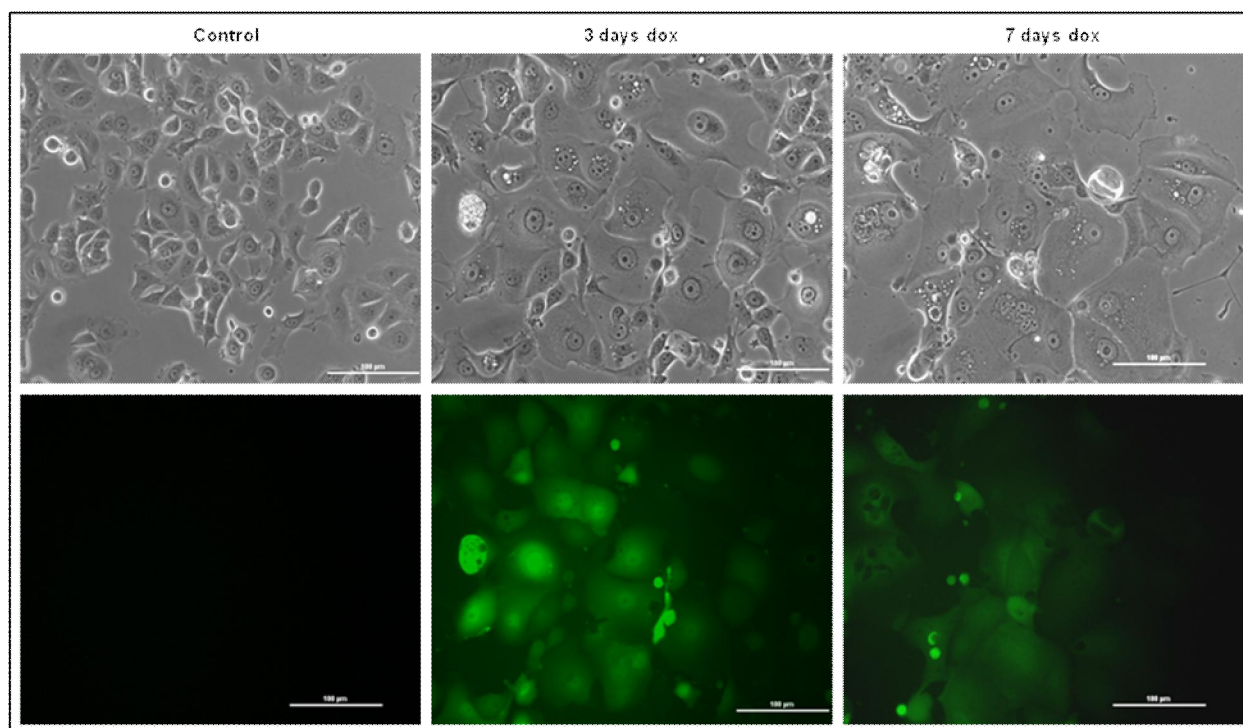


Figure 21: Morphological changes during NeuT oncogene induction. MCF-7/NeuT cells were treated with or without dox at different time points. Cells treated with dox for 3 days displayed an enlarged cytoplasm, increased levels of vacuoles and a centralised nucleolus (upper panels). MCF7/NeuT cells showing these alterations upon dox exposure also expressed the green fluorescent protein, EGFP (bottom pannels). Images are representative for multiple images taken of each condition. Bar, 100 μm .

3.1.3 ERBB2/NeuT over expression induces growth arrest in MCF-7 cells

To further study the effect of oncogenic ERBB2 signaling on proliferation of MCF7 cells, we used the bromodeoxyuridine-incorporation (BrdU) assay. This synthetic analogue is incorporated into DNA instead of thymidine during S phase.

For the BrdU assay, MCF-7/NeuT cells undergoing senescence by addition of dox were incubated with BrdU for 24h. After treatment, the nuclei were stained with an anti-BrdU

antibody to detect incorporated BrdU, in addition to the conventional DAPI staining. In doing so, nuclei that were BrdU positive or negative, i. e. cells that have already undergone DNA replication or have not yet incorporated BrdU, can be easily distinguished because of their different fluorescent colours.

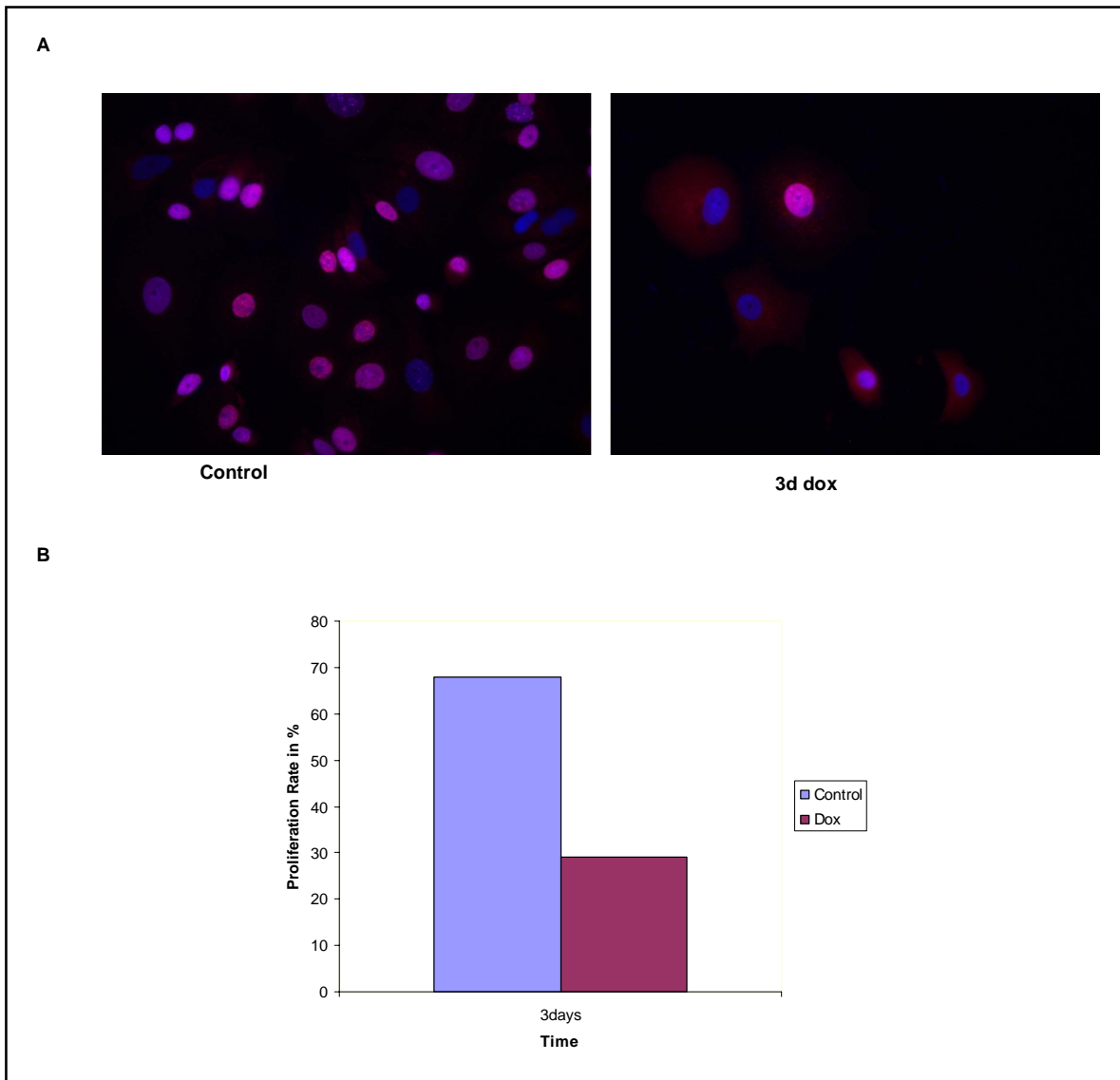


Figure 22: Decreased BrdU-staining in 3 days dox-treated MCF-7/NeuT cells confirms cell cycle arrest upon senescence. A. BrdU-positive (pink) and BrdU-negative (blue) nuclei appear in different fluorescent colours. A representative picture is shown. **B.** Differences in proliferation rate were quantified by calculating the ratio of BrdU-positive cells and total number of cells in 10 random fields per slide.

Quantification of BrdU incorporation was performed by counting all nuclei and the BrdU-positive nuclei, respectively, in randomly chosen fields of the slides using a fluorescent microscope. The proliferation rate was defined as the ratio of BrdU-positive nuclei and total number of nuclei per field denoted in percentage. Our result indicated the decreased cell proliferation upon NeuT induction. This cell cycle arrest was a specific response to oncogene ERBB2/NeuT signaling because no influence on proliferation was seen in the control cells. Therefore, we could confirm the proliferation arrest in MCF-7/NeuT senescent cells.

3.2 ERBB2/NeuT oncogene-induced activation of signaling pathways in senescent cells

NeuT overexpression results in activation of various signaling pathways, including the Ras/Raf/MEK/ERK and the PI3K/AKT pathways (Dissertation Tatjana Trost; Cadenas et al., 2010). p38 becomes also activated at a later time points, whereby it is involved in mediating the senescence transition (Trost et al., 2005). Since the aim of our work was to explore regulation of various cellular events, including senescence and autophagy, by signal transduction pathways, we studied first the time-course activity of three major pathways, the Ras/Raf/MEK/ERK, the AKT/PI3K and the p38 pathway, in the MCF-7/NeuT cells during a 14 days period following doxycycline exposure.

3.2.1 Activation of the Raf/MEK/ERK cascade by the ERBB2/NeuT oncogene

The Ras protein activates multiple downstream pathways, including the Raf-MEK-ERK pathway and induces pleiotropic phenotypes. In many studies overexpression of Ras or Raf protein has been described to elicit growth arrest and premature senescence in several cellular settings (Cox et al., 2006, Zhu et al., 1998). To investigate the activity of

the Raf-MEK-ERK pathway during ERBB2 (NeuT) induced senescence, we monitored the phosphorylation of each of the pathway components by immunoblotting.

We first studied the expression level and activity of the Raf-1/c-Raf protein. The Raf-1/c-Raf (serine/threonine-specific protein kinase) is the first component of this three-tiered protein kinase cascade. Phosphorylation plays a key role in c-Raf activation and both positive and negative regulatory sites have been mapped. Among them, S338 phosphorylation is the key activating site for c-Raf activation (Avruch et al., 2001; Kolch, 2000). Therefore, first we examined phosphorylation of c-Raf protein at different time intervals of dox treatment, using a phospho-specific antibody against S338. Low levels of basal S338 phosphorylation were observed in control cells, but within 6 hours of dox treatment, phosphorylation was elevated and continued to rise over 3 days time period. After reaching the maximum phosphorylation, activation of c-Raf decreased and returned to basal levels after 10 days dox treatment.

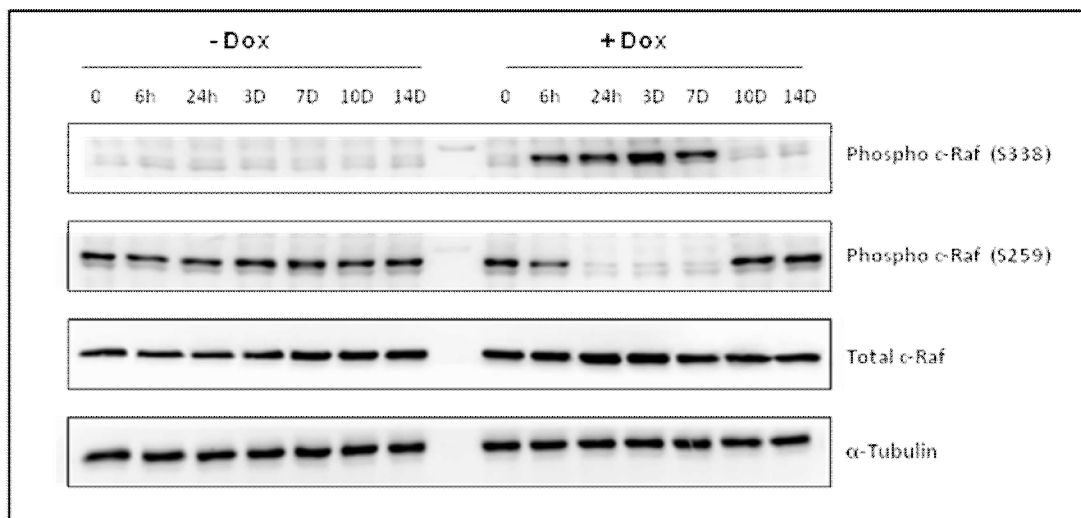


Figure 23: Activation of Raf-1/ c-Raf upon NeuT expression. A representative immunoblot is shown for activation of c-Raf during NeuT-induced senescence. Samples from left to right; non-treated control, treatment of dox in different time intervals. α -Tubulin was used as the loading control.

We next investigated another c-Raf phosphorylation site, S259 (Dhillon et al., 2002). Importantly, the dephosphorylation of S259 is a prerequisite for the activation of c-Raf and S259 dephosphorylated before activating phosphorylation on S338 can occur. In control cells, c-Raf is phosphorylated at the S259 site but already 6h after NeuT induction S259 becomes dephosphorylated concomitant with S338 phosphorylation. In the late senescent stage (10 days after NeuT induction/dox treatment) S259 phosphorylation is restored to initial levels, concomitantly with S338 dephosphorylation.

MEK is the second tier of this cascade and phosphorylation of two serine residues (residues at positions 217 and 221 found in the activation loop) are thought to be important for its synergistic activation by Raf-1/c-Raf (Alessi et al., 1994). MEKs can be partially activated by phosphorylation at either site and substitution of these sites with acidic amino acids enhances basal activity (Mansour et al.1994). To monitor activation of MEK1/2 in senescent cells, cell lysates of different dox treatment time periods were subsequently analyzed for phosphorylation events. Dox treatment induced early MEK12 activation, which peaked to a maximum after 3 days and gradually declined to nearly basal levels during further dox incubation.

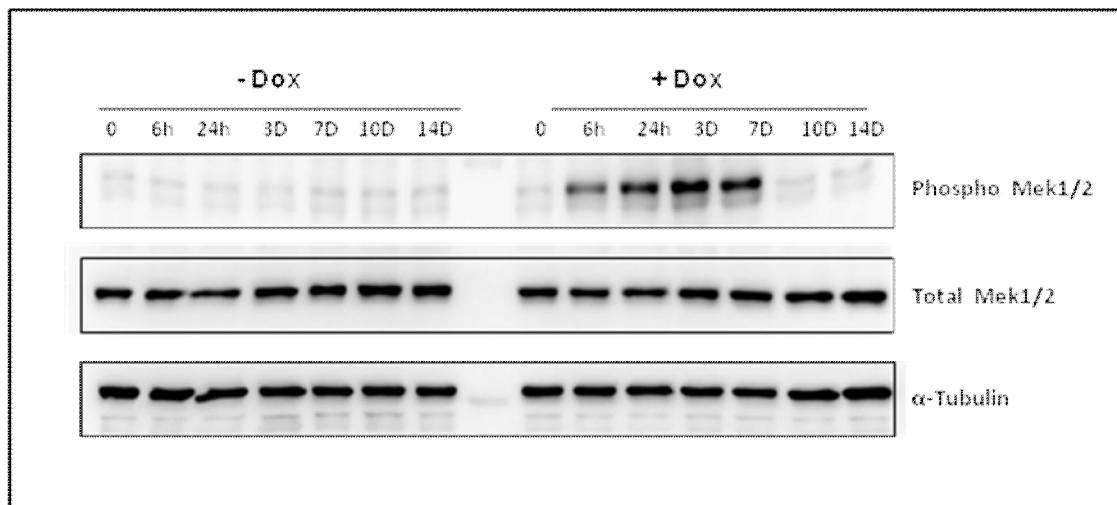


Figure 24: Phosphorylation of MEK1/2 in MCF-7/NeuT cells. Lysates obtained from different time points of dox treatment were subjected to immunoblot analysis using anti-MEK and anti-phosphorylated MEK antibodies. α -Tubulin was used as the loading control.

ERK1 and ERK2 are 44 and 42 kDa serine/threonine kinases, respectively and dual threonine and tyrosine residue phosphorylations activate both ERKs, at Thr202/Tyr204 for human ERK1 and Thr185/Tyr187 for human ERK2. Unlike MEK, significant ERK activation requires phosphorylation at both sites, with tyrosine residue phosphorylation preceding that of threonine (Ferrell, J. and R. Bhatt, 1997). Because ERK is the only downstream-substrate of MEK, it was expected that dox stimulation would quickly induce ERK activation with similar kinetics to that of MEK phosphorylation. As expected, we could show that phosphorylation of ERK appeared 6h after NeuT induction, peaked after 3 days dox-treatment and returned to nearly basal levels after 10 days of incubation.

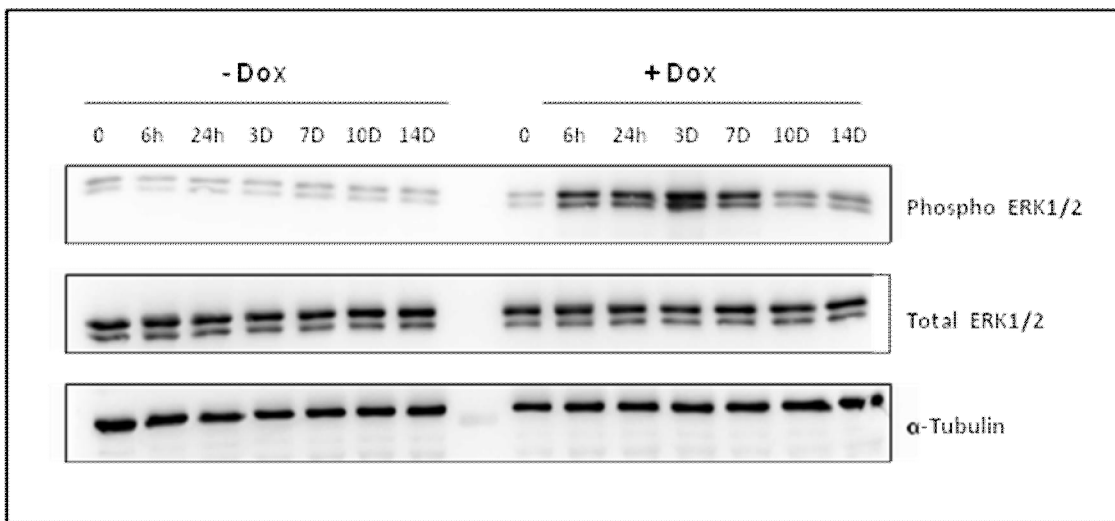


Figure 25: Activation of ERK1/2 during NeuT oncogene-induced senescence. Cells were subjected to immunoblot analysis for studying activation of ERK1/2 in presence or absence of dox at different time periods. α -Tubulin was used as the loading control.

3.2.2 Activation of the PI3K/AKT pathway during NeuT induced senescence

It has been shown that AKT becomes activated during oncogene-induced senescence but its specific contribution remains controversial. Previous studies do not present a clear picture regarding the ability of activated AKT to induce senescence. Some reports

have indicated that activation of the AKT pathway does induce senescence (Chen et al., 2005; Majumder et al., 2008; Miyauchi et al., 2004; Nogueira et al., 2008; Oyama et al., 2007). Other reports have concluded that AKT activity is a weak inducer of senescence (Lin et al., 1998) or is down regulated in senescence (Courtois-Cox et al., 2006; Young et al., 2009) and can antagonize senescence (Courtois-Cox et al., 2006; Kortlever et al., 2006; Tresini et al., 1998). In order to investigate the activity of the PI3K/AKT signaling pathway in our NeuT cell system, the phosphorylation status of AKT was determined by western blot analysis using corresponding phospho-specific antibodies, which are designed to recognize only the activated form of AKT. Our result showed that soon after the onset of Dox exposure AKT phosphorylation increased which peaked at 24hrs and returned to basal levels at the later senescence phase.

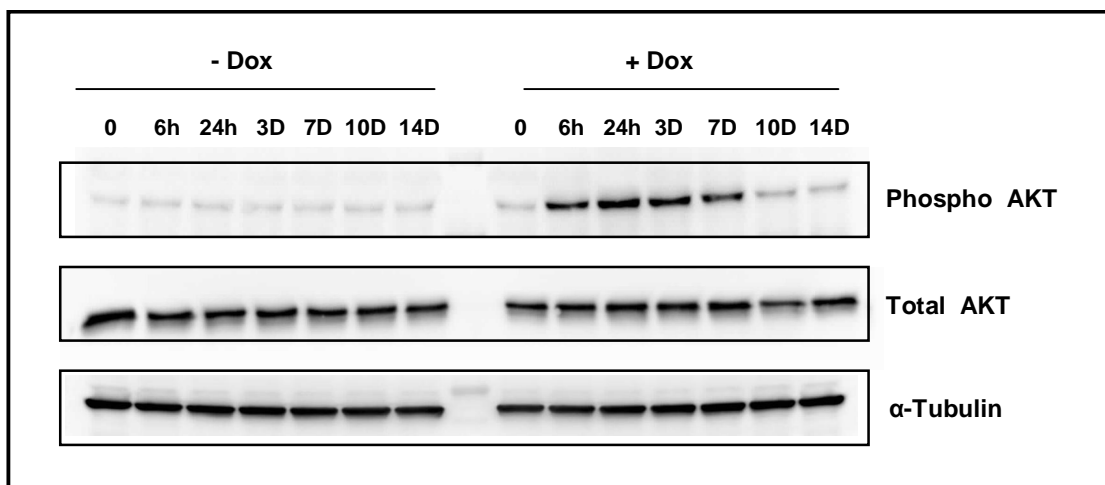


Figure 26: Activation of the AKT pathway in MCF-7/NeuT cells. AKT phosphorylation was induced early after onset of NeuT expression and decreased in late senescence. Samples from left to right: non-treated control, treatment of dox in different time intervals. α -Tubulin was used as the loading control.

A key regulator of protein metabolism, the mammalian target of rapamycin (mTOR), is a serine/threonine protein kinase. mTOR forms two distinct signaling complexes: mTOR complex 1 (mTORC1) and mTORC2. mTOR is a downstream effectors of the AKT/PI3K pathway. To examine the activity of mTOR during senescence, we assessed the

phosphorylation status of mTOR. The level of p-mTOR, showed a similar pattern to p-AKT, initially up-regulated in response to the mitotic signal, while it decreased during the senescence phase.

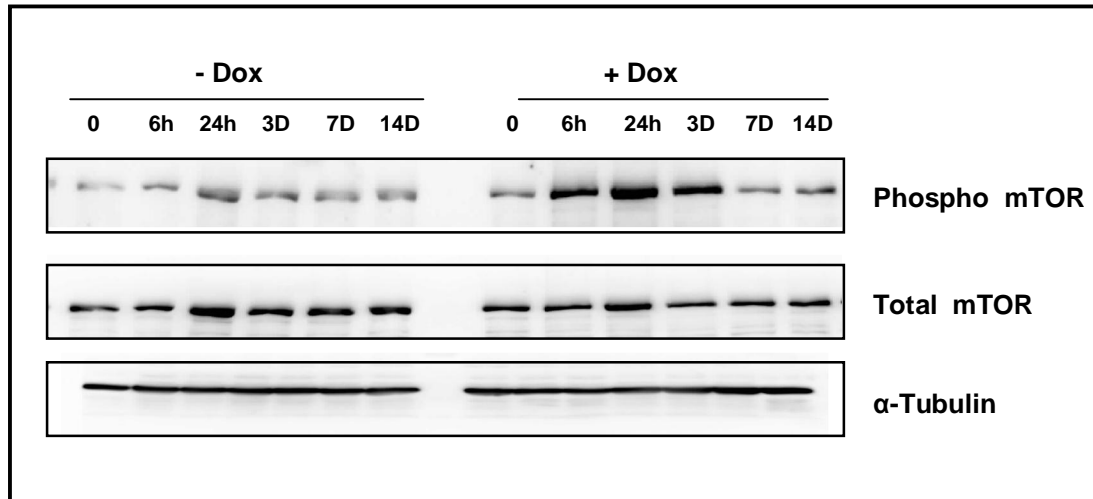


Figure 27: Phosphorylation of mTOR in MCF-7/NeuT cells. Cells were subjected to immunoblot analysis for analysing activation of mTOR in presence or absence of dox at different time periods. α -Tubulin was used as the loading control.

3.2.3 p38 is activated during NeuT induced premature senescence

Several studies, including those previously performed with our MCF-7/NeuT cell line (Troost et al., 2005) have shown that the stress-activated protein kinase p38 mediates senescence. To confirm activation of the p38 pathway and to further explore its role in oncogenic ERBB2-induced senescence, we examined MCF7/NeuT cells undergoing premature senescence at different time points of doxycycline treatment. The phosphorylation of the p38 on Thr180 and Tyr182 is known to lead to the activation of the p38 signaling pathway (Deng et al., 2004). Consistent with prior reports (Troost et al., 2005), phosphorylation of p38 on Thr180 and Tyr182 was observed in western blot analysis using an antibody that specifically recognizes p38 phosphorylation on these

sites. Phosphorylated p38 was clearly observed 3 days after NeuT induction and was sustained throughout senescence (up to 14 days).

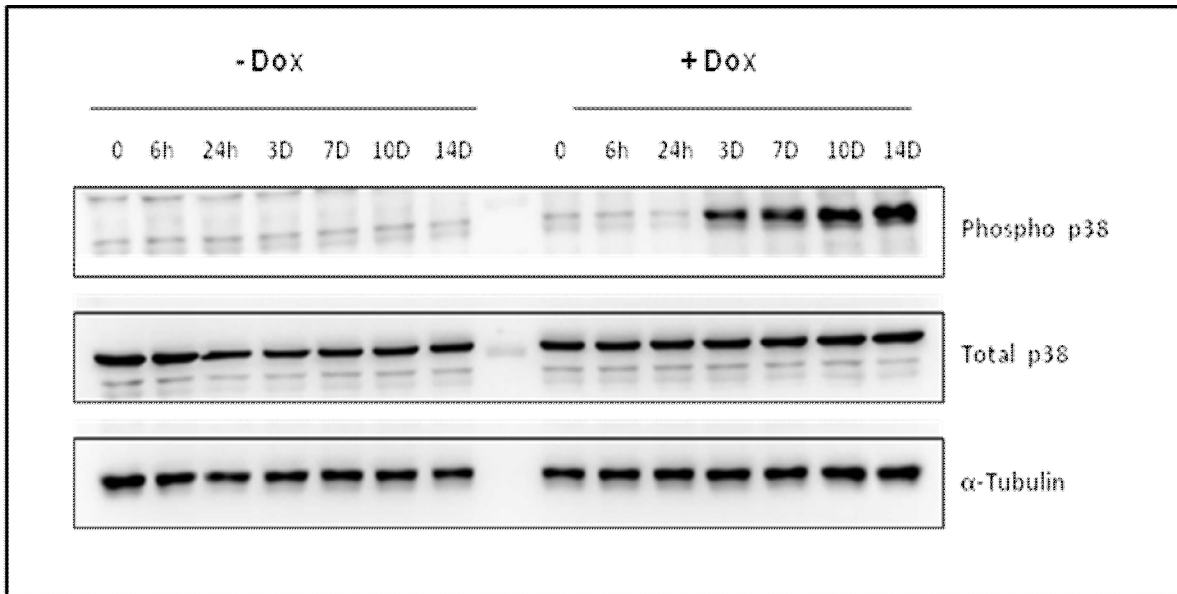


Figure 28: Activation of the p38 signaling pathway upon NeuT expression. A representative immunoblot is shown for activation of p38 in senescence cells. α -Tubulin was used as the loading control.

3.2.4 JNK signaling pathway is not activated during senescence

The c-Jun N-terminal kinase (JNK) is a stress-activated member of MAP kinase family. Therefore, we investigated the role of JNK activation in our senescence cell model. Our result showed that the phosphorylation of JNK levels was unaltered relative to control cells after time dependent dox treatment. This data suggested that activation of JNK has no effect on premature senescence induced by oncogene ERBB2/NeuT.

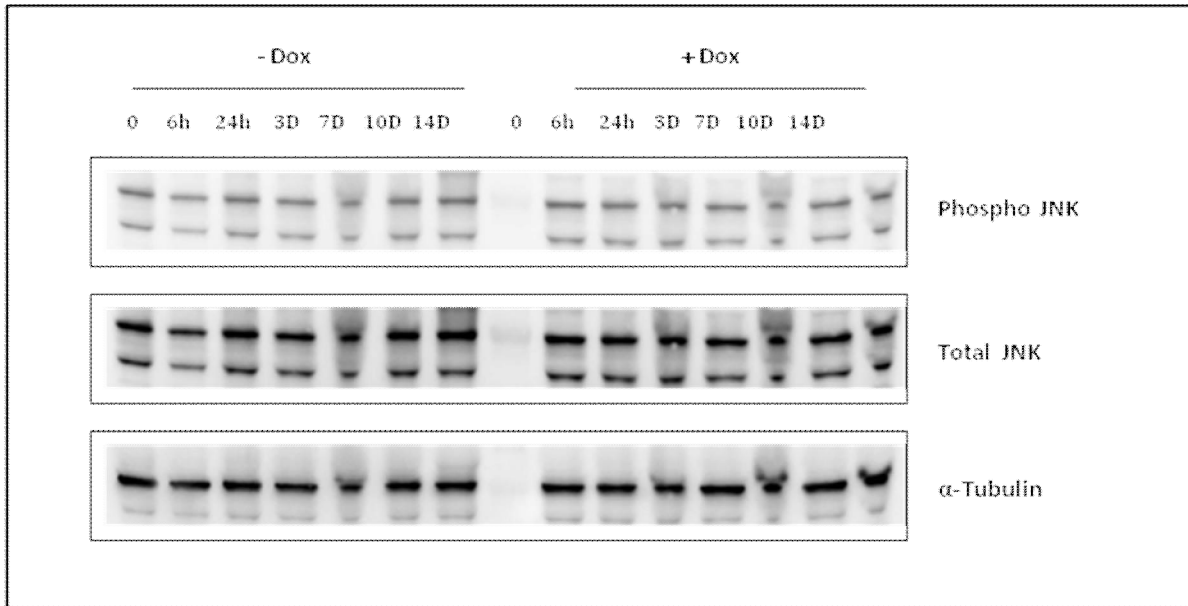


Figure 29: Phosphorylation of JNK pathway in MCF-7/NeuT cells. Lysates obtained from different time points of dox treatment were subjected to immunoblot analysis using anti-JNK and anti-phosphorylated JNK antibodies. α -Tubulin was used as the loading control.

3.3 Autophagy in oncogene-induced senescence cells

Autophagy is an evolutionarily conserved eukaryotic degradation pathway involved in the turnover and elimination/recycling of cellular proteins and organelles.

Several studies have shown that the above described signaling pathways have an influence on the autophagy flux in different ways. While activation of the MEK1/2-ERK1/2 signaling pathway leads to induction of autophagy, activation of the AKT/mTOR pathway has been shown to inhibit it. On the other hand, activation of the p38 signaling cascade is reported to affect autophagy in various ways that appear somehow contradictory. In our cell model, we found that both ERK1/2 and AKT are rapidly phosphorylated upon NeuT induction and become dephosphorylated in the late senescence phase. In contrast, the p38 pathway becomes activated with the onset of

senescence and remains phosphorylated throughout senescence. (Fig-25, Fig-26 and Fig-27).

One of the most prominent morphological alterations observed in the MCF-7/NeuT senescent cells is a strong cytoplasmic accumulation of vacuolar structures. These vacuoles have been shown to be acidic by LysoTracker staining (Cadenas et al., 2012), suggesting that they may be components of the lysosomal degradative system. Strong accumulation of autophagic vacuoles may reflect a deregulated autophagy flux. This observation, together with the activity pattern of signalling pathways involved in regulating autophagy prompted us to explore the regulation and role of autophagy in oncogene induced senescence.

MAP1LC3 (LC3) is a widely used marker of autophagy. Post translational modification of cytosolic LC3-I to LC3-II is followed by LC3-II translocation to nascent autophagosomal membranes, which is a useful index of autophagosome formation (Mizushima, 2010). The lipid conjugated form of LC3 (LC3-II) can be separated from the nonconjugated form (LC3-I) by SDS-PAGE and LC3-II levels reflect the abundance of autophagosomes. Therefore, the first approach was to study levels of LC3-II during NeuT-induced senescence.

In our MCF-7/NeuT cell system, LC3-II levels were elevated after 24 hr dox treatment and increased further in the senescence phase, reflecting higher numbers of autophagosomes. In addition to LC3 II, we also monitored the levels of an autophagosomal cargo adaptor, p62/SQSTM1. p62 directly binds to LC3 and becomes itself degraded during the autophagic process (Pankiv et al., 2007; Ichimura et al., 2008). According to the literature, increased amounts of p62 may indicate a blockade of autophagy. Our results showed accumulation of p62 after onset of senescence, which might represent the impairment of autophagy in our senescence cell model.

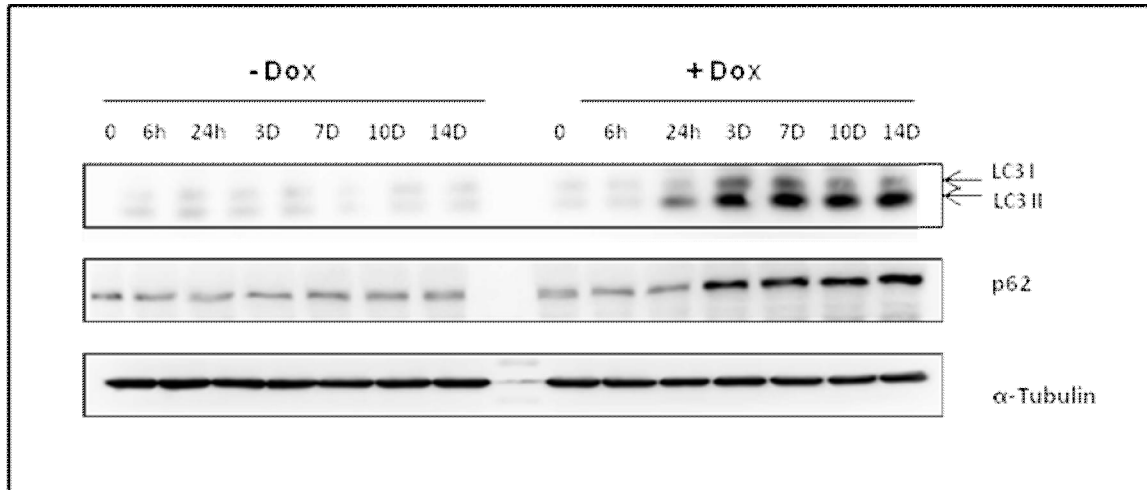


Figure 30: Increased levels of autophagosomes in senescent cells. Western blot analyses showing increased amounts of the autophagosome marker LC3-II and the cargo-adaptor protein p62 in senescent cells. α -Tubulin was used as the loading control.

In order to provide evidence that the increased vacuolization and LC3-II levels are related to autophagy, we treated our cells with 3-methyladenine (3-MA) at different dox-treatment time intervals. 3-MA is one of the most widely used inhibitor of autophagy that suppresses the autophagic/lysosomal pathway by inhibiting class III PI3Ks (Lin et al., 2012). We found that in senescent cells the cytoplasmic vesicles were diminished by incubating with 3-MA (Fig-31A). We also analyzed the expression of the autophagosome marker LC3-II by immunoblot. LC3-levels became reduced to the basal level in presence of 3-MA (Fig-31B). This result indicated that the vacuolization observed in senescent cells was due to accumulation of autophagic vesicles.

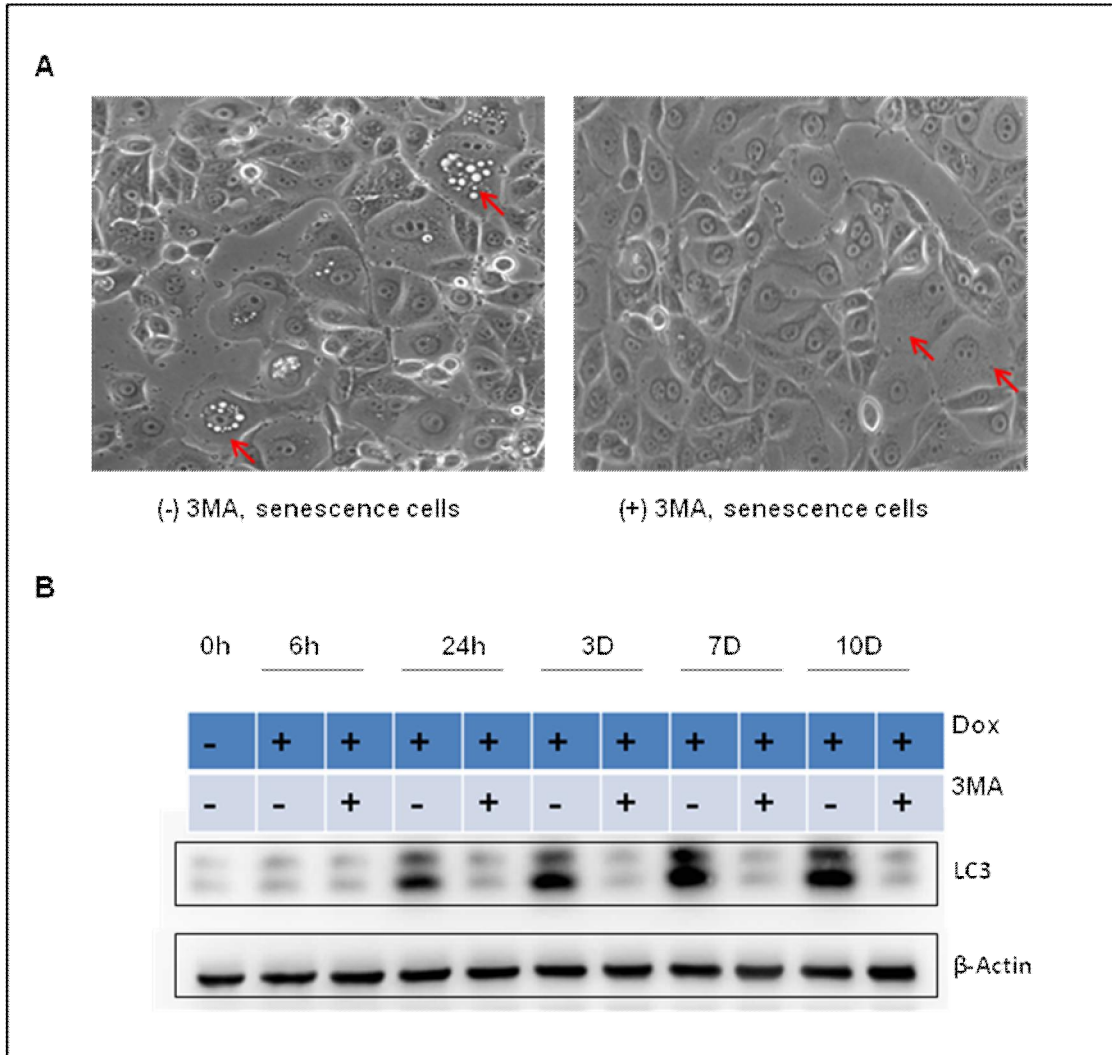


Figure 31: Inhibition of autophagy by 3-MA treatment. A. Morphological changes of senescent cells by incubation with 5 mM of 3-MA. B. Expression of the autophagic marker LC3-II after treatment with 5 mM 3-MA at different times of dox exposure.

3.4 Autophagy maturation is impaired in senescent cells

Since LC3-II is itself degraded during the autophagy process due to its localization in autophagosomes, LC3-II accumulation may reflect either autophagic induction by enhanced formation of autophagosomes or blockade of autophagosome degradation. In order to discriminate between these two possibilities we performed the LC3-II turnover assay according to the proposed guidelines (Klionsky, 2008).

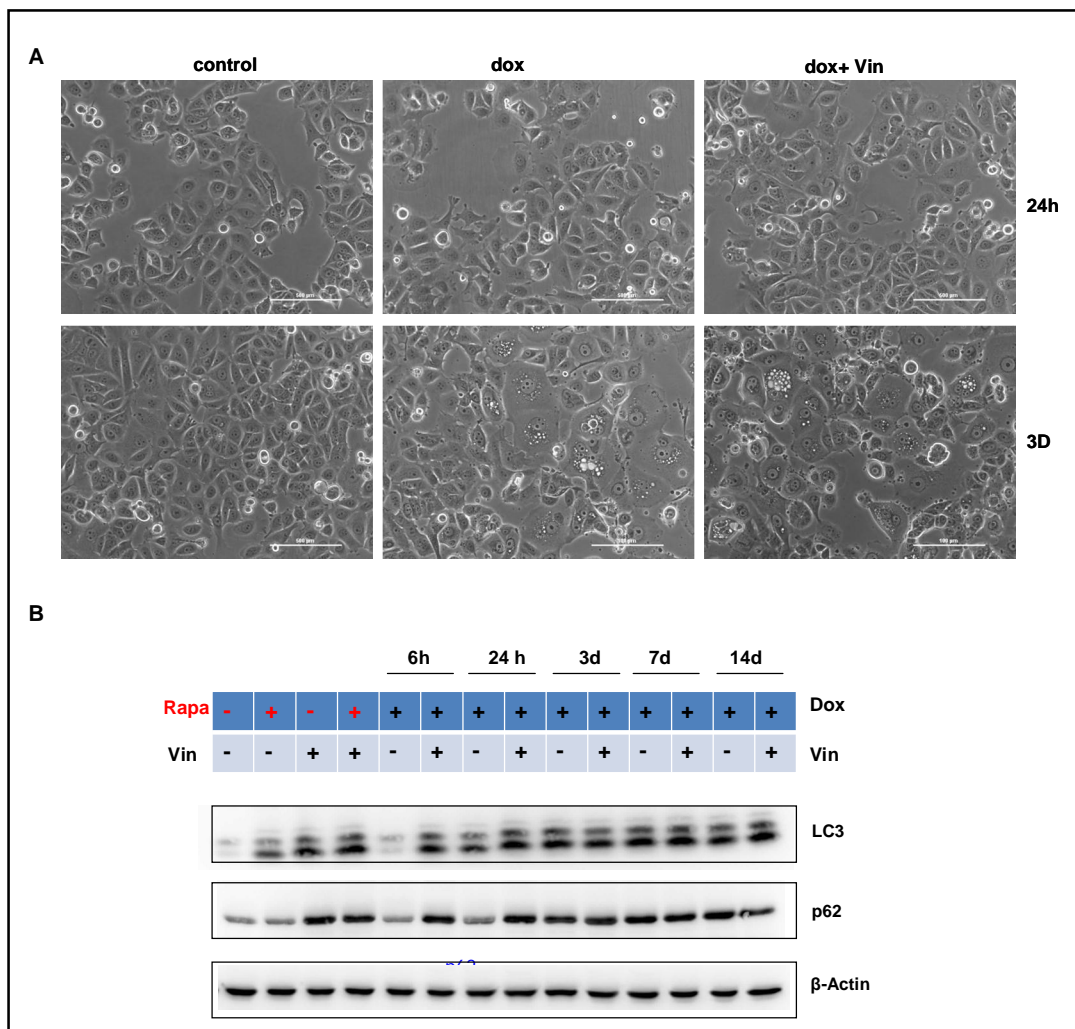


Figure 32: LC3-II turnover assay reveals a biphasic behavior of autophagy. Cells were incubated overnight with rapamycin (100nM) as a positive control for autophagy induction. In the turnover assay, cells were treated with 50 μ M of vinblastine for 2 hours before lysate extraction. Induction of autophagy is shown at 24h+dox, whereas the block of autophagosome (LC3-II) degradation is shown after 3d-14d+dox. β -Actin was used as the loading control.

In this assay the autophagy flux is monitored by experimentally blocking lysosomal degradation. Accumulation of the autophagosome marker LC3-II or of any cargo protein during this block is an indicator of a previously active autophagy flux. To monitor the autophagic flux in our MCF-7/NeuT cells we incubated cell cultures for 2 hours with vinblastine before harvesting. Vinblastine is a microtubule destabilizer which is known to

impair fusion of autophagosomes with lysosomes. In pre-senescent MCF-7/NeuT cells (6h-24h+dox), vinblastine induced a dramatic increase of LC3 II suggesting that the autophagy flux is induced at this stage. The levels of p62 expression also accumulated by vinblastine treatment. In contrast, after exposure to vinblastine in the senescent stage (3d-14d+dox), neither the autophagic marker LC3-II nor the cargo protein p62 showed further accumulation, showing that senescent MCF-7/NeuT cells have already an impaired flux .

To further confirm this result we also assessed the LC3-II turnover assay in the presence of bafilomycin A1, a specific inhibitor of the vacuolar type H(+)-ATPase, which inhibits lysosome acidification. As expected, similar results were obtained when levels of LC3-II and p62 were monitored, which confirmed the two phases in the autophagy flux upon oncogene overexpression: i) enhanced flux in the pre-senescent stage (high LC3, low p62) and ii) blocked flux in the senescence stage (high LC3, high p62).

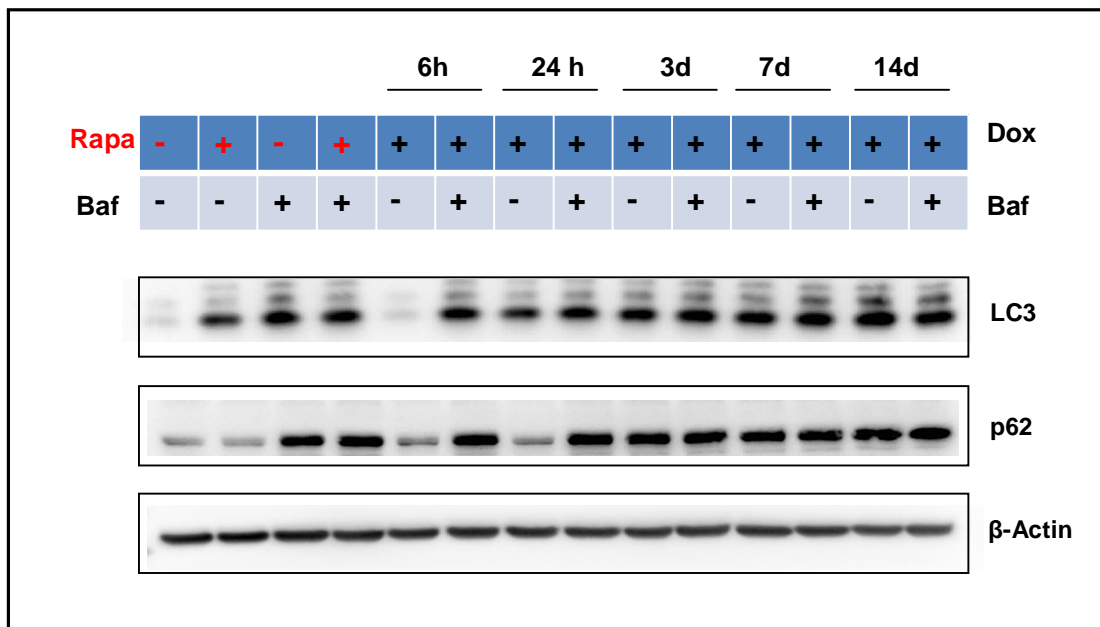


Figure 33: Impairment of autophagy maturation in senescence. Cells were treated with 200 nM of bafilomycin for 2 hours before cell lysate extraction. Induction of autophagy is shown at 24h+dox, whereas block of autophagosome (LC3-II) degradation is shown after 3d-14d+dox. β-Actin was used as the loading control and rapamycin (100nM) as a positive control for autophagy induction.

In conclusion, our data shows that NeuT expression leads initially to induction of autophagy. However, after the onset of senescence, accumulation of autophagosomes is due to a blockade in autophagosome turnover.

3.5 Senescence-associated blockade of the autophagic flux is triggered by the p38-MAPK pathway

In order to investigate the mechanisms that lead to the initial induction of autophagy and the later block of its flux in senescence, we applied small molecule inhibitors of the pathways previously shown to be induced upon NeuT expression. Since phosphorylation of p38 matched to the appearance of the autophagy flux blockade, we investigated whether the p38 pathway would be responsible for the impaired autophagy flux by applying a pharmacological inhibitor of p38, SB203580. After treating MCF-7/NeuT cells with the SB203580 inhibitor, we found absence of autophagic vacuoles in senescence. This indicated the participation of the p38 pathway in accumulation of autophagosomes (Fig- 34A).

To further study the role of p38 in autophagy during senescence, we performed the turnover assay. Inhibition of p38 by the SB203580 inhibitor has no effect on LC3-II levels in untreated MCF-7/NeuT cells or in MCF7/NeuT cells in the pre-senescent stage (6h-24h+dox). This can be explained by the fact that p38 is not maximally activated at this stage, as shown by lack of phosphorylation of the p38-substrate MSK1. In addition, this shows that induction of autophagy in the pre-senescence phase is p38-independent. In contrast, incubation of MCF7/NeuT senescent cells (3d-7d+dox) with the SB203580 inhibitor completely blocked accumulation of LC3-II (Fig-34B). The efficiency of p38-inhibition by SB203580 was confirmed by monitoring phosphorylation of MSK1. Addition of vinblastine to SB-treated cells resulted in a new accumulation of LC3-II.

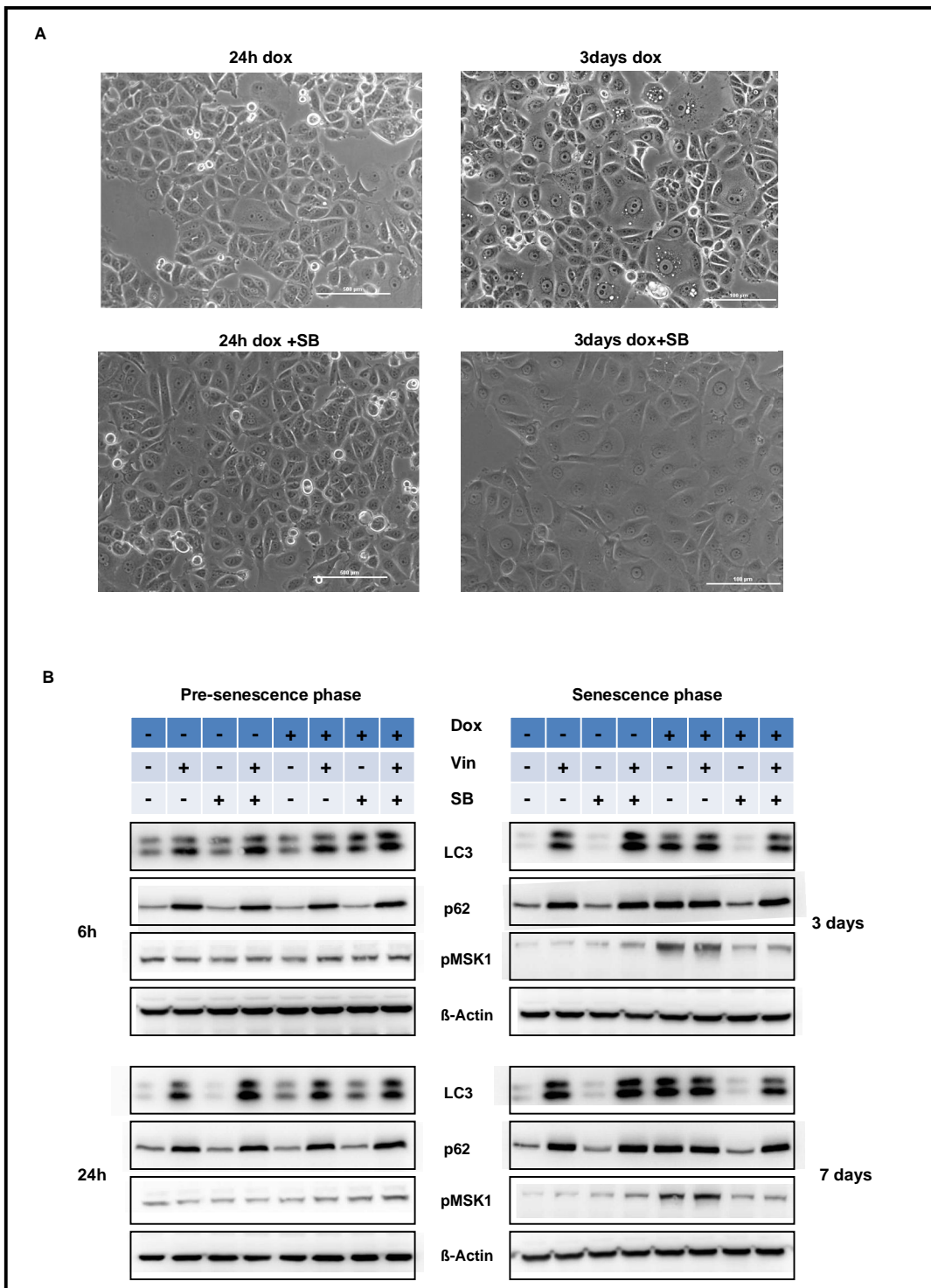


Figure 34: Impaired autophagic flux is mediated by the p38 signaling pathway in senescence. MCF-7/ NeuT cells were pre-incubated with SB203580 (20μM) for 1hr before time dependent dox treatment. Before protein lysate extraction cells were exposed for 2 hours to vinblastine (50μM). β-Actin was used as the loading control.

This showed that p38 blocks the completion/maturation of the autophagy process and SB203580 restored a basal-like autophagic flux that can be impaired by additional treatment with autophagy flux inhibitors. We also studied the impact of SB203580 mediated inhibition of p38 on p62/SQSTM1 abundance: (As shown in Fig-34B), i) p62 only accumulates in senescent (and not in pre-senescent) cells as a result of impaired autophagy, ii) its accumulation in senescence is not further enhanced by vinblastine treatment, showing that the flux is already blocked and iii) SB-treatment impairs accumulation of p62 in senescent MCF-7/NeuT cells (3D-7D+Dox), which can accumulate by additional vinblastine treatment.

Identical results were obtained when bafilomycin A1 was used instead of vinblastine to confirm the blockade of autophagy by p38 pathway in senescence cells .

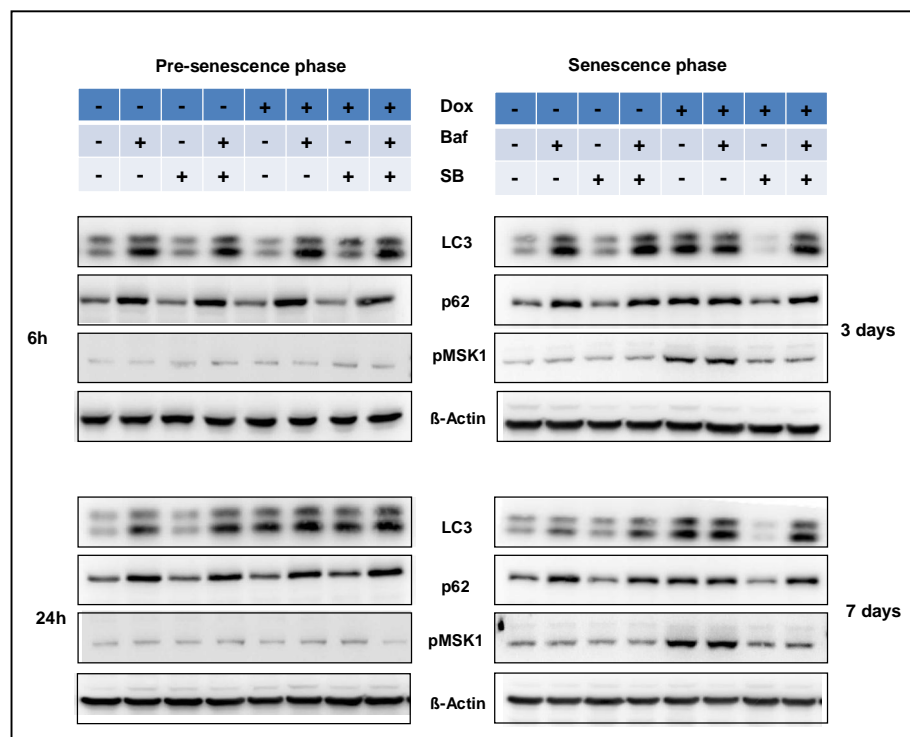


Figure 35: p38 signaling pathway mediates blockade of autophagy in oncogene-induced senescence. MCF-7/ NeuT cells were pre-incubated with SB203580 (20 μ M) for 1 hr before time dependent dox treatment. Before protein lysate extraction, cells were exposed for 2 hours to bafilomycin (200nM). β -Actin was used as the loading control.

Monitoring LC3 puncta formation by immunofluorescence of endogenous LC3 (Mishuzima et al., 2007, Klyonki et al., 2008, Mishuzima et al., 2010) in presence or absence of SB and/or autophagy flux inhibitors further confirmed our results and

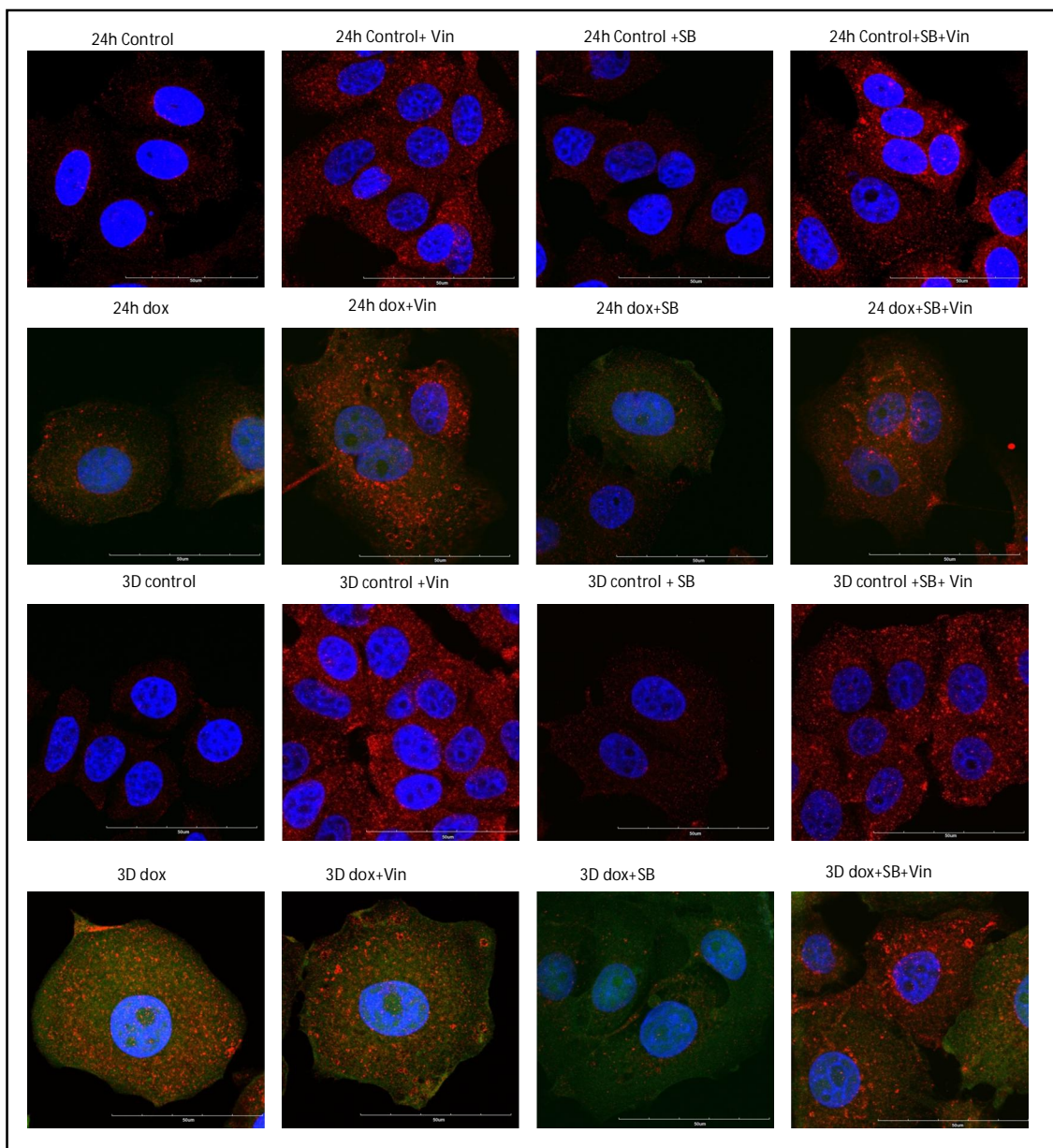


Figure 36: Detection of LC3-puncta by confocal microscopy. Cells were subjected to dox-treatment at the indicated time points. Pre-incubation with SB203580 (20 μ M) was done for 1 hr before dox treatment. Before fixation, cells were exposed for 2 hours to vinblastine and detection of LC3 was performed by immuno staining. The nuclei were labelled with DAPI; blue (DAPI), red (LC3) and green (EGFP). Images are representative of multiple images taken of each condition. Bar; 50 μ m.

showed that LC3-puncta (and thus autophagosomes) that accumulate in senescence (3d+dox) cannot be increased by treatment with vinblastine. As described above, SB203580 treatment lead to reduced levels of LC3-puncta, which further increased by treatment with vinblastine. Blockage of the autophagy flux by the p38 pathway and release of this blockage by adding SB203580 inhibitor was therefore confirmed as well by immunofluorescence of LC3 puncta.

3.6 The MEK1/2-ERK1/2 signaling pathway is involved in initial induction of autophagy upon NeuT induction

Activation of extracellular signal-regulated kinases (ERK1/2) has been shown to induce autophagy in different cell types such as in neurons (Zhu et al., 2003) and in human colon cancer cells (Pattingre et al., 2003). Therefore, we also investigated the role of ERK signaling pathway in our oncogene-induced cell system. To do so, we treated our MCF-7/NeuT cells with the MEK inhibitor PD98059. Our first results showed that PD did not alter senescence cell morphology, since senescence-associated flattening and vacuolization were still observed after PD98059 treatment (Fig-37A).

To explore the regulation of autophagy by the MEK-ERK1/2 signaling pathway, we performed the turnover assay in combination with the PD98059 inhibitor.

Our results showed that in the pre-senescent stage (6h-24h+dox), the MEK/ERK1/2 pathway is responsible for the enhanced autophagy flux since addition of PD98059 inhibits the accumulation of LC3-II-positive autophagosomes observed at this stage. In contrast, incubation of MCF7/NeuT senescent cells (3d-7D+dox) with PD showed no effect on LC3-II and cargo protein p62 levels. Although activity of the ERK signaling pathway is still high at this stage (phospho-ERK1/2 is observed in dox-treated cells), it has no influence on the autophagy flux in senescent cells (Fig-37B).

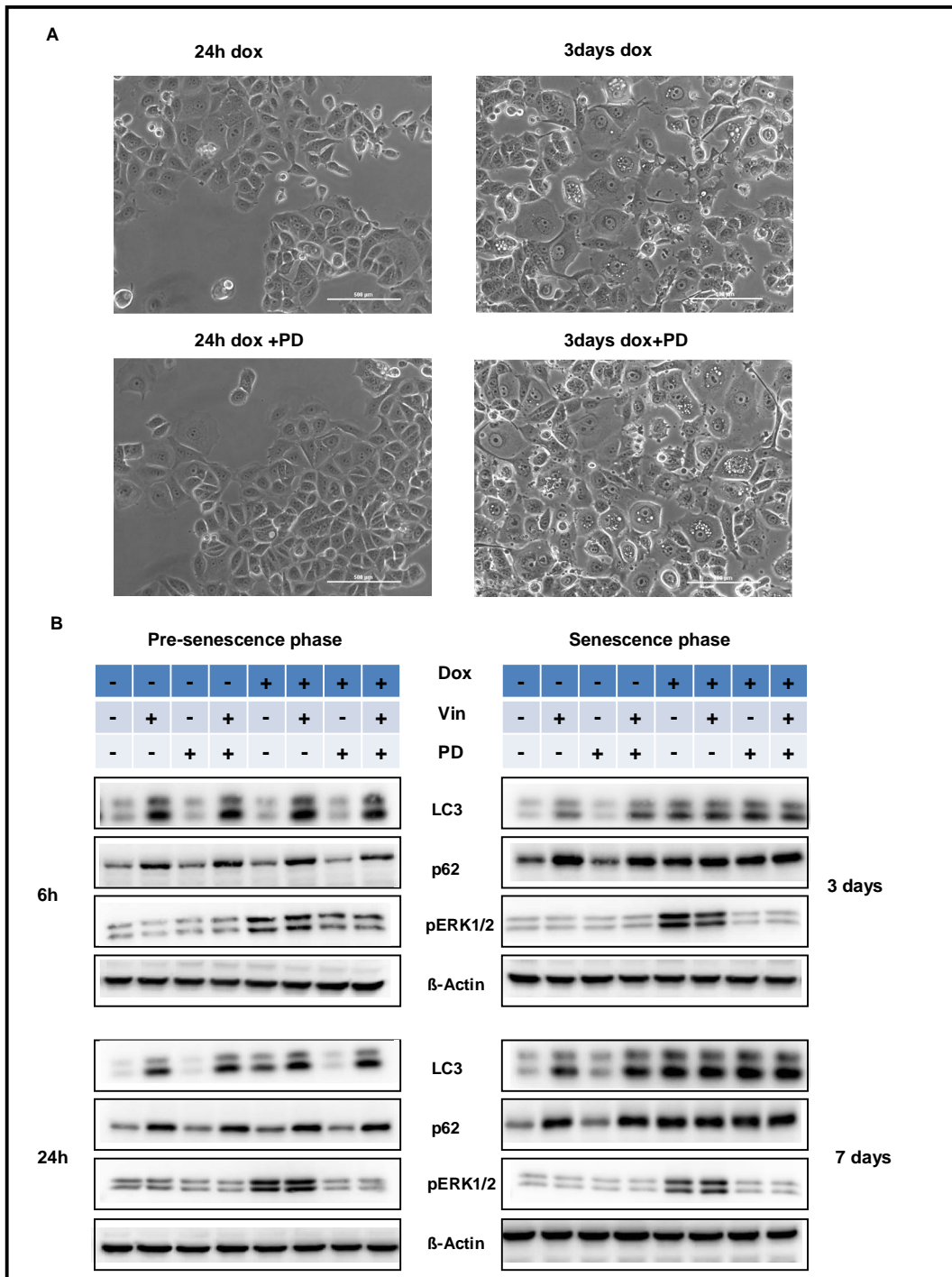


Figure 37: Inhibition of the ERK signaling pathway influences early (24h) LC3-II levels but has no effect on autophagy maturation in late senescence (3-7 days). MCF-7/NeuT cells were pre-incubated with PD98059 (50 μ M) for 1h before time-dependent dox-treatment. Before protein lysate extraction cells were exposed to vinblastine (50 μ M) for 2h. β -Actin was used as the loading control.

This result suggested that the p38 signaling pathway is the major player in blocking the maturation of the autophagy process in senescent MCF-7/NeuT cells. The participation of the PI3K (class I)/AKT signaling pathway was not investigated because the available inhibitors are unspecific and block also class III PI3K, which are directly involved in autophagy.

3.7 Mechanism underlying p38-mediated block of autophagy maturation

In the previous section evidence for an impaired completion of autophagy in oncogene-induced senescence via p38 was presented. The next goal of the work was to identify p38 targets involved in mediating the blockade of the autophagy flux. Based on the literature, we first considered several factors whose inactivation or deficiency leads to perturbed maturation of autophagic vacuoles. Then, we investigated whether they are controlled by the p38 signaling pathway.

3.7.1 Cytoskeleton-mediated transport of autophagosomes (delivery of autophagosomes to lysosomes) is impaired in senescent cells via p38

3.7.1.1 Regulation of microtubule-associated protein activity by p38

Microtubules facilitate both autophagosomal biogenesis and fusion of autophagosomes with lysosomes by trafficking of mature autophagosome (Webb et al., 2004). Microtubule stability and dynamics are regulated by microtubule-associated proteins. Two of these, the microtubule-associated protein 4 (MAP4) and stathmin/oncoprotein 18 have recently been implicated in hypoxia-induced microtubule destabilization via p38 (Hu et al., 2010). This report has shown that hypoxia induces microtubule depolymerization via the activation of the p38 signaling pathway and changes the phosphorylation levels of its downstream effectors, Map4 and op18. MAP4 binds to and stabilizes microtubules, however p38-mediated phosphorylation of MAP4 results in disassembly of microtubules (Hu et al., 2010). In contrast, STMN1/OP18 is a microtubule depolymeriser in its dephosphorylated state. While normally found

inactivated as a phospho-protein, STMN1/OP18 dephosphorylation triggered by p38, destabilizes microtubules (Hu et al., 2010).

In order to investigate whether a similar mechanism is involved in the senescence-associated block of autophagy flux observed in our MCF-7/NeuT cell model, we first analyzed levels of MAP4 and STMN1/OP18 and their corresponding phosphorylated forms in the course of oncogene-induced senescence. As shown in Figure 38, MAP4 is phosphorylated in senescent cells. Vice versa oncoprotein 18 was dephosphorylated which predicts depolymerisation of microtubules.

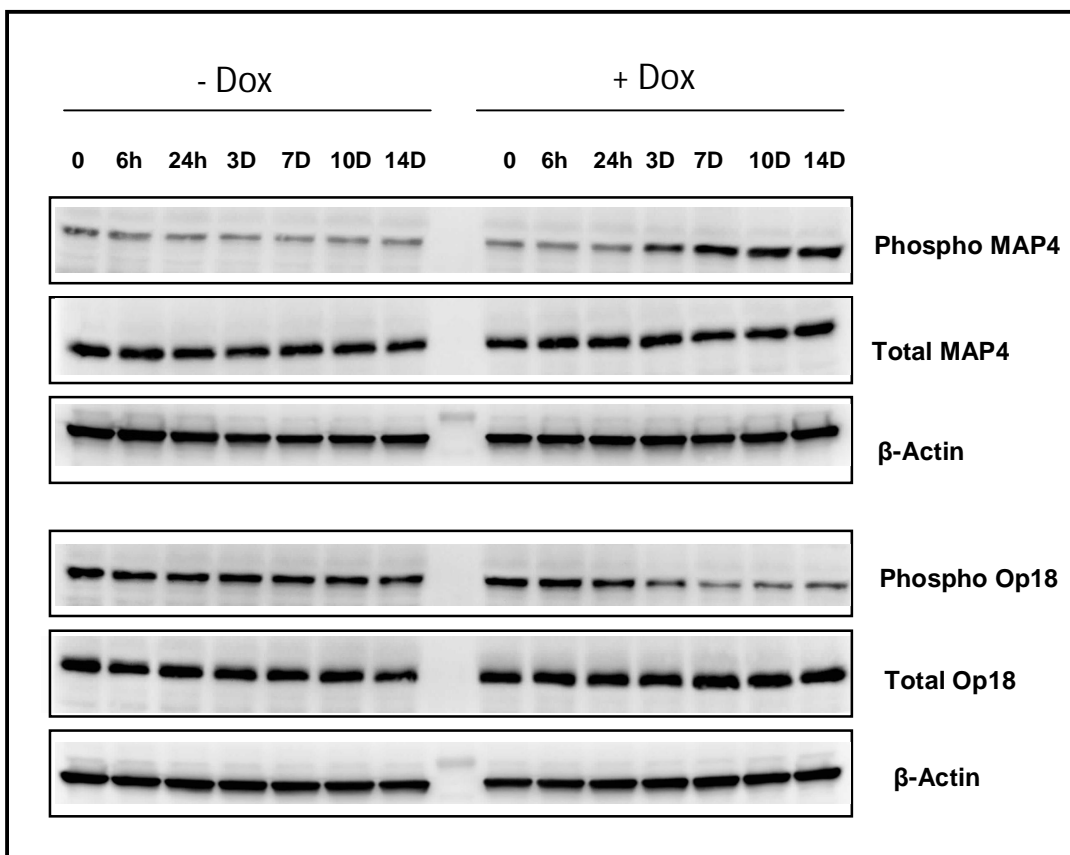


Figure 38: Destabilization of microtubules in senescent cells through phosphorylation of MAP4 and dephosphorylation of oncoprotein18. Representative western blot analysis for phosphorylated MAP4, total MAP4, phosphorylated Op18 and total Op18. β-Actin was used as the loading control.

To explore the role of the p38 signaling pathway in the regulation of MAP4 and STMN1/OP18, we treated our cells with the p38 inhibitor SB203580. Our results showed dephosphorylation of MAP4 in senescent cells in presence of SB203580. On the other hand SB-mediated inhibition of p38 resulted in phosphorylation of oncoprotein 18 similar to the control level.

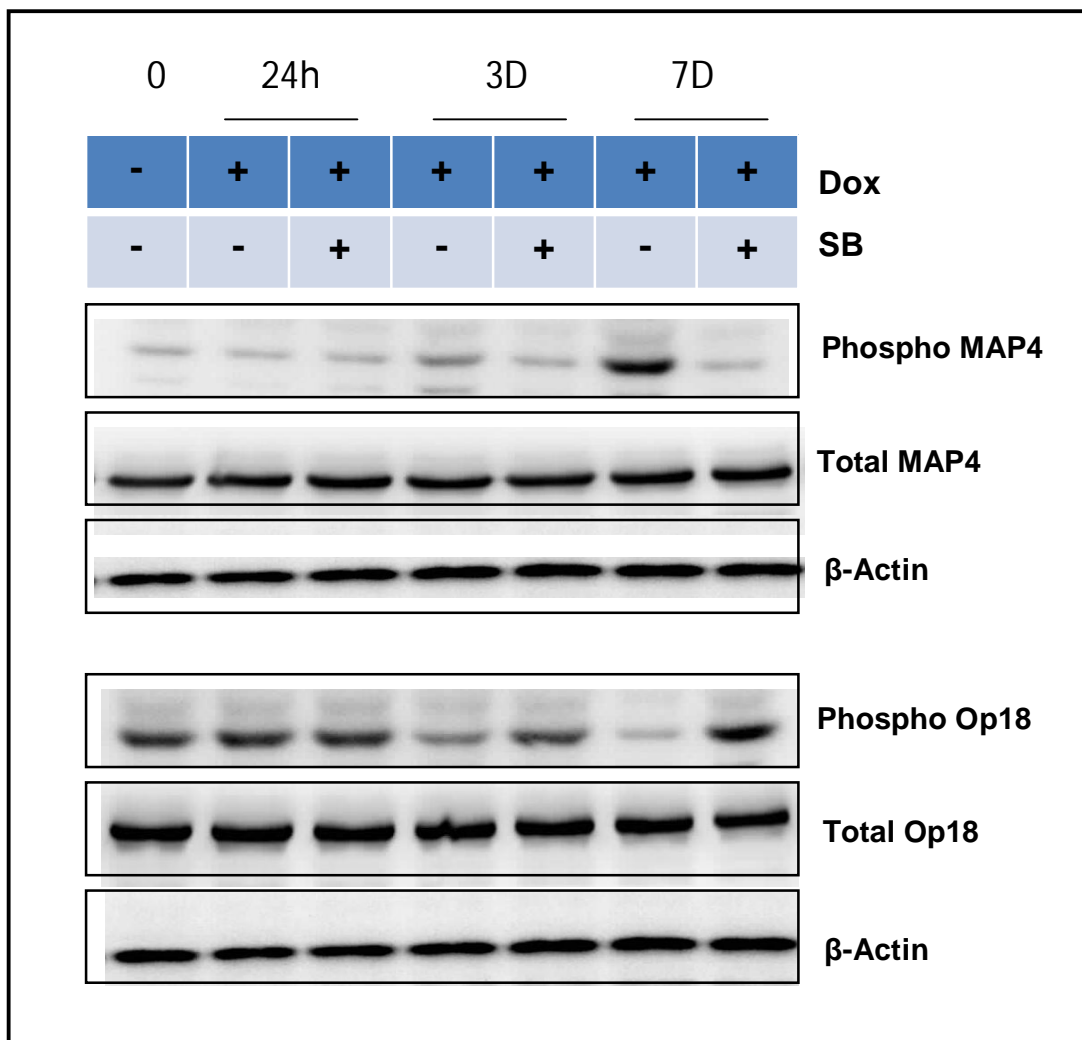


Figure 39: Destabilization of microtubules in senescence cells via the p38 signaling pathway. MCF-7/ NeuT cells were pre-incubated with the SB203580 inhibitor (20 μ M) 1 hr before dox treatment. Representative western blot analysis for phosphor MAP4, total MAP4, phosphor Op18 and total Op18. β -Actin was used as the loading control.

Staining of alpha-tubulin by immunofluorescence confirmed that the microtubule network is intact in pre-senescent but disrupted in senescent MCF-7/NeuT cells, as it was expected by the concomitant phosphorylation of MAP4 and the dephosphorylation of STMN1/OP18 that act as microtubule depolymerizers. Treatment of MCF-7/NeuT senescent cells (3d+dox) with vinblastine did not aggravate depolymerization, which supports the finding that microtubules are already affected in senescence. Inhibition of the p38 MAPK with SB203580 inhibitor results in apparently intact microtubule architecture, probably as a result of normal levels of dephosphorylated MAP4 and phosphorylated levels of STMN1/OP18. Additional treatment with vinblastine was shown to cause microtubule disruption again.

In conclusion, our results suggest that the microtubule network is compromised in senescence via p38 signaling (Fig-40).

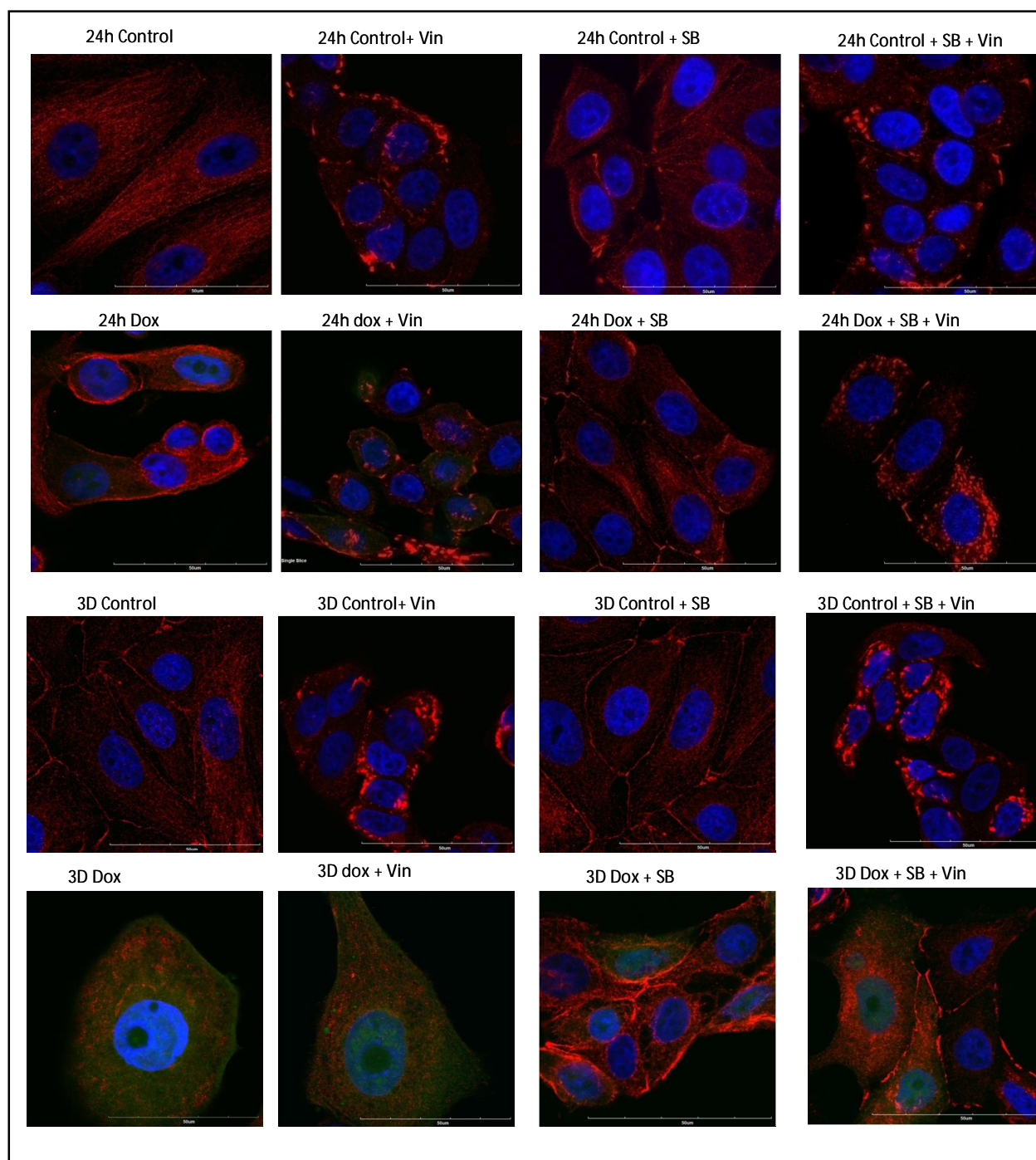


Figure 40: Disruption of the microtubule network in senescent MCF-7/NeuT cells via p38. Cells were subjected to dox-treatment at the indicated time points. Pre-incubation with SB203580 (20µM) was done for 1 hr before addition of dox. Vinblastine treatment was performed 2 h before fixation. Detection of the microtubule network was performed by immuno staining with an anti- α -tubulin antibody. blue (DAPI), red (α -tubulin) and green (EGFP). Images are representative of multiple images taken of each condition. Bar; 50 μ m

3.7.1.2 Regulation of dynein light chain 1 (DYNLL1) expression by p38

Microtubules facilitate autophagosome trafficking. Once formed, the autophagosome moves towards the lysosome along the microtubules by means of the dynein motors. Loss of dynein leads to an impairment of the clearance of aggregate-prone proteins by autophagy and to increased levels of LC3-II, reflecting a defect in the fusion between autophagosomes and lysosomes (Ravikumar et al., 2005). To determine the expression

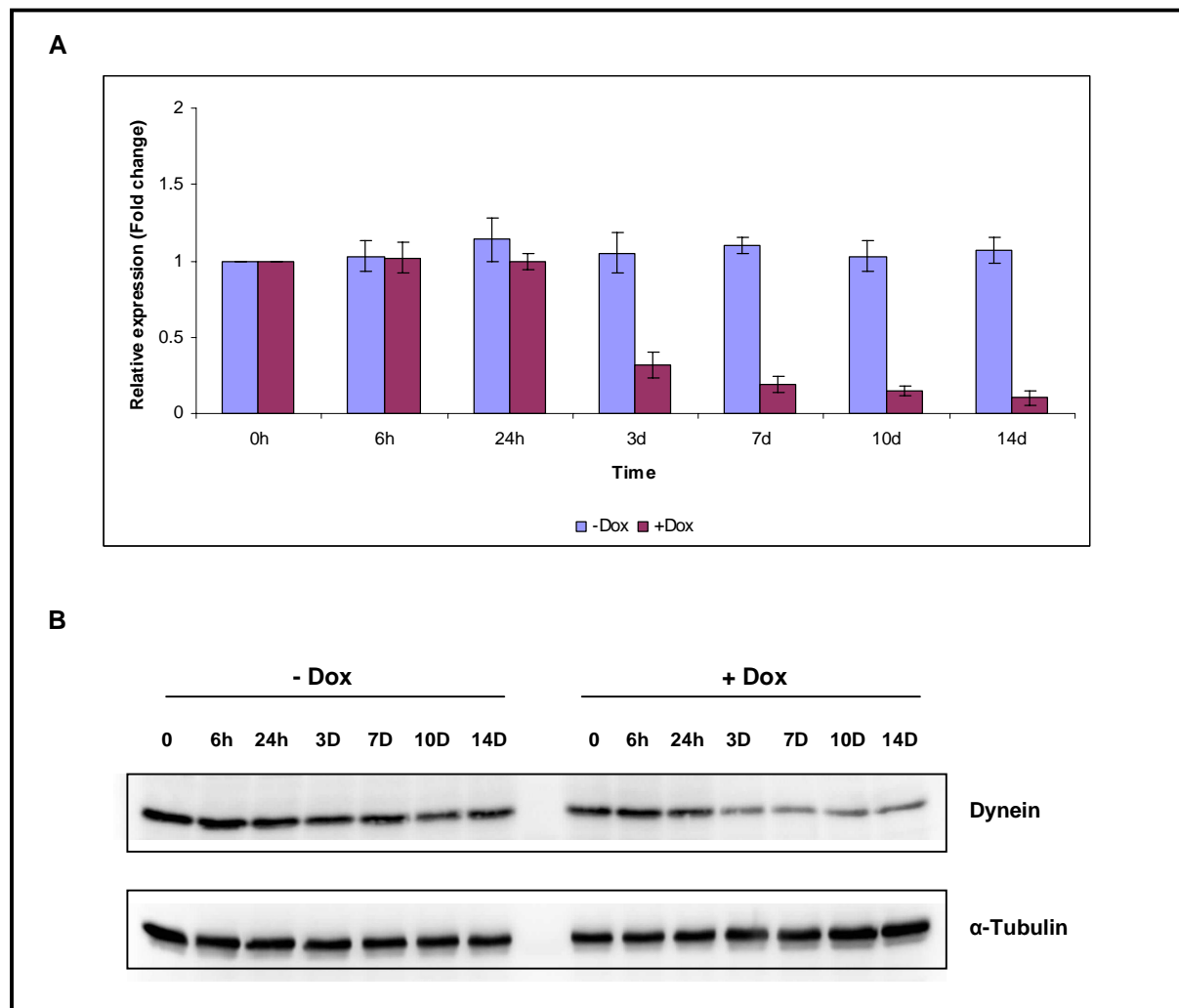


Figure 41: Down regulation of the dynein motor protein subunit DYNLL1 in senescence. A. Expression of dynein by qRT-PCR. The result presented here is the mean of three independent experiments, with error bars to represent standard deviations from mean. **B.** Western blot analysis of the dynein motor protein subunit DYNLL1.

level of dynein motor protein in senescent cells, a time-course study was performed from 0h to 14 days of dox treatment by using qRT-PCR to measure mRNA expression. Our result showed down regulation of the dynein motor protein subunit DYNLL1 (dynein light chain 1) upon NeuT induction. This result was confirmed at the protein level by immunoblotting using a specific antibody against DYNLL1.

To further investigate whether p38 is the major signaling pathway responsible for down regulation of DYNLL1 we treated MCF7/NeuT cells with the SB inhibitor and analyzed

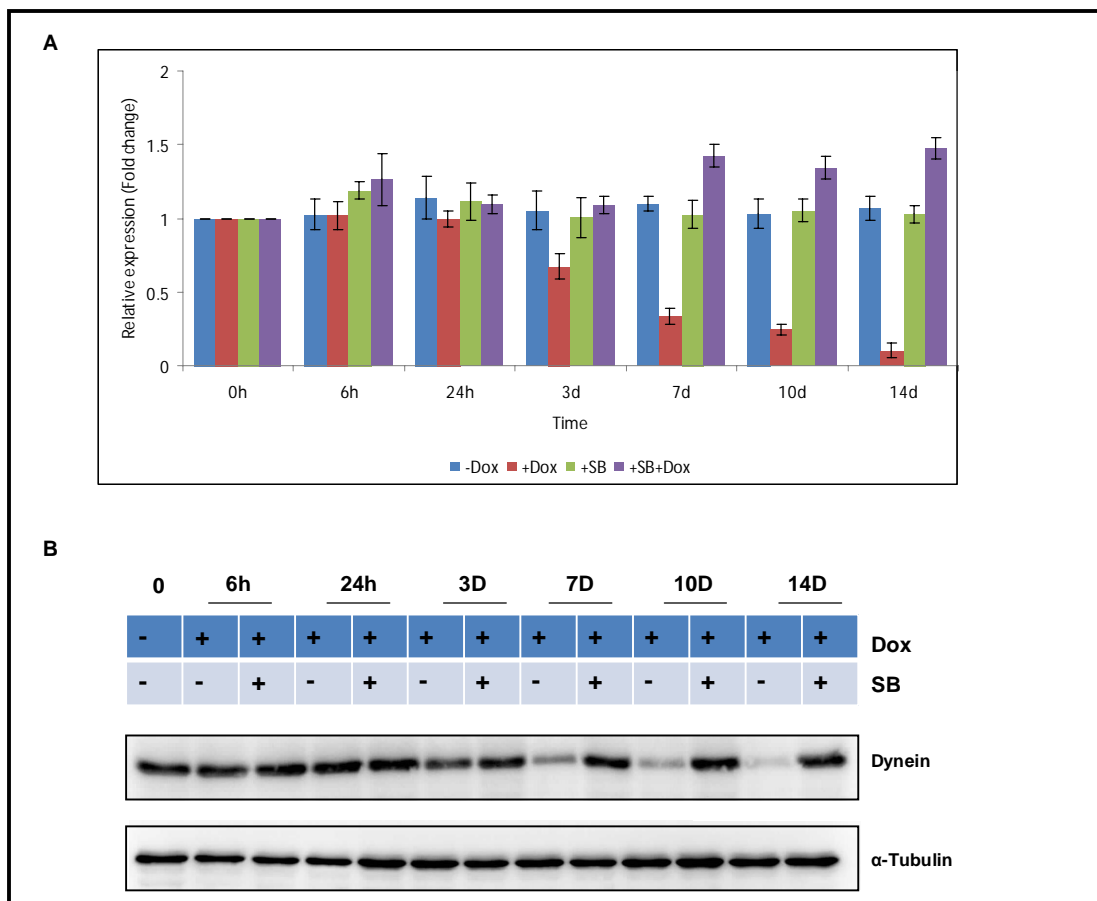


Figure 42. Down regulation of dynein motor protein subunit DYNLL1 by the p38 signaling pathway. MCF-7/NeuT cells were pre incubated with SB203580 inhibitor (20 μ M) 1 hr before dox treatment. **A.** Expression of dynein motor protein subunit DYNLL1 by qRT-PCR. The result presented is the mean of three independent experiments, with error bars to represent standard deviations. **B.** Western blot analysis for DYNLL1.

DYNLL1 both at mRNA and protein level. This results showed that the SB inhibitor can restore DYNLL1 expression, which coincided with restoration of the autophagic flux in senescence.

3.7.2 Regulation of acidification and composition of lysosomes by p38 pathway

The late stage of autophagy depends on acidification and composition of lysosomes and lysosomal membranes and studies have shown that impairment of lysosomal function or biogenesis results in an accumulation of autophagosomes, which inevitably slows down or interrupts the autophagic flux.

3.7.2.1 Down-regulation of cathepsin D expression by p38 signaling pathway in senescent cells

Cathepsins are a major family of hydrolases that mediate protein degradation. They are synthesized as inactive precursors and are normally activated in the acidic environment of lysosomes. Previous published work described that reduced cathepsins cause impaired autophagic degradation (Tatti et al., 2012).

In order to explore this mechanism, we investigated cathepsin gene expression in senescence cells by RT-qPCR. Our result showed down-regulation of cathepsin D upon NeuT induction which was restored by SB inhibition.

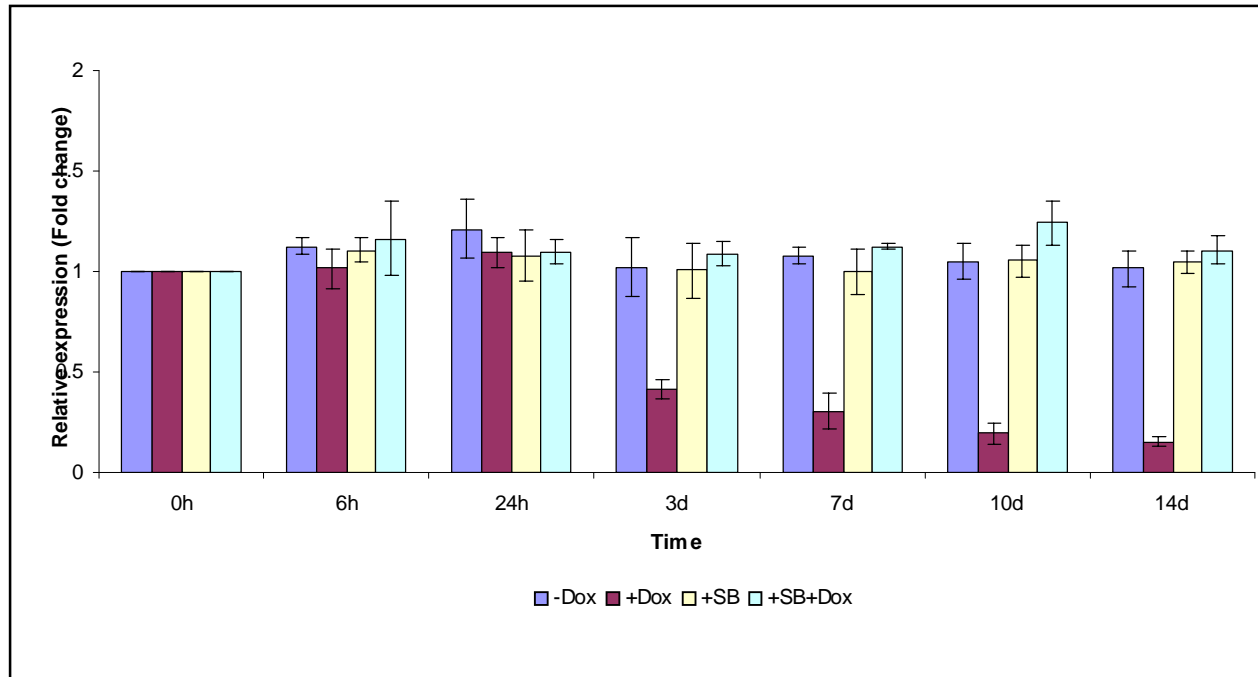


Figure 43: Down regulation of cathepsin D in senescent cells via p38 signaling pathway. MCF-7/NeuT cells were pre incubated with SB203580 inhibitor (20 μ M) for 1 hr before dox treatment. The result is representative of three independent experiments, with error bars to represent standard deviations.

3.7.2.2 The p38/MAPK pathway mediates down-regulation of the vacuolar ATPase

Vacuolar ATPases (v-ATPases) are ubiquitous, multi-subunit proteins located in the cellular acidic compartment (endosomes, lysosomes). Their function is to transport protons across the vacuolar membrane by coupling ATP hydrolysis. Acidification of the vacuolar compartment is required to activate proteases necessary for degradation; therefore inhibition of v-ATPases impairs proteolysis. It has been proposed that an additional consequence of the inhibition of v-ATPase is the interruption of the autophagic flux, as determined by the inhibition of lysosomal degradation of autophagic cargo (Kinouchi et al., 2010).

In senescent cells expression of the v-ATPase was analyzed by qRT-PCR. We observed that the ATP6V0A2 subunit, a component of the V(0) domain of the V-ATPase that is involved in proton translocation, is reduced in senescent MCF-7/NeuT cells and that this down-regulation is triggered by the p38 signaling pathway.

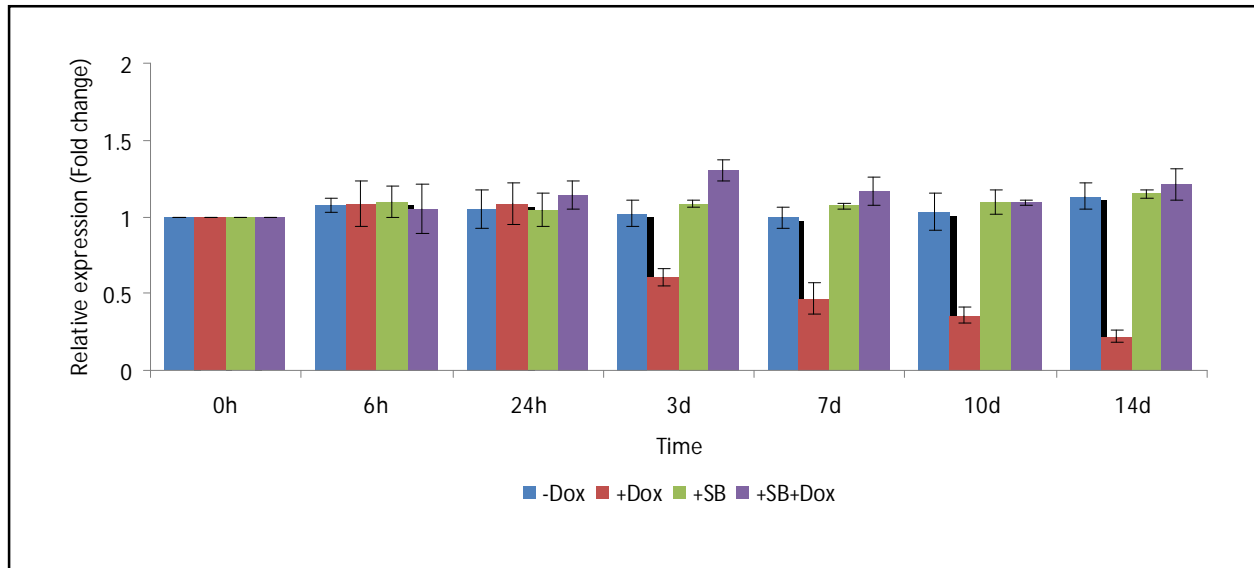


Figure 44: p38 activation down regulated the vacuolar ATPase subunit ATP6V0A2. MCF-7/ NeuT cells were pre incubated with SB203580 inhibitor (20 μ M) for 1 hr before time depended dox treatment. The result is representative of three individual experiments. Error bars represent standard deviations.

In summary, multiple factors that are known to play a role in autophagy maturation were shown to be altered in senescence. In addition, it was shown that these factors are regulated by p38. This suggests that p38 provokes a blockade in autophagosome turnover by acting on multiple levels, including disruption of the microtubule network and of lysosomal functionality.

3.8 Attenuation of p38 by SB203580 in senescence rescues the microtubule network and restores the autophagy flux in a time-dependent manner

The results above prompted us to investigate whether exposure of senescent cells to SB would revert the phenotypes observed. In contrast to previous experiments, we first induced senescence with dox and then applied SB203580 to MCF-7/NeuT senescent cells (3days+dox) in a time-dependent manner. This experiment showed that already 6h of SB203580 exposure lead to reduced vacuolization and after 24 hours cells were almost deprived from autophagic vesicles.

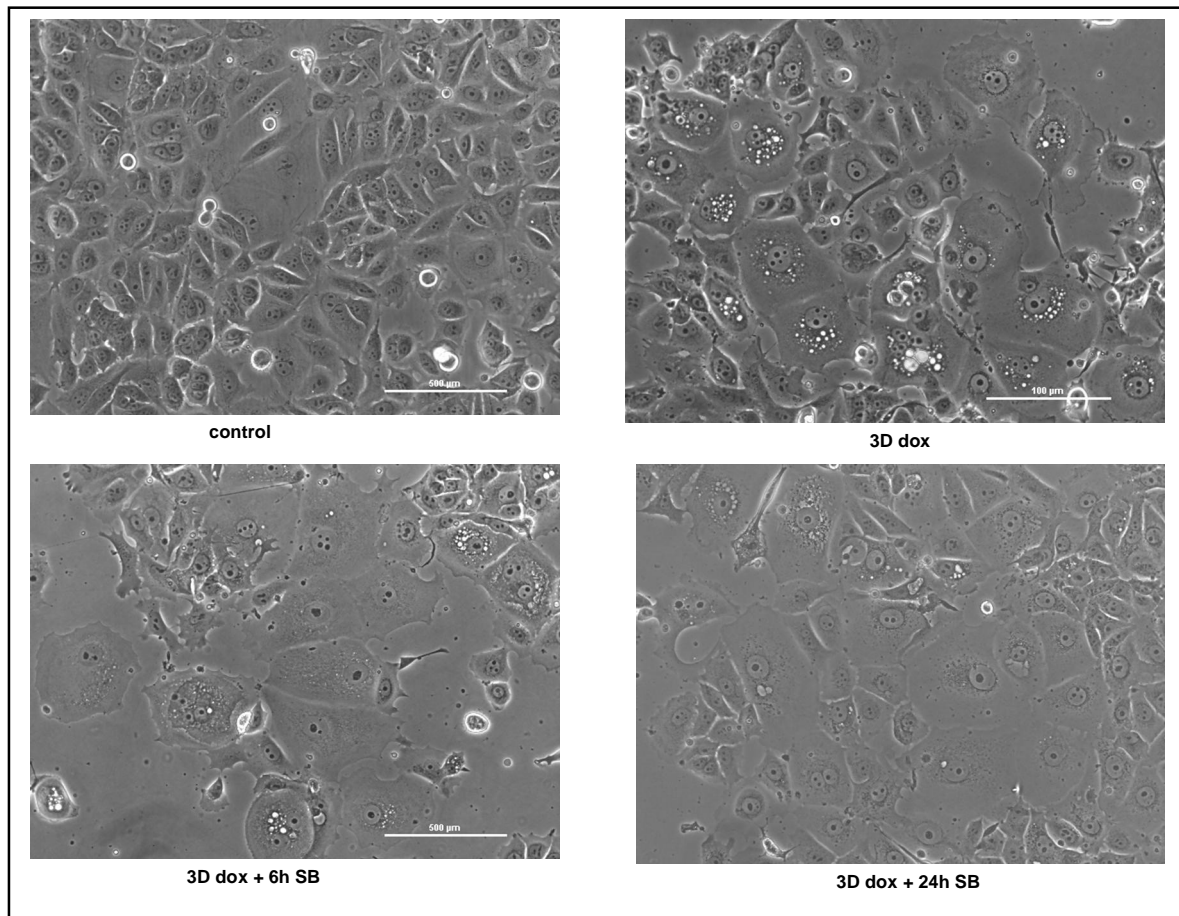


Figure 45: Vacuolization in MCF-7/NeuT senescent cells is abolished by treatment with the SB203580 inhibitor. Cells were exposed to doxycycline (1 µg/ml) for 3 days and then SB inhibitor (20 µM) was applied in a time dependent manner. Bar; 100 µm

Then we also checked whether SB203580 inhibition can rescue the expression of the autophagic marker LC3-II and the cargo protein p62. Our result showed lower levels of LC3-II and p62 expression indicating that the autophagy flux can be restored by SB203580.

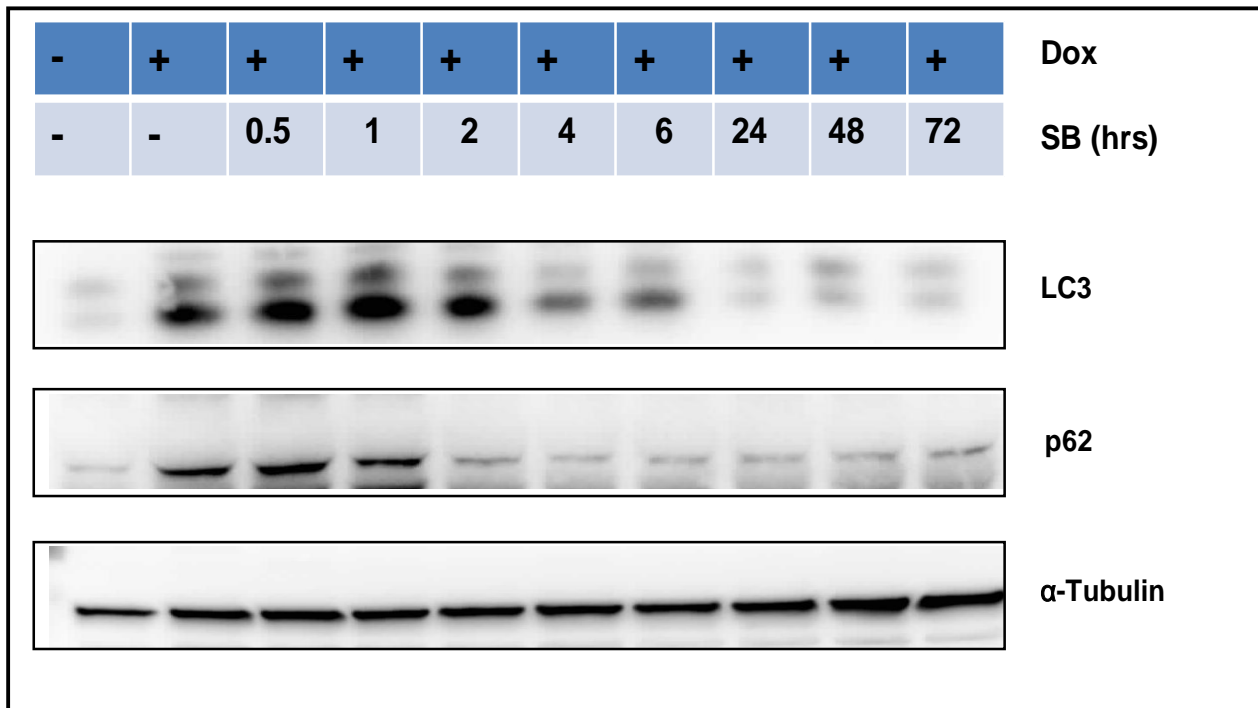


Figure 46: Effect of time-dependent SB inhibition of p38/MAPK pathway on LC3-II (autophagosomes) and p62 accumulation. Senescence cells were exposed to SB inhibitor (20 μ M) at different time points and LC3 and p62 protein were analyzed by western blot technique. α -Tubulin was used as the loading control.

In order to confirm that the reduction of LC3-II by SB203580 was not due to inhibition of autophagy but to restoration of the flux we applied vinblastine to 1h, 6h and 24h-SB-treated cells. This led to accumulation of LC3-II and p62 in the 6h and 24h-SB-treated cells, showing that SB had released the autophagy flux blockade and that vinblastine succeeded in blocking it.

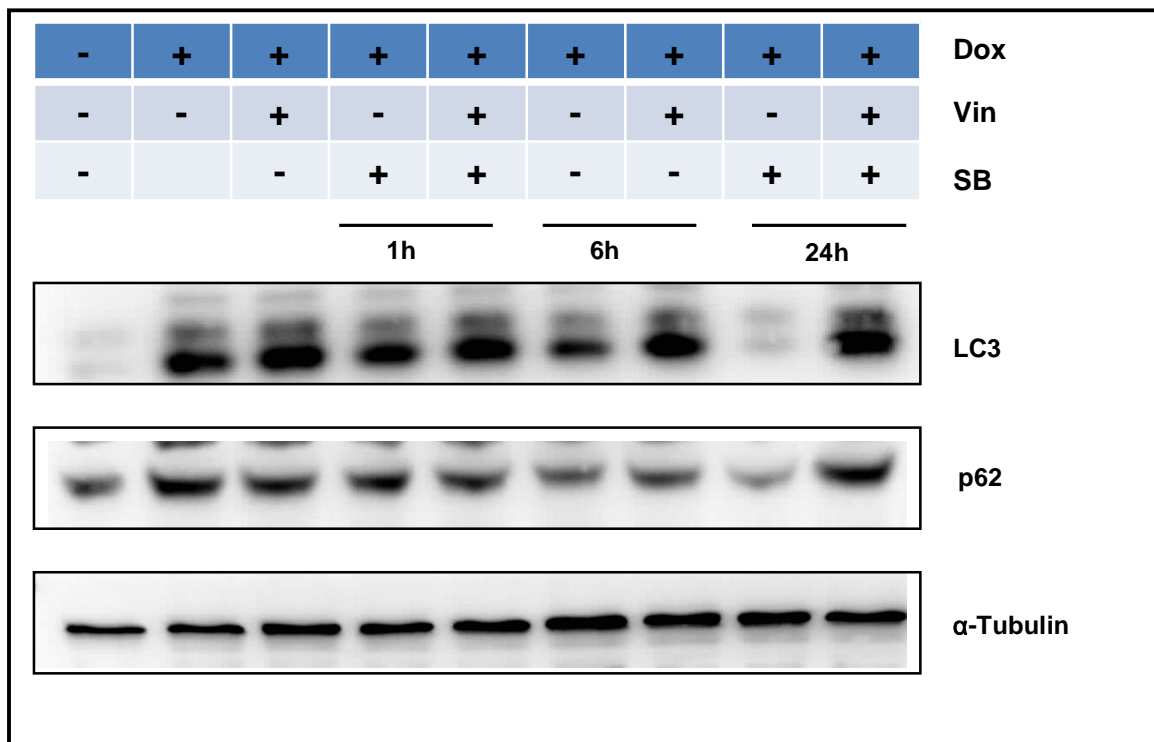


Figure 47: The p38 pathway negatively regulates autophagy and SB inhibitor restores autophagic flux. MCF-7/ NeuT cells were incubated with SB203580 (20 μ M) for 1hr, 6hr and 24hrs. Before protein lysate extraction, cells were exposed for 2 hours to vinblastine (50 μ M). α -Tubulin was used as the loading control.

We further investigated the rescue effect of the SB203580 inhibitor on microtubule dynamics. Concomitant dephosphorylation of MAP4 and phosphorylation of OP18 was observed upon SB203580 treatment, suggesting that polymerization of microtubules and thus restoration of the p38-damaged microtubule network begin to occur when the p38 pathway becomes silenced

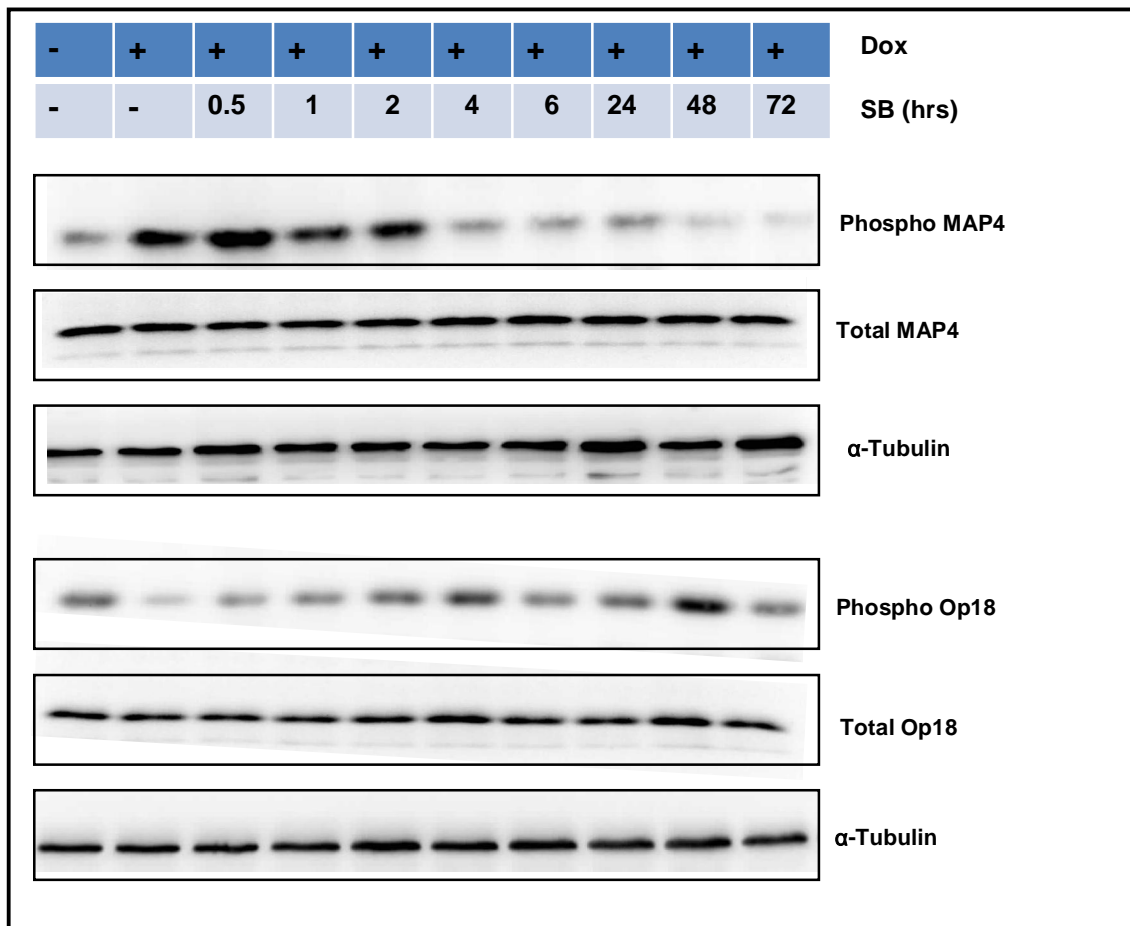


Figure 48: Effect of SB inhibition of p38/MAPK pathway on MAP4 phosphorylation and Op18 dephosphorylation. Phosphorylated MAP4, total MAP4, phosphorylated Op18 and total Op18 were analyzed by Western blot. α -Tubulin was used as the loading control.

For confirmation of the microtubule disruption and its restoration by SB203580 inhibitor we performed α -tubulin immunofluorescence staining. Senescent cells showing microtubule disruption started to restore their microtubule network after 6h SB203580 inhibitor and completely recovered it after 24hrs SB203580 treatment.

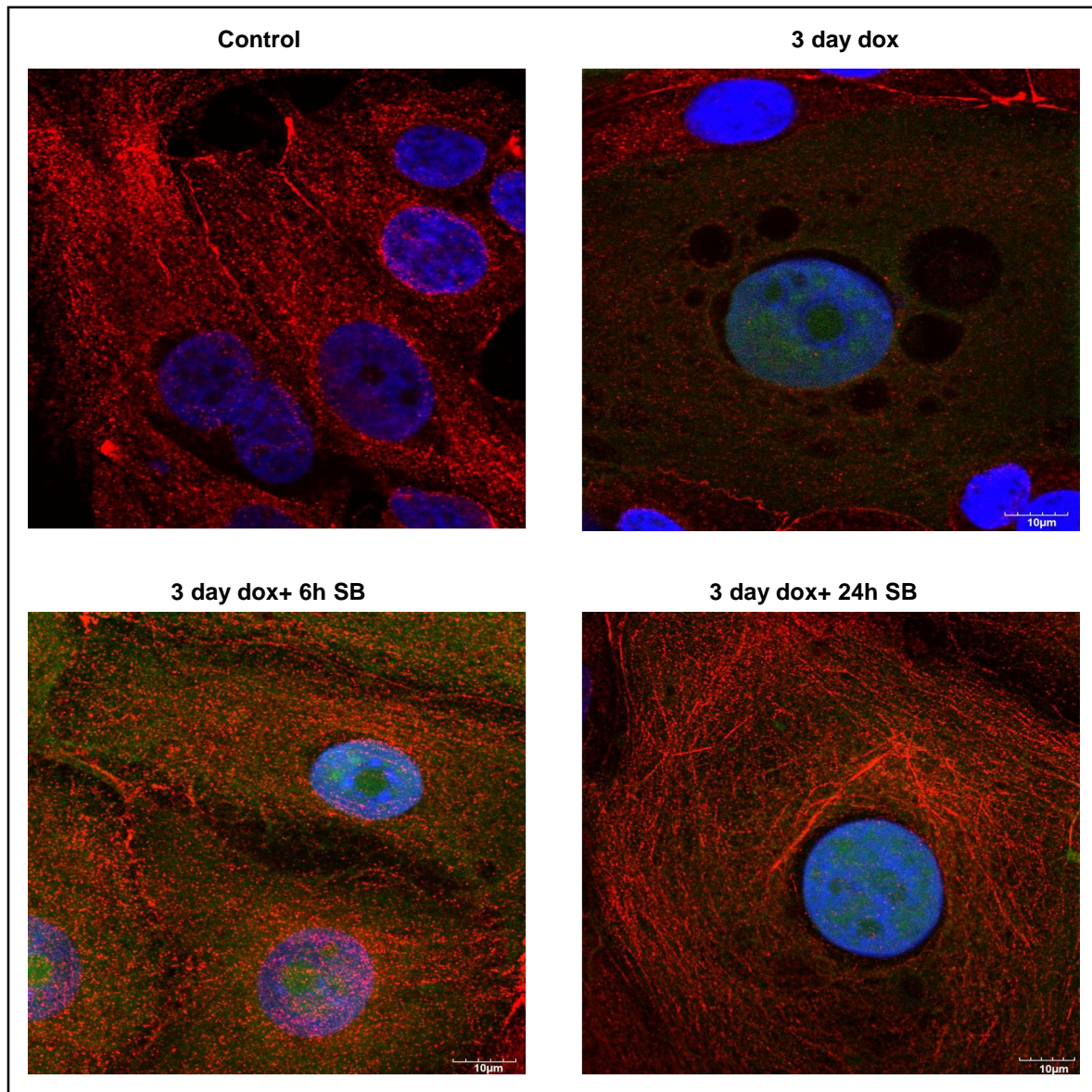


Figure 49: SB inhibition of p38/MAPK pathway recued the tubulin formation. Cells were subjected to SB203580 (20 μ M) treatment at the indicated time points. Detection of the microtubule network was performed by immuno staining with red (α -tubulin), blue (DAPI),and green (EGFP). Images are representative of multiple images taken of each condition. Bar; 10 μ m

In summary, p38 activation during oncogene induced senescence promotes microtubule network disruption. This, in turn, is assumed to impair fusion between autophagosomes and lysosomes and results in accumulation of autophagosomes. SB203580 inhibitor is able to restore the microtubule network and to normalize the autophagic flux.

3.8 p38 regulates the autophagy flux by a similar mechanism in other cell lines upon different kinds of stress

Our results on the MCF7/NeuT cell line prompted us to investigate whether p38 regulates the autophagy flux in other cell lines in a similar manner. For this purpose MCF-7, HeLa and HEK293 cells were treated with anisomycin, an inhibitor of protein synthesis that has previously been shown to trigger activation of the p38 MAPK pathway (Törocsik, 2000; Geiger, 2005).

In MCF-7 proliferating cells, phosphorylation of p38 is already clearly observed 30 minutes after anisomycin exposure and increases considerably after 4 hours, reaching highest levels at 48 h exposure. This suggests that perseverance of stress conditions is reflected by stronger p38 signaling. Interestingly, levels of LC3-II became higher already after 6h whereas p62 started to accumulate only after 48h.

Accumulation of both LC3-II and autophagic cargo after longer anisomycin treatment suggested again a blockade of the autophagic flux. This finding was confirmed by the LC3-II turnover assay with vinblastine treatment. In a similar manner than in NeuT oncogene-induced senescence (OIS) model, vinblastine was added for 2h at different time points of anisomycin exposure in order to block fusion of autophagosomes to lysosomes.

Our results clearly show a bi-phasic behavior of the autophagy flux upon anisomycin treatment: induction of autophagy during 6h-24h anisomycin exposure and blockade of autophagy after longer exposure.

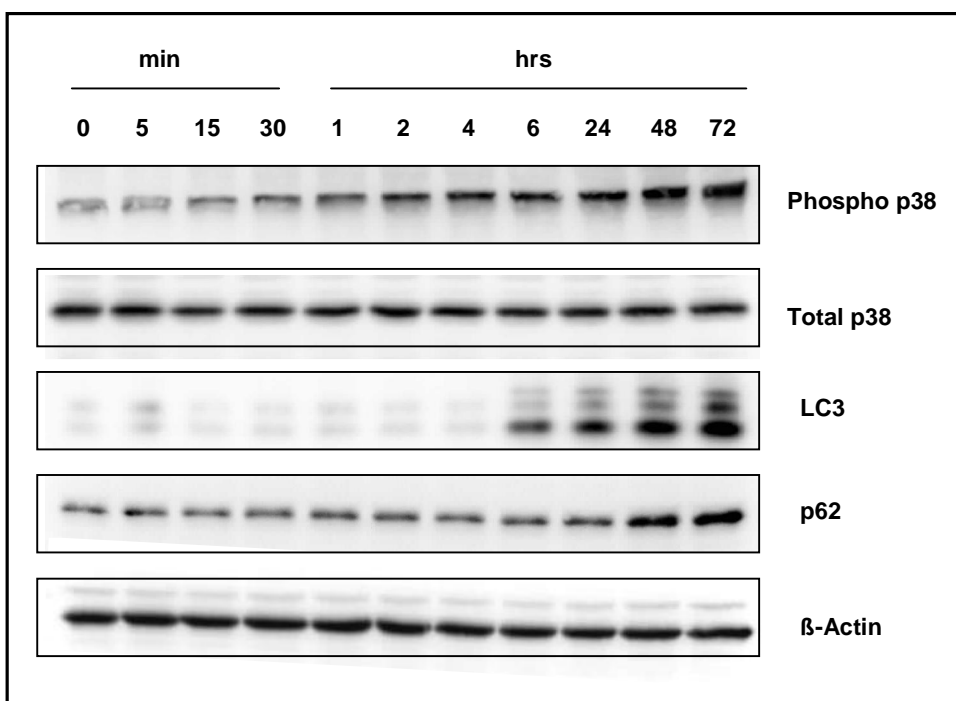


Figure 50: Activation of p38 signaling pathway and autophagosome formation by anisomycin. Proliferating MCF-7 were treated with anisomycin (10 μ M) for different time periods. Western blot analyses showing increased amounts of the autophagosome marker LC3-II and the cargo-adaptor protein p62 in senescent cells. β -Actin was used as the loading control.

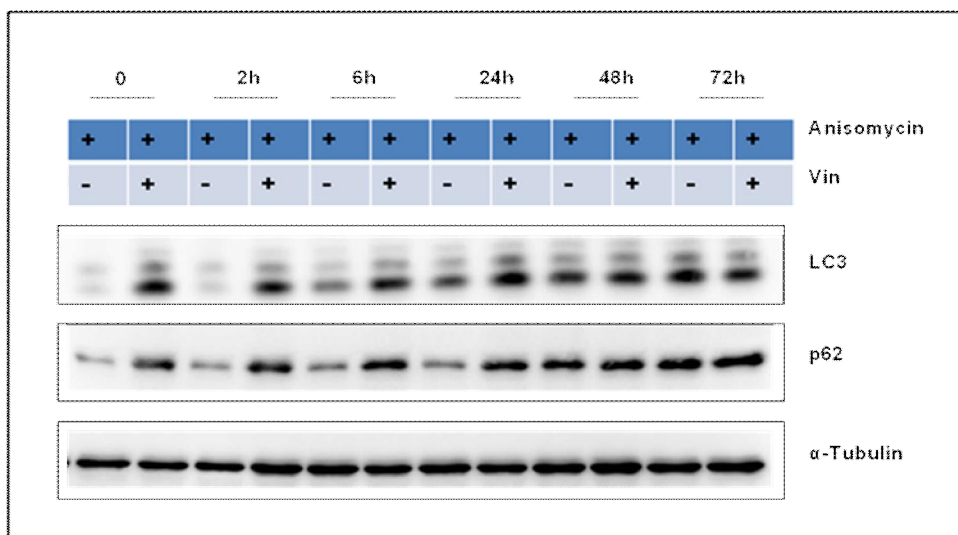


Figure 51: Autophagy is impaired by sustained activation of the p38 signaling pathway. In the turnover assay, cells were treated with 50 μ M of vinblastine for 2 hours before lysate extraction and LC3 and p62 were analyzed by immunoblots. α -Tubulin was used as the loading control.

To determine the effect of the anisomycin-activated p38 signaling pathway in blockade of autophagy in MCF-7 cells, the LC3-II turnover assay was performed in presence or absence of the SB inhibitor. Two different time points of anisomycin exposure, 24h + anisomycin, representative for induction of autophagy and 3d+anisomycin, representative for blockade of the flux, were investigated.

Our result showed that both induction of autophagy at 24h anisomycin exposure and blockade of autophagy maturation at 72 anisomycin exposure are mediated by p38.

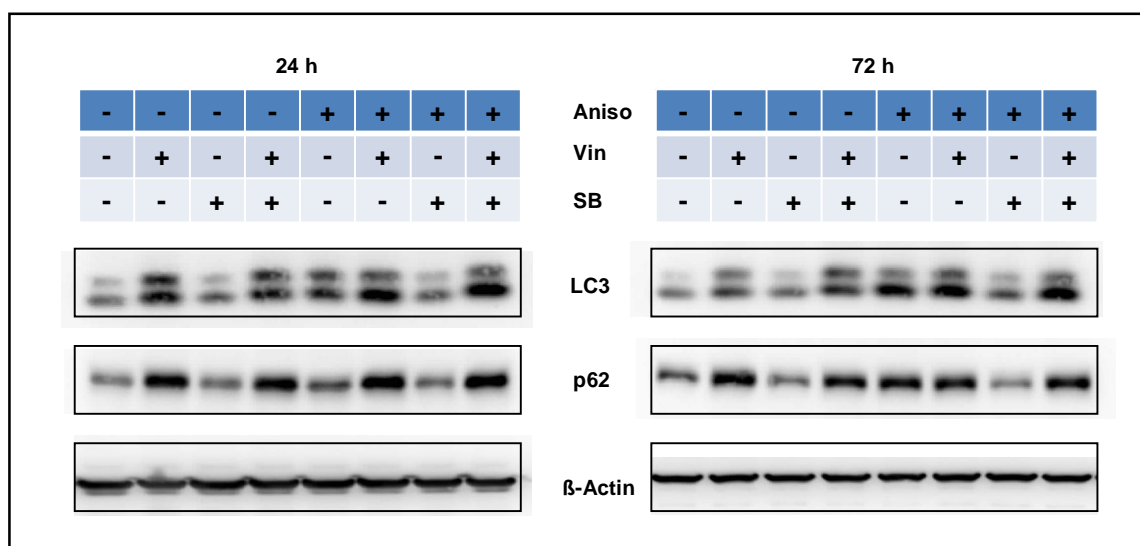


Figure 52: Sustained activation of p38 signaling pathway mediates blockade of autophagy. MCF-7 cells were pre-incubated with SB203580 (20 μ M) for 1 hr before time dependent anisomycin (10 μ M) treatment. Before protein lysate extraction cells were exposed for 2 hours to vinblastine (50 μ M). β -Actin was used as the loading control.

Next also LC3-puncta formation was analyzed and the influence of the p38 pathway on the levels of LC3-puncta was studied by confocal microscope images. The results of the LC3-II immunoblotting and immunofluorescence of LC3-puncta in the anisomycin (stress)-treated cells showed comparable results to those obtained in the oncogene induced senescence model.

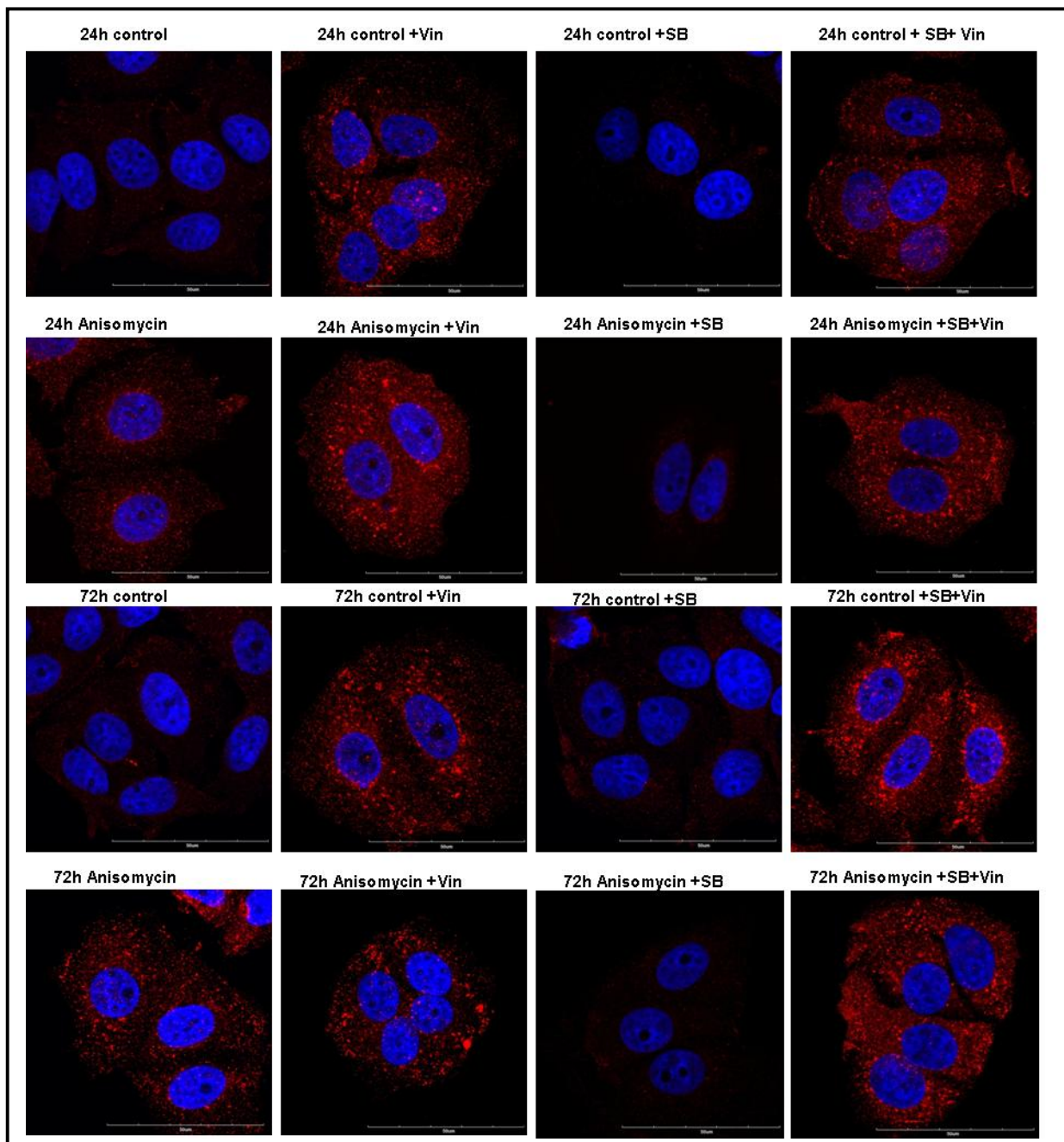


Figure 53: Subcellular localization of LC3 puncta. MCF-7 cells were subjected to anisomycin (10 μ M) treatment at the indicated time points. Pre-incubation with SB203580 (20 μ M) was done for 1 hr before addition of anisomycin. Vinblastine treatment was performed 2 h before fixation. Detection of the LC3 puncta was performed by immuno staining with an anti-LC3 antibody (red). The nuclei were labeled with DAPI (Blue). Images are representative of multiple images taken of each condition. Bar; 50 μ m

This reinforces the idea that stress signals initially induce autophagy but that sustained activation of the p38 pathway by prolonged stress conditions finally lead to a block in autophagy maturation. As in the oncogene induced senescence model, the mechanism by which anisomycin leads to a defective autophagosome turnover was also investigated. We focused on the role of the microtubule network. We also found that exposure of cells to anisomycin for longer than 48h led to p38-dependent phosphorylation of MAP4 and dephosphorylation of STMN1/OP18 and that disruption of the microtubule network, as shown by immunofluorescence staining of alpha-tubulin, accompanied these events.

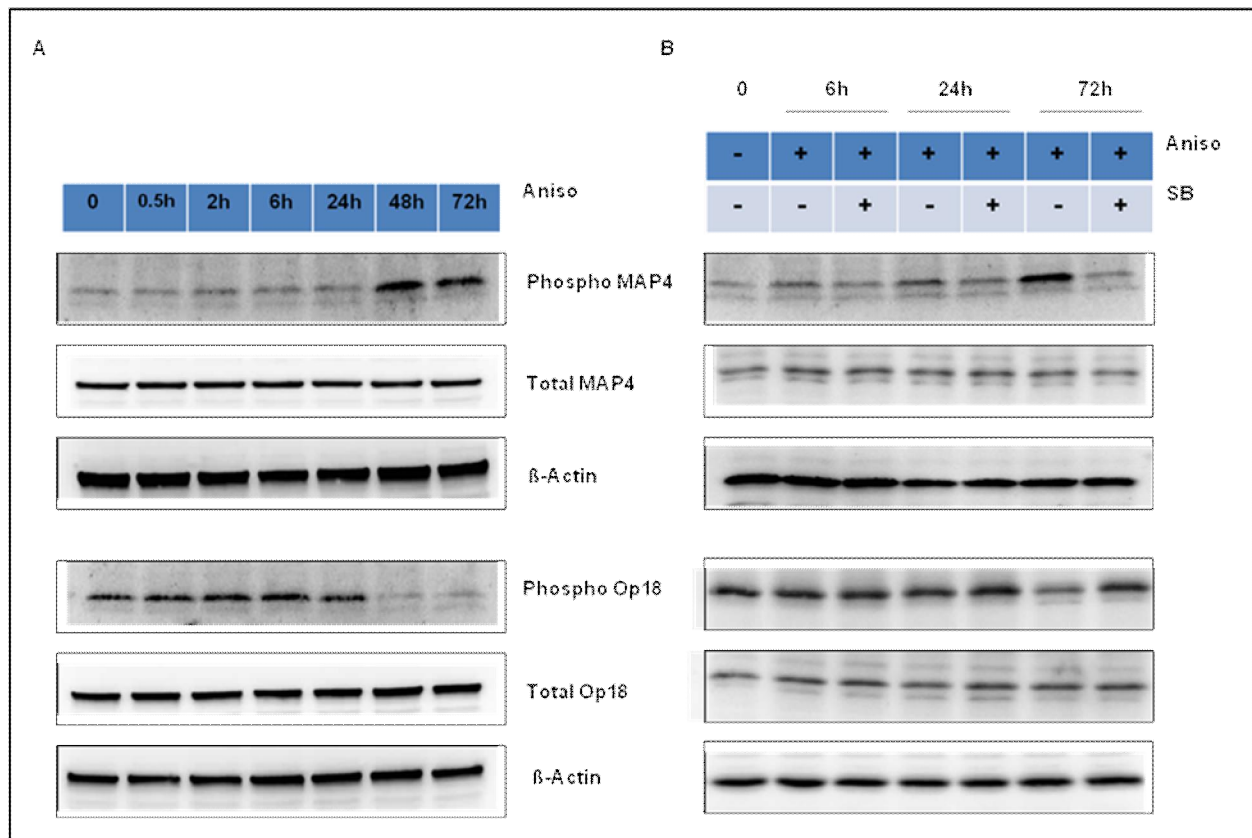


Figure 54: Destabilization of microtubules in anisomycin treated MCF-7 cells. A. Western blot analysis for phosphorylated MAP4, total MAP4, phosphorylated Op18 and total Op18. B. Cells were pre-incubated with the SB203580 inhibitor (20μM) 1 hr before anisomycin treatment. β-Actin was used as the loading control.

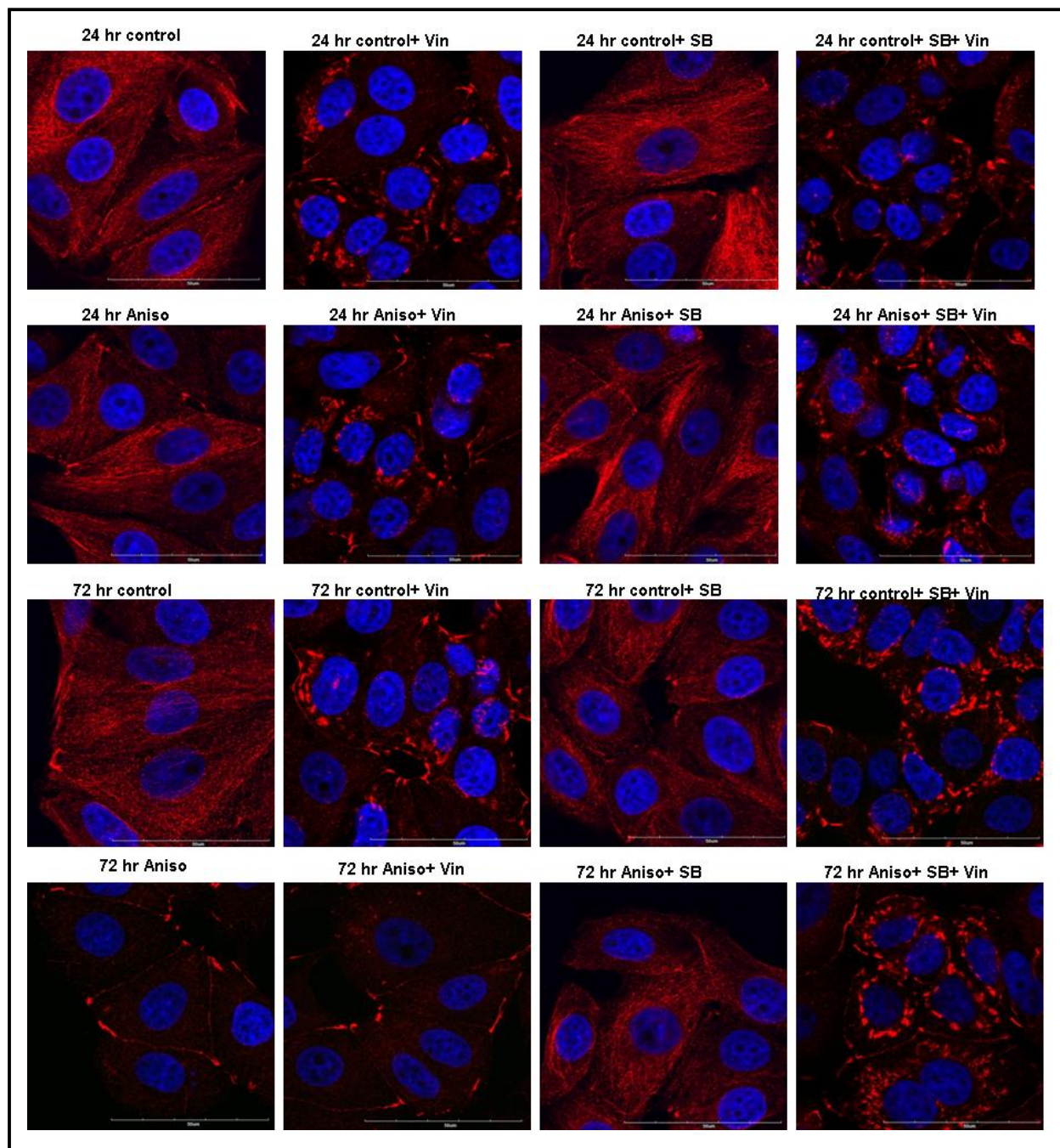


Figure 55: Disassembly of the microtubule network in MCF-7 cells via p38. Cells were subjected to treatment at the indicated time points. Pre-incubation with SB203580 (20 μM) was done for 1 hr before anisomycin. Vinblastine (50 μM) treatment was performed 2 h before fixation. Detection of the microtubule network was performed by immuno staining with α -tubulin (red), DAPI (blue). Images are representative of multiple images taken of each condition. Bar; 50 μm

Next we again analyzed the expression level of the dynein motor protein subunit DYNLL1 in anisomycin model. Our result showed the down regulation of dynein protein after 72 hours anisomycin incubation when the autophagic flux was impaired. This reduced protein level is also triggered by p38 signaling pathway.

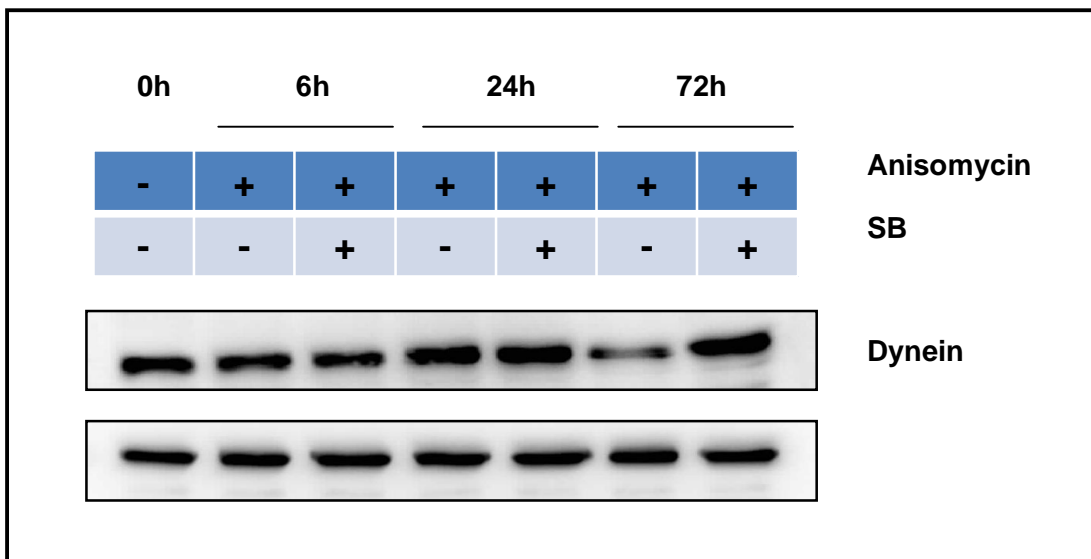


Figure 56: Down regulation of dynein motor protein subunit DYNLL1 by sustained activation of the p38 signaling pathway. Proliferating MCF-7 were treated with anisomycin (10 μ M) for different time periods and dynein motor protein subunit DYNLL1 was analyzed by westernblot. α -Tubulin was used as the loading control

In order to find out whether this mechanism is also operating in other cell lines in addition to breast cancer MCF-7 cells we performed the same set of experiments in HEK293 and HeLa cells. Anisomycin treatment of these two cell lines also activated the p38 pathway and led to the previously described biphasic behaviour in the autophagy flux.

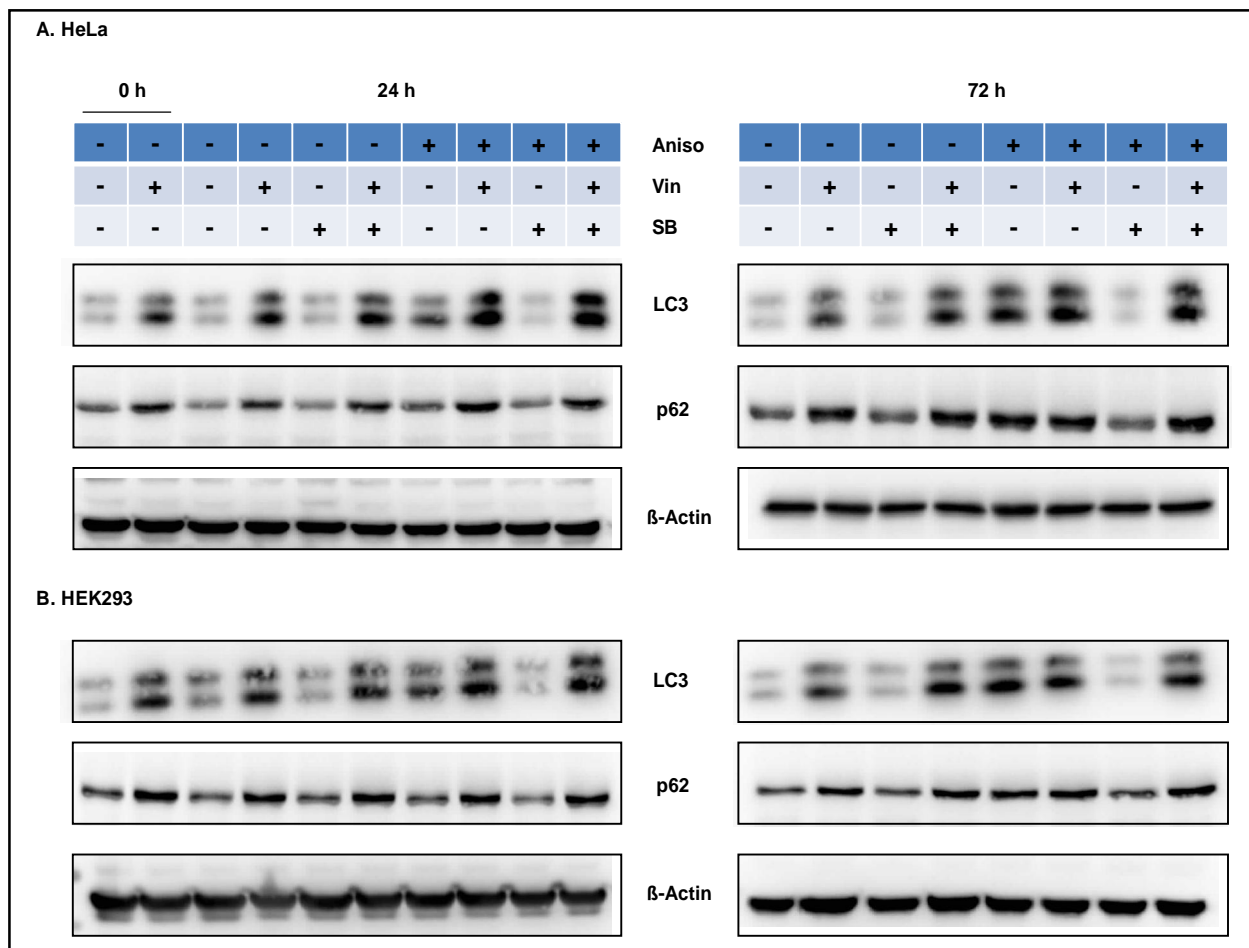


Figure 57: Autophagy maturation is impaired in HEK and HeLa cells by sustained activation of the p38 signaling pathway. A. HeLa. B. HEK293. Cells were pre-incubated with SB203580 (20 μ M) for 1 hr before time dependent anisomycin (10 μ M) treatment. In the LC3 turn over assay, cells were exposed for 2 hours to vinblastine (50 μ M) before protein lysate extraction. β -Actin was used as the loading control.

Moreover, the phosphorylation of MAP4 and dephosphorylation of Op18 by p38 also proved to be involved in these two additional cell lines.

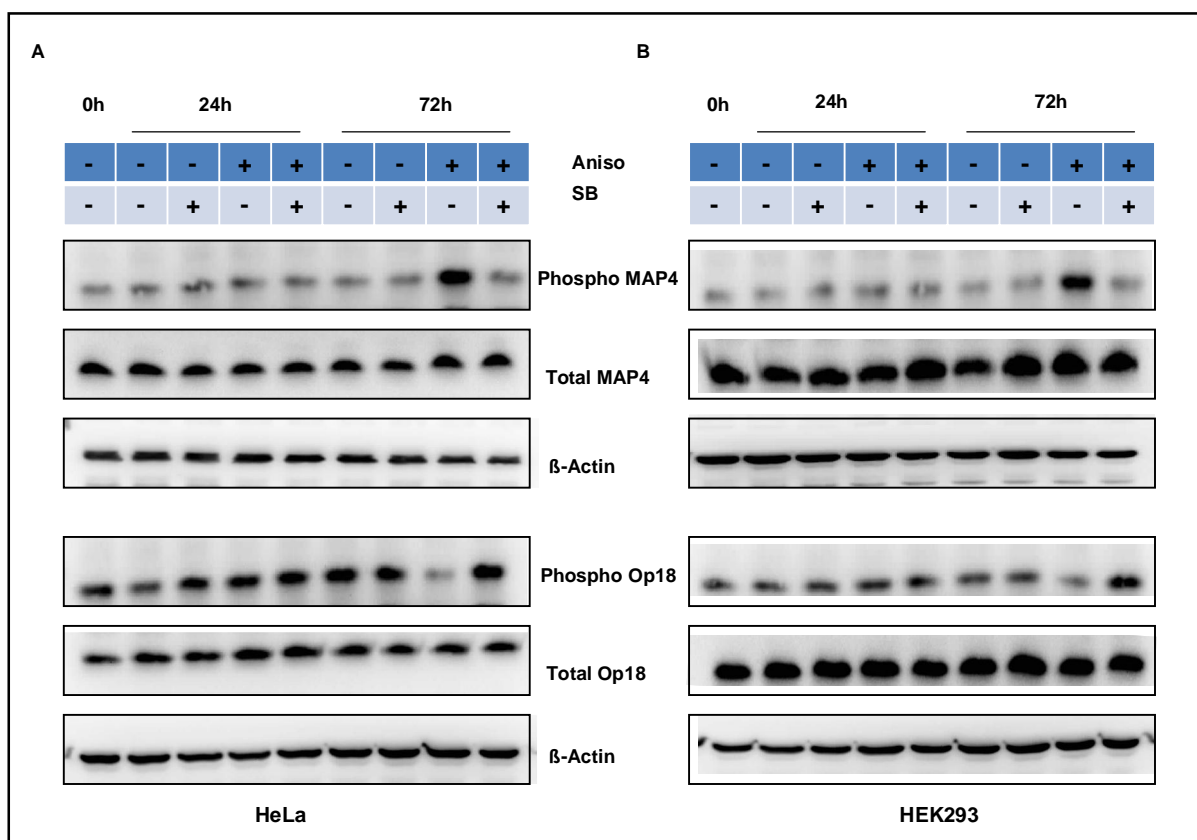


Figure 58: p38-MAPK-triggered autophagy flux blockade occurs via disruption of the microbule network. Cells were pre-incubated with the SB203580 inhibitor (20 μ M) 1 hr before anisomycin treatment. Western blot analysis for phosphorylated MAP4, total MAP4, phosphorylated Op18 and total Op18. β -Actin was used as the loading control.

In conclusion, the p38-mediated block of autophagy maturation happens in different contexts and cell lines in response to persistent stress conditions.

3.9 Biological consequences of the blockade in the autophagy flux

At present, the exact role of autophagy is highly controversial. Autophagy generally serves as a cell survival mechanism under stress conditions. Many recent studies have shown the cytoprotective role of autophagy in mammalian cells. Paradoxically, autophagy has also been implicated in cell death, called autophagic or type II programmed cell death. To determine the relationship between autophagy and cell survival in senescent cells we monitored cleavage of the PARP, poly (ADP-ribose) polymerase by western blot. Cleavage of PARP facilitates cellular disassembly and serves as a marker of cells undergoing apoptosis. Our result showed that in general senescent cells were resistance to PARP cleavage although we found cleavage at very late stage of senescence (14d+dox). This indicates that blockage of the autophagy flux during senescence does not compromise the survival ability of the cells.

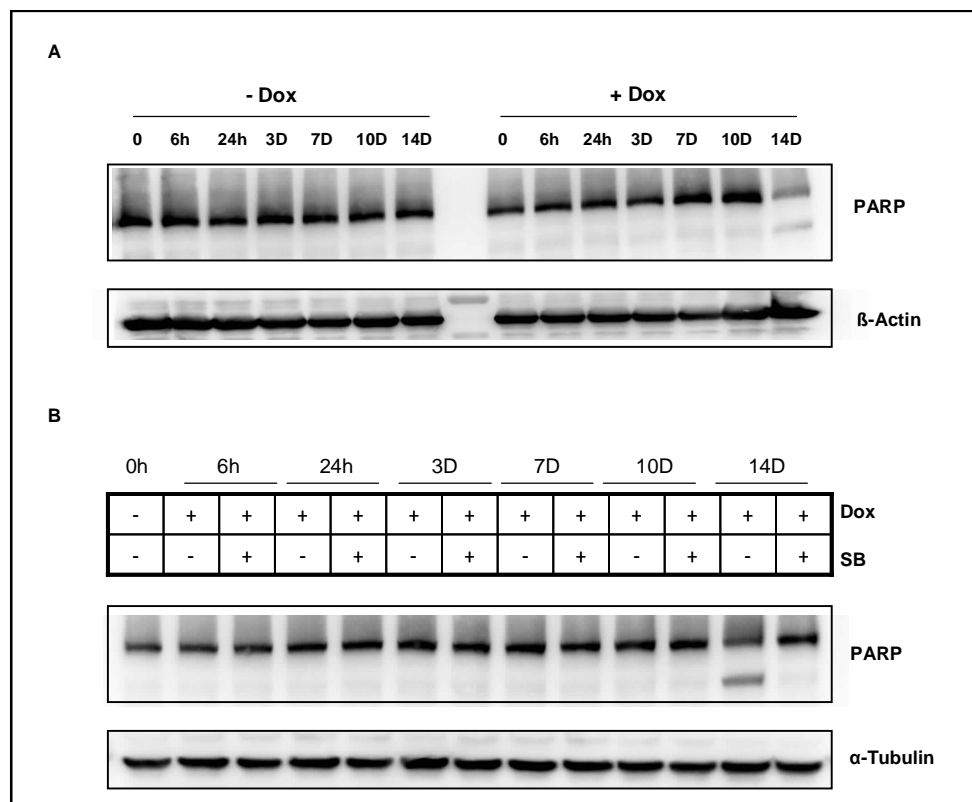


Figure 59: PARP cleavage in senescent cells. A. cells were analyzed for PARP cleavage by western blot analysis. B. Cells were pre-incubated with the SB203580 inhibitor (20 μ M) 1 hr before dox treatment and analyzed by western blot.

We also monitored PARP cleavage in our anisomycin model. After 24 hours incubation with anisomycin, when the autophagic flux was induced, no PARP cleavage was detected. However, PARP cleavage occurred when autophagy was impaired after longer anisomycin treatment. Because several studies have been shown that anisomycin is an apoptosis inducer in many cell types, we hypothesized that PARP cleavage in MCF-7 and HEK cells might be the p38-independent toxic effect of anisomycin. However, exposure of cells to the p38 inhibitor SB abolished PARP cleavage, demonstrating the role for the p38 pathway in promoting apoptosis after longer periods of anisomycin exposure.

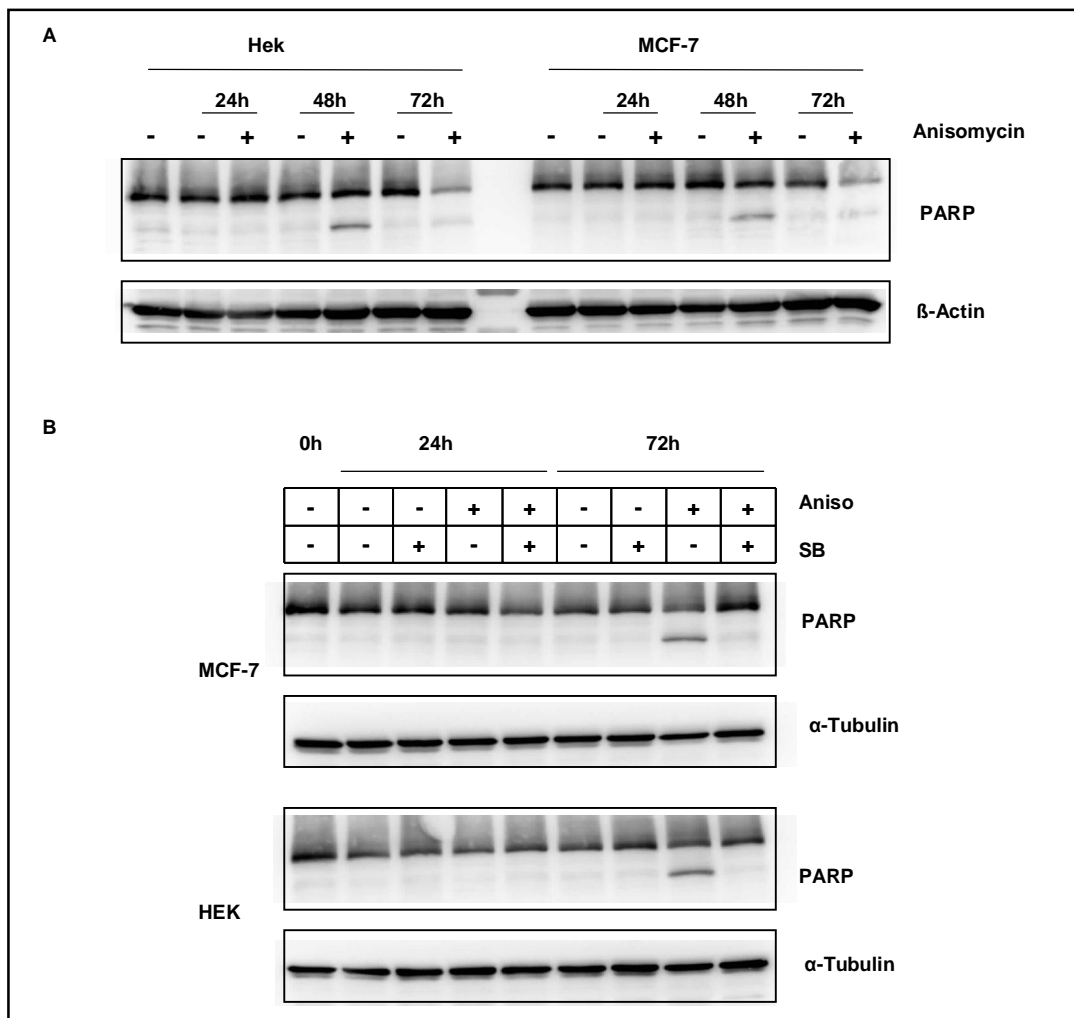


Figure 60: PARP cleavage in anisomycin treated cells. PARP cleavage was analyzed by Western blot in MCF-7 and Hek cells. B. Cells were pre-incubated with the SB203580 inhibitor (20 μ M) 1 hr before anisomycin (10 μ M) treatment.

CHAPTER FOUR
DISCUSSION

4.0 Discussion

4.1 Role of p38 in autophagy in oncogene induced senescence cells

It is well acknowledged that p38 plays a key role in autophagy regulation (Tang et al., 2008; Webber and Tooze, 2010; Keil et al., 2012; Mei et al., 2012; Choi et al., 2010; Moruno-Manchon et al., 2013; Vom Dahl et al., 2001; Homer et al., 2012; Paillas et al., 2012). However, a currently unresolved discrepancy is that approximately half of all publications addressing this question report a positive (Table-8), whereas the other half found an inhibitory influence of p38 on autophagy (Table-9). Negative feedback regulation of mTOR has been suggested as a possible mechanism of positive autophagy regulation by p38 (Tang et al., 2008), while compromised autophagosome formation (Webber and Tooze, 2010), maturation (Keil et al., 2012), downregulation of ULK1 (Mei et al., 2012) and microtubule disruption (Haussinger et al., 1999) may explain the negative influence on the autophagic flux. However, an explanation of the discrepancy (positive but also negative regulation by the same signaling pathway) is not possible considering the current literature. In order to bridge this gap, the question addressed in this work was how p38 regulates autophagy during the time-course of exposure to a stress stimulus.

First we applied a cell model of oncogene-induced senescence, where an oncogenic variant of ERBB2 (NeuT) can be inducibly expressed (Trost et al., 2005; Spangenberg et al., 2006; Cadenas et al., 2010; 2012). In this cell system NeuT expression leads to permanent p38 activation up to the longest studied time period of 14 days. We observed an early (24h) induction of the autophagic flux in contrast to a late inhibition (3-14 days). To test another stress stimulus besides NeuT overexpression, we used the protein synthesis inhibitor anisomycin (that is able to activate stress-activated kinases independently of its ability to block protein synthesis). Also anisomycin provoked an early induction and late inhibition of the autophagic flux. Both effects (induction and inhibition) could be reversed by the p38 inhibitor SB. The results could be reproduced in three different cell lines (MCF-7, HeLa and HEK293). It is important to note that in order to verify the effects of p38 on the autophagy flux both LC3-II and p62 levels were systematically analyzed in combination with the flux inhibitors vinblastine and bafilomycin A1, according to the proposed guidelines (Klionsky, DJ et al., 2008). In

addition, Western blot-based LC3-II turnover assays were in good agreement with the imaging of the LC3-punctae.

4.2 A model for regulation of autophagy by p38

The results obtained in this work show both p38-induced enhancements as well as inhibition of the autophagic flux. An important aspect is the duration and intensity of p38 activation. Therefore, in the model proposed (Fig-61) low or transitory stress conditions that moderately activate p38 stimulate the autophagic flux.

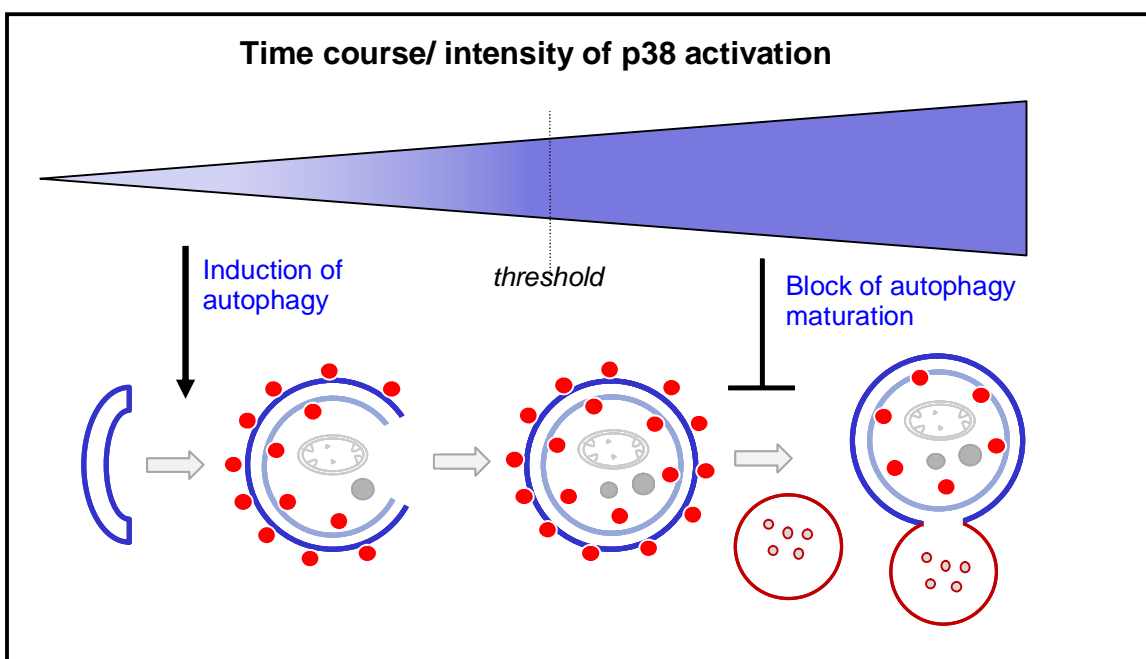


Figure 61: Proposed model for the role of p38 in autophagy. This model takes into account the duration and intensity of p38 activity. Low or transitory stress conditions that moderately activate p38 stimulate the autophagic flux by inducing early steps of the autophagic process. In contrast, more permanent and intensive stress that causes a strong activation of p38 blocks the autophagic flux at the maturation step.

In contrast, more permanent and intensive stress that causes a strong activation of p38 blocks the autophagic flux. The principle that short-term activation of p38 stimulates autophagy whereas long-term activation blocks it was confirmed in different cell systems

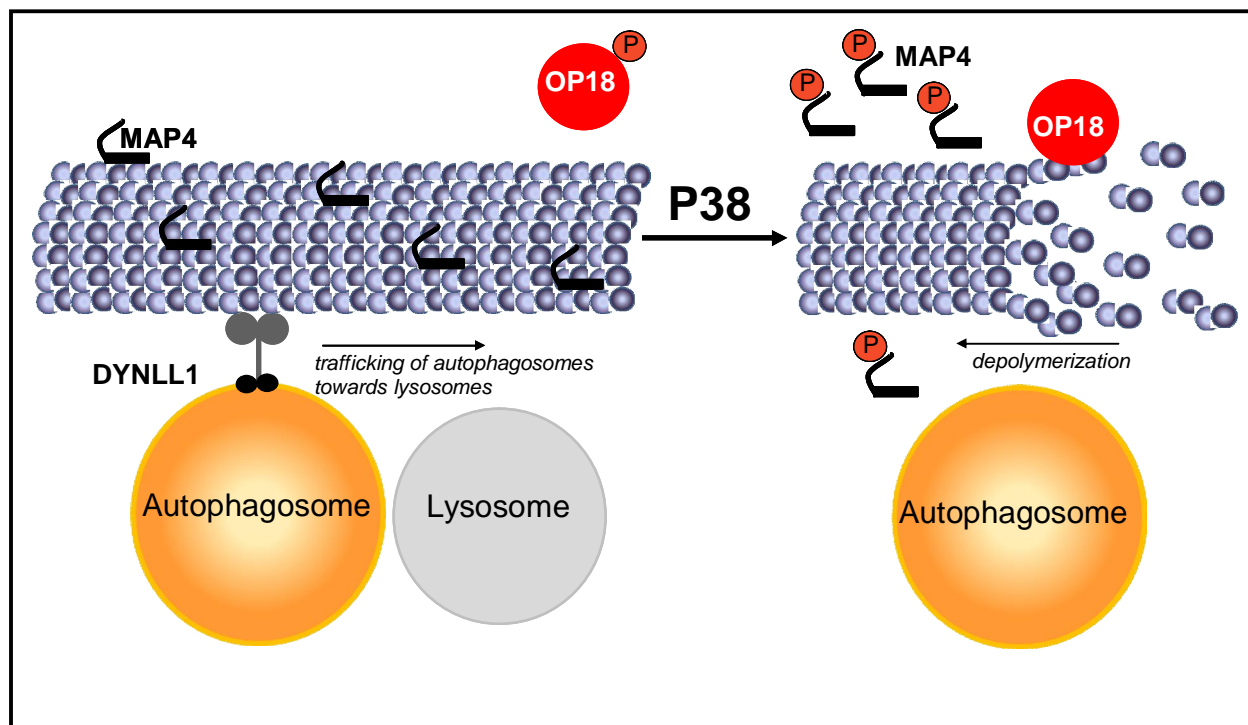
under stress stimuli, as mentioned above. The molecular mechanisms by which p38 was found to exert these effects are discussed in the following sections.

4.3 Mechanism of late block of autophagy by p38

The block of the autophagic flux is the more prominent phenomenon observed in this work. It could be shown that this block is accompanied by a compromised microtubule network (Fig-38 in Results). In addition it was found that modulating the phosphorylation status of the microtubule associated proteins MAP4 and STMN1/OP18 is one important mechanism by which p38 controls microtubule dynamics (Fig-62 in Discussion and Fig-39 in Results). Accordingly, p38-mediated microtubule depolymerization involves phosphorylation and thus inactivation of the microtubule stabilizing protein MAP4 and concomitant dephosphorylation followed by activation of the microtubule de-stabilizing protein STMN1/OP18.

The roles of the microtubule network and of the dynein motor protein complex in autophagy have been investigated in numerous studies (Fass et al., 2006; Jahreiss, L. et al., 2008; Kochl, R. et al., 2006; Webb, J.L. 2004; Ravikumar, B et al., 2005; Kimura S. et al., 2008). It has also been shown that p38MAPK can modulate cytoskeleton dynamics by directly regulating microtubule associated proteins (Hu J.Y. et al., 2010). But this study is, to the best of our knowledge, the first one to recognize that p38 affects autophagosome maturation by compromising microtubule stability and downregulating motor proteins. This study suggests also for the first time that MAP4 and STMN1/OP18 can influence the autophagy flux via their their microtubule assembly-disassembly properties.

In addition to these p38-triggered post-translational modifications of MAPS, also a "late stage" p38-dependent downregulation of the dynein motor subunit DYNLL1 at both gene and protein levels was observed in our senescence model and confirmed in the anisomycin model. Regulation of DYNLL1 expression by p38 had never been reported



before and thus it represents a novel mechanism of regulating autophagy.

Figure 62: Mechanism by which p38 leads to a blocked autophagic flux. P38 signaling dephosphorylates, and thus activates the microtubule depolymerizer OP18/STMN1; it phosphorylates MAP4 provoking its detachment from microtubules and their subsequent destabilization and it downregulates expression of dynein subunits, such as DYNLL1. These events impair trafficking of autophagosomes

Since both microtubules and the dynein motor complex have been shown to be involved in autophagosome trafficking to the lysosome (Ravikumar, B et al., 2005; Kimura S. et al., 2008), the afore-mentioned events lead to impaired autophagosome-lysosome fusion. Thus, the demonstrated late stage after p38 activation characterized by blocked autophagic flux is a consequence of impaired trafficking via microtubules. Other p38-mediated alterations in gene expression observed in this study such as downregulation

of the cathepsin D and lysosomal vacuolar ATPase subunit ATP6VOA2 (Fig-43 and Fig- 44 in result part) are also found to play an important role in inhibiting the autophagic flux by compromising lysosomal activity. This suggests that p38 signaling directs inhibition of autophagy by acting on a multitude of downstream substrates.

4.4 Mechanism of early induction of autophagy by p38

Further studies will be required to identify the specific mechanisms used by p38 to positively regulate autophagy induction under low-stress conditions. Interestingly, p38 has been predicted to phosphorylate ULK1 (Mack et al., 2012) at a consensus p38 phosphorylation site. Unfortunately, no antibody that specifically recognizes this putative p38-phosphorylation site is commercially available up to date. It is also noteworthy that DYNLL1 has been implicated in a recent study in the control of autophagosome formation (Di Bartolomeo, S.D. et al., 2010). The authors could show that the interaction between DYNLL1/2 and the Beclin1-interacting protein AMBRA1 keeps the Beclin1-Vps34 complex attached to the cytoskeleton. Induction of autophagy releases the AMBRA1-Beclin1-Vps34 complex from dynein and enables its localization to the endoplasmic reticulum where autophagosome formation is thought to occur. Moreover, the same study showed that knockdown of DYNLL1 resulted in enhanced LC3 lipidation. This prompted us to hypothesize p38-mediated downregulation of DYNLL1 as a possible mechanism to induce autophagy. However, decreased levels of DYNLL1 in our experimental models are only observed at late stages of p38 activation, when autophagy is impaired. Therefore, this mechanism can not be responsible for the initial induction of autophagy.

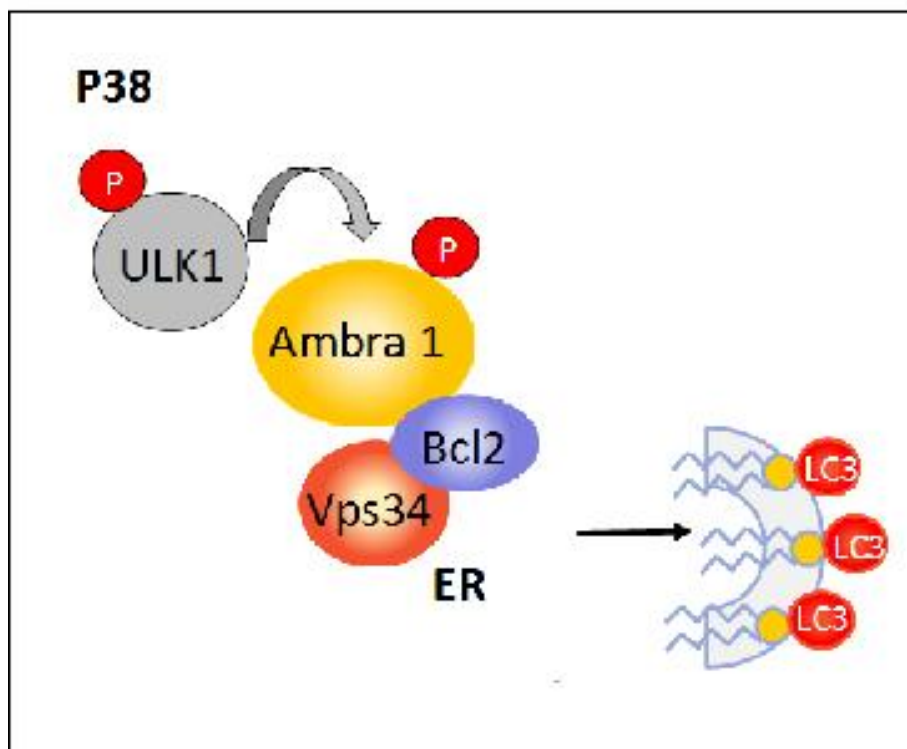


Figure 63: Possible mechanism by which p38 may induce autophagy (this is a speculation). p38 could phosphorylate ULK1, which is essential for induction of autophagy by promoting assembly of the AMBRA1-Bcl2-Vps34 complex and autophagosome formation.

4.5 Does p38 regulate autophagy in other stress/pathological conditions by a similar mechanism?

The results obtained by both experimental models in different cell lines suggest a general role of the p38 MAPK-cytoskeleton axis in the negative regulation of late steps of autophagy. Interestingly, in several neurodegenerative diseases that are characterized by an impaired autophagy flux and accumulation of autophagosomes/autolysosomes (Alzheimer disease, AD, Parkinson disease, PD) there is evidence for p38 playing a role in the pathophysiology of disease. One of the suggested functions of p38 in AD is phosphorylation of *tau* (MAPT), which is a neuron-specific microtubule-associated protein with a similar function in microtubule dynamics as MAP4.

Hyperphosphorylated *tau* causes its aggregation and therefore compromises microtubule-dependent axonal transport (Shahpasand et al., 2012). Pharmacological inhibition of p38 has been shown to alleviate the pathophysiology of the disease. However the underlying mechanisms remain to be elucidated. In light of our results, it could be plausible that p38-mediated phosphorylation of *tau* leads to AD-associated impaired autophagic clearance *via* destabilization of microtubules. In this case we would assume that p38-inhibition releases the blockade of autophagy in neurodegenerative diseases. This requires further investigation.

4.5 Biological consequences of impaired autophagy

Autophagy is believed to support cellular metabolism and cell survival under starvation and stress conditions. Many studies have reported a cytoprotective role of autophagy in mammalian cells (Wang et al., 2012; Tu et al., 2012; Moreau et al., 2010). On the other hand, autophagy has also been implicated in cell death, either directly by the so called autophagic or type II programmed cell death (Clarke, 1990; Kroemer et al., 2005; Bursch et al., 2001; Tsujimoto, 2005) or through its crosstalk with apoptosis (Salminen, A et al., 2012; Shi, M et al., 2012; Rikiishi, 2012), suggesting that excessive autophagy can also be detrimental. Our findings that compromised autophagy maturation is accompanied by apoptosis (observed in 3d anisomycin-treated cells and in 14 days senescent cells) are consistent with a cytoprotective role of autophagy. An intriguing observation was the late onset of apoptosis in the oncogene-induced senescence model. Here we observed PARP cleavage only after a relatively long period of blocked autophagy (14 days), whereas in the anisomycin model apoptosis became evident much earlier (Fig-59 and Fig-60).

Having demonstrated the biphasic nature of a p38-controlled autophagic flux its possible biological significance should be addressed. The consequences of initially induced autophagy are obvious. Initial stress sensors activate the well-known stress activated pathway p38 which in turn facilitates the removal of damaged cell components by increased autophagic flux. As already discussed by others, this supports cell survival

(Bernales et al., 2006; Ostefeld et al., 2008; Iwata et al., 2006). In this context it is of interest that p38 but not its sister stress pathway JNK plays a role in regulation of autophagy in MCF-7/NeuT cells. The explanation of the biological implications of blocked autophagy maturation after permanent p38 is much more difficult. One may expect that upon permanent stress, reflected by continuous p38 activation, the cell actively directs its fate towards cell death. On the other hand, the late block of autophagy may also serve a protective purpose. Two aspects in this scenario may be important: i) Blocking fusion of autophagosomes with lysosomes might be cytoprotective in situations in which excess of autophagy compromises the integrity of lysosomes (Pivtoraiko et al., 2009) ii) these cells may develop alternative mechanisms for clearance of cell damage in order to survive. A completely different explanation would be that it may be an advantage for an organism to remove cells by apoptosis that have experienced high levels of prolonged stress. The described autophagy block upon long term P38 activation may contribute to the cell's decision to undergo active cell death.

4.6 Role of autophagy in senescence

The relationship between autophagy and senescence has been previously investigated in a model of oncogenic Ras-induced senescence (Young et al., 2009) in IMR90 cells. In this experimental model autophagy was shown to be induced during the transition from the mitotic to the senescent state. Moreover, autophagy was shown to be essential for the establishment of senescence. In our study we also observed initial induction of autophagy upon oncogenic ERBB2 expression, however attenuation of the autophagic flux occurs simultaneously with the onset of senescence. In previous work with our MCF-7/NeuT cell line it was found that p38-mediated activation/upregulation of p21 is responsible for the establishment of senescence. Since in the current study p38 was found to negatively regulate autophagy, we assume that this negative effect of p38 on autophagy is part of the anti-tumor/fail-safe mechanism senescence is considered to be. This is in agreement with the classical view that autophagic activity decreases during aging and that the impaired autophagic clearance contributes to the aging-related accumulation of cellular damage.

In conclusion, in this work it could be shown that transient p38 activation causes enhanced autophagic flux whereas permanent p38 signaling blocks autophagy by compromising microtubule-mediated transport. This study demonstrates the importance of considering dynamics and kinetics of p38 activation to understand its importance on autophagy.

Tabel 8: p38 as positive regulator of autophagy

Reference	Stimulus	Cell line	Statement/ Proposed mechanism	Method employed to investigate p38 role	Method employed to detect autophagy
Tang et al., 2008	Accumulation of GFAP	U251 astrocytoma cells overexpressing GFAP	p38 becomes phosphorylated upon GFAP accumulation and induces autophagy via inhibition of mTOR	Pharmacological inhibition of p38 with SB 203580 Knockdown with p38 siRNA	LC3-II/LC3-I ratio by immunoblotting
Choi et al., 2010	Capsaicin exposure	MCF-7 and MDA-MB231 breast cancer cell lines	p38 becomes activated upon capsaicin exposure and induces autophagy by positively regulating the sequestration step		
Homer et al., 2012	Muramyl dipeptide (MDP)	HCT116 human colorectal adenocarcinoma	Autophagy induction requires p38	Pharmacological inhibition of p38 with SB 203580 Knockdown with p38 siRNA	
Paillas et al., 2012	SN-38 (the active metabolite of irinotecan)	HCT116 human colorectal adenocarcinoma	p38 becomes activated upon SN-38 exposure and induces autophagy		
Moruno-Manchon et al., 2013	Addition of glucose under starvation conditions	NIH/3T3, MEFs	p38 becomes activated upon glucose exposure and induces autophagy	Pharmacological inhibition of P38 with SB 203580 Knockdown with p38 siRNA	LC3-II levels +/- NH4Cl and Leupeptin by immunoblotting

Table 9: p38 as a negative regulator of autophagy

Reference	Stimulus	Cell line	Proposed mechanism	Method employed to investigate p38 role	Method employed to detect autophagy
Haussinger et al., 1999	Swelling induced by hypoosmolarity or glutamine, ethanol, or insulin	Rat hepatocytes	p38 becomes activated by hypo-osmotic live perfusion and leads to a decrease in cell proteolysis and inhibition of autophagic vacuole formation	Pharmacological inhibition of p38 with SB203580	Proteolysis
Vom Dahl et al, 2001	Swelling by hypoosmolarity	Rat hepatocytes	p38 becomes activated by hypo-osmotic live perfusion and leads to a decrease in autophagic vacuoles in a microtubule-dependent manner	Pharmacological inhibition of p38 with SB203580	Quantification of volume of autophagic vacuoles
Weber and Tooze 2010	Starvation	HEK293	Phosphorylated p38alpha leads to inhibition of autophagy through sequestering of p38IP, which is required for mAtg9 trafficking and thus autophagosome formation	Overexpression of p38alpha	LC3-II/LC3-I ratio +/- Leupeptin

Keil et al., 2012	Overexpression of Gadd45 β +/- Starvation	NIH3T3	p38 becomes targeted to autophagosomes by Gadd45 β /MEKK4 and inhibits fusion to lysosomes via phosphorylation of Atg5		
Mei et al., 2012	Cholesterol loading with LDL	Macrophage cell line THP1	p38 becomes phosphorylated upon LDL loading and inhibits induction of autophagy by downregulating ULK1 expression	Pharmacological inhibition of P38 with SB 203580 Knockdown with p38 siRNA	LC3-II/LC3-I ratio by immunoblotting GFP-LC3 dot formation by fluorescence microscopy

CHAPTER FIVE
LITERATURE

5.0 Literatures

- Alessil, D. R., Saito, Y., Campbell, D. G., Cohen, P., Sithanandam, G., Rapp, U., Ashworth, A., et al. (1994). Identification of the sites in MAP kinase kinase-1 phosphorylated by p74raf1. *EMBO J*, 13(7), 1610–1619.
- Amaravadi, R. K., Yu, D., Lum, J. J., Bui, T., Christophorou, M. A., Evan, G. I., Thomas-tikhonenko, A., et al. (2007). Autophagy inhibition enhances therapy-induced apoptosis in a Myc-induced model of lymphoma. *The Journal of clinical Investigation*, 117(2), 326–336.
- Aplin, A., Jasionowski, T., Tuttle, D., Lenk, S., & Dunn, W. (1992). Cytoskeletal elements are required for the formation and maturation of autophagic vacuoles. *J Cell Physiol*, 152, 458–466.
- Arico, S., Petiot, A., Bauvy, C., Dubbelhuis, P. F., Meijer, A J., Codogno, P., & Ogier-Denis, E. (2001). The tumor suppressor PTEN positively regulates macroautophagy by inhibiting the phosphatidylinositol 3-kinase/protein kinase B pathway. *The Journal of biological chemistry*, 276(38), 35243–35246.
- Avruch, J., Khokhlatchev, a, Kyriakis, J. M., Luo, Z., Tzivion, G., Vavvas, D., & Zhang, X. F. (2001). Ras activation of the Raf kinase: tyrosine kinase recruitment of the MAP kinase cascade. *Recent progress in hormone research*, 56, 127–55.
- Badger, A., Cook, M. N., Lark, M. W., Newman-Tarr, T. M., Swift, B. a, Nelson, a H., Barone, F. C., et al. (1998). SB 203580 inhibits p38 mitogen-activated protein kinase, nitric oxide production, and inducible nitric oxide synthase in bovine cartilage-derived chondrocytes. *Journal of immunology*, 161(1), 467–473.
- Baehrecke, E. H. (2003). Autophagic programmed cell death in Drosophila. *Cell death and differentiation*, 10(9), 940–945.

- Barth, S., Glick, D., & Macleod, K. F. (2010). Autophagy: assays and artifacts. *The Journal of pathology*, 221(2), 117–124. doi:10.1002/path.2694.
- Bartkova, J., Rezaei, N., & Lontos, M. (2006). Oncogene-induced senescence is part of the tumorigenesis barrier imposed by DNA damage checkpoints. *Nature*, 444(7119), 633–637.
- Berg, T. O., Fengsrud, M., Strømhaug, P. E., Berg, T., & Seglen, P. O. (1998). Isolation and Characterization of Rat Liver Amphisomes. *The Journal of biological chemistry*, 273(34), 21883–21892.
- Bernales, S., McDonald, K., & Walter, P. (2006). Autophagy counterbalances endoplasmic reticulum expansion during the unfolded protein response. *PLoS Biol*, 4(12), e423.
- Bhui, K., Tyagi, S., Prakash, B., & Shukla, Y. (2010). Pineapple bromelain induces autophagy, facilitating apoptotic response in mammary carcinoma cells. *Biofactors*, (36), 474–482.
- Borsello, T., Croquelois, K., Hornung, J. P., & Clarke, P. G. (2003). N-methyl-d-aspartate-triggered neuronal death in organotypic hippocampal cultures is endocytic, autophagic and mediated by the c-Jun N-terminal kinase pathway. *Eur. J. Neurosci.*, 18, 473–485.
- Boya, P., Gonzalez-Polo, R., Casares, N., Perfettini, J., Dessen, P., Larochette, N., Metivier, D., et al. (2005). Inhibition of macroautophagy triggers apoptosis. *Mol Cell Biol*, 25(3), 1025–1040.
- Braig, M., Lee, S., & Loddenkemper, C. (2005). Oncogene induced senescence as an initial barrier in lymphoma development. *Nature*, 436(7051), 660–650.
- Brancho, D., Tanaka, N., Jaeschke, A., Ventura, J.-J., Kelkar, N., Tanaka, Y., Kyuuma, M., et al. (2003). Mechanism of p38 MAP kinase activation in vivo. *Genes & development*, 17(16), 1969–78.

- Bulavin, D. V., Demidov, O. N., Saito, S., Kauraniemi, P., Phillips, C., Amundson, S. a, Ambrosino, C., et al. (2002). Amplification of PPM1D in human tumors abrogates p53 tumor-suppressor activity. *Nature genetics*, 31(2), 210–215.
- Bursch, W. (2001). The autophagosomal-lysosomal compartment in programmed cell death. *Cell death and differentiation*, 8(6), 569–81.
- Bélanger, M., Rodrigues, P. H., Dunn, W. A., & Progulske-fox, A. (2006). Autophagy, A highway for porphyromonas gingivalis in Endothelial Cells. *Autophagy*, 2(3), 165–170.
- Cadenas, C., Franckenstein, D., Schmidt, M., Gehrmann, M., Hermes, M., Geppert, B., Schormann, W., et al. (2010). Role of thioredoxin reductase 1 and thioredoxin interacting protein in prognosis of breast cancer. *Breast Cancer Res.*, 12(3), R44.
- Cadenas, C., Vosbeck, S., Hein, E., Hellwig, B., Langer, A., Hayen, H., Franckenstein, D., et al. (2012). Glycerophospholipid profile in oncogene-induced senescence. *Biochim Biophys Acta*, 1821(9), 1256–1268.
- Campisi, J. (2000). Cancer, aging and cellular senescence. *In Vivo*, 14(1), 183–188.
- Campisi, J. (2005). Senescent cells, tumor suppression, and organismal aging: good citizens, bad neighbors. *Cell*, 120(4), 513–522.
- Campisi, J., & d'Adda di Fagagna, F. (2007). Cellular senescence: when bad things happen to good cells. *Nature Reviews Molecular Cell Biology*, 8, 729–740.
- Cardone, M. H., Salvesen, G. S., Widmann, C., Johnson, G., & Frisch, S. M. (1997). The regulation of anoikis: MEKK-1 activation requires cleavage by caspases. *Cell*, 90(2), 315–323.
- Chan, E. (2009). mTORC1 phosphorylates the ULK1-mAtg13-FIP200 autophagy regulatory complex. *Sci. Signal.*, 2, pe51.

- Chan, H., Narita, M., Lowe, S., & Livingston, D. (2005). The p400 E1A-associated protein is a novel component of the p53 - p21 senescence pathway. *Genes & development*, 19, 196–201.
- Chen, J. L., Lin, H. H., Kim, K. J., Lin, A., Forman, H. J., & Ann, D. K. (2008). Novel roles for protein kinase C delta-dependent signaling pathways in acute hypoxic stress-induced autophagy. *J Biol Chem*, 283, 34432–34444.
- Chen, Q., Prowse, K., Tu, V., Purdom, S., & Linskens, M. (2001). Uncoupling the senescent phenotype from telomere shortening in hydrogen peroxide-treated fibroblasts. *Exp Cell Res*, 265, 294–303.
- Chen, Z., Trotman, L., Shaffer, D., Lin, H., Dotan, Z., Niki, M., Koutcher, J., et al. (2005). Crucial role of p53-dependent cellular senescence in suppression of Pten-deficient tumorigenesis. *Nature*, 436, 725–730.
- Cheng, Y., Qiu, F., Tashiro, S., Onodera, S., & Ikejima, T. (2008). ERK and JNK mediate TNFalpha-induced p53 activation in apoptotic and autophagic L929 cell death. *Biochem. Biophys. Res. Commun*, 376, 483–488.
- Choi, C. H., Jung, Y. K., & Oh, S. H. (2010). Autophagy induction by capsaicin in malignant human breast cells is modulated by p38 and extracellular signal-regulated mitogen-activated protein kinases and retards cell death by suppressing endoplasmic reticulum stress-mediated apoptosis. *Mol. Pharmacol*, 78, 114–125.
- Clarke, P. (1990). Developmental cell death: morphological diversity and multiple mechanisms. *Anat Embryol (Berl)*, 181(3), 195–213.
- Collado, M., Gil, J., & Efeyan, A. (2005). Tumour biology: senescence in premalignant tumours. *Nature*, 436(7051), 642.
- Colosetti, P., Puissant, A., Robert, G., Luciano, F., Jacquelin, A., Gounon, P., Cassuto, J., et al. (2009). Autophagy is an important event for megakaryocytic differentiation of the chronic myelogenous leukemia K562 cell line. *Autophagy*, 5, 1092–1098.

- Corcelle, E., Nebout, M., Bekri, S., Gauthier, N., Hofman, P., Poujeol, P., Fenichel, P., et al. (2006). Disruption of autophagy at the maturation step by the carcinogen lindane is associated with the sustained mitogen-activated protein kinase/extracellular signal-regulated kinase activity. *Cancer Res*, *66*, 6861–6870.
- Courtois-Cox, S., Jones, S., & Cichowski, K. (2008). Many roads lead to oncogene-induced senescence. *Oncogene*, *27*, 2801–2809.
- Courtois-Cox, S., Williams, S. M., Reczek, E. E., Johnson, B. W., McGillicuddy, L. T., Johannessen, C. M., Hollstein, P. E., et al. (2006). A negative feedback signaling network underlies oncogene-induced senescence. *Cancer cell*, *10*(6), 459–472.
- Crichton, D., Wilkinson, S., O'Prey, J., Syed, N., Smith, P., Harrison, P. R., Gasco, M., et al. (2006). DRAM, a p53-induced modulator of autophagy, is critical for apoptosis. *Cell*, *126*(1), 121–34.
- Cui, Q., Tashiro, S., Onodera, S., Minami, M., & Ikejima, T. (2007). Oridonin induced autophagy in human cervical carcinoma HeLa cells through Ras, JNK, and P38 regulation. *J. Pharmacol. Sci.*, *105*, 317–325.
- Da Silva, J., Pierrat, B., Mary, J. L., & Lesslauer, W. (1997). Blockade of p38 mitogen-activated protein kinase pathway inhibits inducible nitric-oxide synthase expression in mouse astrocytes. *The Journal of biological chemistry*, *272*(45), 28373–28380.
- Deak, M., Clifton, a D., Lucocq, L. M., & Alessi, D. R. (1998). Mitogen- and stress-activated protein kinase-1 (MSK1) is directly activated by MAPK and SAPK2/p38 and may mediate activation of CREB. *The EMBO journal*, *17*(15), 4426–4441.
- Debacq-Chainiaux, F Erusalimsky, J., Campisi, J., & O., T. (2009). Protocols to detect senescence-associated beta-galactosidase (SA-beta-gal) activity, a biomarker of senescent cells in culture and in vivo. *Nat Protoc*, *4*(12), 1798–1806.

- Degenhardt, K., Mathew, R., Beaudoin, B., Bray, K., Anderson, D., Chen, G., Mukherjee, C., Shi, Y., et al. (2006). Autophagy promotes tumor cell survival and restricts necrosis, inflammation, and tumorigenesis. *Cancer cell*, 10, 51–64.
- Degenhardt, K., Mathew, R., Beaudoin, B., Bray, K., Anderson, D., Chen, G., Mukherjee, C., et al. (2010). Autophagy promotes tumor cell survival and restricts necrosis, inflammation and tumorigenesis. *Cancer cell*, 10(1), 51–64.
- Deng, Q., Liao, R., Wu, B., & P, S. (2004). High intensity ras signaling induces premature senescence by activating p38 pathway in primary human fibroblasts. *J Biol Chem*, 279(2), 1050–1059.
- Denoyelle, C., Abou-Rjaily, G, Bezrookove, V., Verhaegen, M., Johnson, T., Fullen, D., Pointer, J., Gruber, S., et al. (2006). Anti-oncogenic role of the endoplasmic reticulum differentially activated by mutations in the MAPK pathway. *Nat Cell Biol*, 8, 1053–1063.
- Dhillon, A. S., Meikle, S., Yazici, Z., Eulitz, M., & Kolch, W. (2002). Regulation of Raf-1 activation and signalling by dephosphorylation. *The EMBO journal*, 21(1-2), 64–71.
- Di Bartolomeo, S., Corazzari, M., Nazio, F., Oliverio, S., Lisi, G., Antonioli, M., Pagliarini, V., et al. (2010). The dynamic interaction of AMBRA1 with the dynein motor complex regulates mammalian autophagy. *The Journal of cell biology*, 191(1), 155–68.
- Dimri, G., Lee, X., Basile, G., Acosta, M., Scott, G., Roskelley, C., Medrano, E., et al. (1995). A biomarker that identifies senescent human cells in culture and in aging skin in vivo. *Proc Natl Acad Sci*, 92, 9363–9367.
- Ding, W., Ni, H., Gao, W., Hou, Y., Melan, M., Chen, X., Stolz, D., et al. (2007). Differential effects of endoplasmic reticulum stress-induced autophagy on cell survival. *J Biol Chem*, 282(7), 4702–4710.

- Dorn, B. R., Dunn, W. A., & Progulske-fox, A. (2002). Bacterial interactions with the autophagic pathway. *Cellular Microbiology*, 4(1), 1–10.
- Duan, W., Li, Q., Xia, M., Tashiro, S., & Onodera, S. (2011). Silibinin activated p53 and induced autophagic death in human fibrosarcoma HT1080 cells via reactive oxygen species-p38 and c-Jun N-terminal kinase pathways. *Biol. Pharm. Bull.*, 34, 47–53.
- Dunn, W. A. (1990). Studies on the mechanisms of autophagy: formation of the autophagic vacuole. *The Journal of cell biology*, 110(6), 1923–1933.
- Edinger, A. L., & Thompson, C. B. (2003). Defective autophagy leads to cancer. *Cancer cell*, 4(6), 422–4.
- Ellington, A., Berhow, M., & Singletary, K. (2006). Inhibition of Akt signaling and enhanced ERK1/2 activity are involved in induction of macroautophagy by triterpenoid B-group soyasaponins in colon cancer cells. *Carcinogenesis*, 27, 298–306.
- Emr, K. (2009). Autophagy as a Regulated Pathway of Cellular Degradation. *Science*, 290(5497), 1717–1721.
- Engelman, J. A., Lisanti, M. P., & Scherer, P. E. (1998). Specific inhibitors of p38 mitogen-activated protein kinase block 3T3-L1 adipogenesis. *The Journal of biological chemistry*, 273(48), 32111–20.
- Eskelinen, E.-L., Tanaka, Y., & Saftig, P. (2003). At the acidic edge: emerging functions for lysosomal membrane proteins. *Trends in Cell Biology*, 13(3), 137–145.
- Fass, E., Shvets, E., Degani, I., Hirschberg, K., & Elazar, Z. (2006). Microtubules support production of starvation-induced autophagosomes but not their targeting and fusion with lysosomes. *J Biol Chem*, 281, 36303–36316.

- Feng, L., Zhou, X., Liao, J., & Omary, M. B. (1999). Pervanadate-mediated tyrosine phosphorylation of keratins 8 and 19 via a p38 mitogen-activated protein kinase-dependent pathway. *Journal of cell science*, 112, 2081–90.
- Ferrell, J. E., & Bhatt, R. R. (1997). Mechanistic studies of the dual phosphorylation of mitogen-activated protein kinase. *The Journal of biological chemistry*, 272(30), 19008–16.
- Freshney, N. W., Rawlinson, L., Guesdon, F., Jones, E., Cowley, S., Hsuan, J., & Saklatvala, J. (1994). Interleukin-1 activates a novel protein kinase cascade that results in the phosphorylation of Hsp27. *Cell*, 78(6), 1039–49.
- Fukunaga, R., & Hunter, T. (1997). MNK1, a new MAP kinase-activated protein kinase, isolated by a novel expression screening method for identifying protein kinase substrates. *The EMBO journal*, 16(8), 1921–33.
- Furuta, S., Hidaka, E., Ogata, A., Yokota, S., & Kamata, T. (2004). Ras is involved in the negative control of autophagy through the class I PI3-kinase. *Oncogene*, 23(22), 3898–3904.
- Ganley, I. G., Lam, D. H., Wang, J., Ding, X., Chen, S., & Jiang, X. (2009). ULK1-ATG13-FIP200 complex mediates mTOR signaling and is essential for autophagy. *The Journal of biological chemistry*, 284(18), 12297–305.
- Geiger, P. C., Wright, D. C., Han, D.-H., & Holloszy, J. O. (2005). Activation of p38 MAP kinase enhances sensitivity of muscle glucose transport to insulin. *American journal of physiology. Endocrinology and metabolism*, 288(4), E782–E788.
- Goel, V., Ibrahim, N., & Jiang, G. (2009). Melanocytic nevuslike hyperplasia and melanoma in transgenic BRAFV600E mice. *Oncogene*, 28(23), 2289–2298.
- Guan, Z., Buckman, S. Y., Pentland, a P., Templeton, D. J., & Morrison, a R. (1998). Induction of cyclooxygenase-2 by the activated MEKK1 --> SEK1/MKK4 --> p38

- mitogen-activated protein kinase pathway. *The Journal of biological chemistry*, 273(21), 12901–8.
- Gutierrez, M. G., Munafó, D. B., Berón, W., & Colombo, M. I. (2004). Rab7 is required for the normal progression of the autophagic pathway in mammalian cells. *Journal of cell science*, 117(Pt 13), 2687–2697.
- Gwinn, D., Shackelford, D., Egan, D., Mihaylova, M., Mery, A., Vasquez, D., Turk, B., et al. (2008). AMPK phosphorylation of raptor mediates a metabolic checkpoint. *Mol. Cell*, 30, 214–226.
- Han, J., & Ulevitch, J. (1994). A map kinase targeted by endotoxin and hyperosmolarity in mammalian cells. *Science*, 265(5173), 808–811.
- Hanaoka, H., Noda, T., Shirano, Y., Kato, T., Hayashi, H., Shibata, D., Tabata, S., et al. (2002). Leaf Senescence and Starvation-Induced Chlorosis Are Accelerated by the Disruption of an Arabidopsis Autophagy Gene. *American Society of Plant Biologists*, 129(July), 1181–1193.
- Hanks, S. K., & Hunter, T. (1995). Protein kinases 6. The eukaryotic protein kinase superfamily: kinase (catalytic) domain structure and classification. *FASEB J.*, 9(8), 576–596.
- Hansen, K., Wagner, B., Hamel, W., Schweizer, M., Haag, F., Westphal, M., & Lamszus, K. (2007). Autophagic cell death induced by TrkA receptor activation in human glioblastoma cells. *J. Neurochem.*, 103, 259–275.
- Haq, R., Brenton, J. D., Takahashi, M., Finan, D., Rottapel, R., & Zanke, B. (2002). Constitutive p38HOG Mitogen-activated Protein Kinase Activation Induces Permanent Cell Cycle Arrest and Senescence. *cancer Res*, 62, 5076–5082.
- Hara, T., & Mizushima, N. (2009). Role of ULK-FIP200 complex in mammalian autophagy. *Autophagy*, 5(1), 85–87.

- Hayflick, L., & Moorhead, P. (1961). The serial cultivation of human diploid cell strains. *Experimental Cell Research*, 25, 585–621.
- Heidenreich, O., Neininger, a, Schratt, G., Zinck, R., Cahill, M. a, Engel, K., Kotlyarov, a, et al. (1999). MAPKAP kinase 2 phosphorylates serum response factor in vitro and in vivo. *The Journal of biological chemistry*, 274(20), 14434–43.
- Heidenreich, K. A., & Kummer, J. L. (1996). Inhibition of p38 mitogen-activated protein kinase by insulin in cultured fetal neurons. *The Journal of biological chemistry*, 271(17), 9891–9894.
- Henkart, P. A., (1996). ICE family proteases: mediators of all apoptotic cell death? *Immunity*, 4(3), 195–201.
- Hollenbach, E., Neumann, M., Vieth, M., Roessner, A., Malfertheiner, P., & Naumann, M. (2004). Inhibition of p38 MAP kinase- and RICK/NF-kappaB-signaling suppresses inflammatory bowel disease. *The FASEB journal*, 18(13), 1550–2.
- Homer, C., Kabi, A., Marina-García, N., Sreekumar, A., Nesvizhskii, A., Nickerson, K., Chinnaiyan, A., et al. (2012). A dual role for receptor-interacting protein kinase 2 (RIP2) kinase activity in nucleotide-binding oligomerization domain 2 (NOD2)-dependent autophagy. *J Biol Chem*, 287(30), 25565–25576.
- Hosokawa, N, Hara, T., Kaizuka, T., Kishi, C., Takamura, A., Miura, Y., Iemura, S., et al. (2009). Nutrient-dependent mTORC1 association with the ULK1-Atg13-FIP200 complex required for autophagy. *Mol. Biol. Cell*, 20, 1981–1991.
- Hosokawa, Nao, Sasaki, T., Iemura, S., Natsume, T., Hara, T., & Mizushima, N. (2009). Atg101, a novel mammalian autophagy protein interacting with Atg13. *Autophagy*, 5(7), 973–9.
- Hu, J., Chu, Z., Han, J., Dang, Y., Yan, H., Zhang, Q., Liang, G., et al. (2010). The p38/MAPK pathway regulates microtubule polymerization through phosphorylation of MAP4 and Op18 in hypoxic cells. *Cell Mol Life Sci.*, 67(2), 321–333.

- Huang, C. K., Zhan, L., Ai, Y., & Jongstra, J. (1997). LSP1 is the major substrate for mitogen-activated protein kinase-activated protein kinase 2 in human neutrophils. *The Journal of biological chemistry*, 272(1), 17–19.
- Huang, J., & Manning, B. (2009). A complex interplay between Akt, TSC2 and the two mTOR complexes. *Biochem. Soc. Trans.*, 37, 217–222.
- Huang, S., Jiang, Y., Li, Z., Nishida, E., Mathias, P., Lin, S., Ulevitch, R. J., et al. (1997). Apoptosis signaling pathway in T cells is composed of ICE/Ced-3 family proteases and MAP kinase kinase 6b. *Immunity*, 6(6), 739–49.
- Häussinger, D., Schliess, F., Dombrowski, F., & Vom Dahl, S. (1999). Involvement of p38MAPK in the regulation of proteolysis by liver cell hydration. *Gastroenterology*. 1999 Apr;116(4):921-35., 116(4), 921–935.
- Høyvik, H., Gordon, P., Berg, T., Stromhaug, P., & Seglen, P. (1991). Inhibition of autophagic-lysosomal delivery and autophagic lactolysis by asparagine. *J Cell Biol*, 113, 1305–1312.
- Ichimura, Y., Kominami, E., Tanaka, K., & Komatsu, M. (2008). Selective turnover of p62/A170/SQSTM1 by autophagy. *Autophagy*, 4(8), 1063–1066.
- Inoki, K., Zhu, T., & Guan, K. (2003). TSC2 mediates cellular energy response to control cell growth and survival. *Cell*, 115, 577–590.
- Itakura, E., Kishi, C., Inoue, K., & Mizushima, N. (2008). Beclin 1 Forms Two Distinct Phosphatidylinositol 3-Kinase Complexes with Mammalian Atg14 and UVRAG. *Molecular Biology of the cell*, 19(12), 5360–5372.
- Iwasa, H., Han, J., & Ishikawa, F. (2003). Mitogen-activated protein kinase p38 defines the common senescence-signalling pathway. *Genes to cells*. 8(2), 131–44.

- Iwata, J., Ezaki, J., Komatsu, M., Yokota, S., Ueno, T., Tanida, I., Chiba, T., et al. (2006). Excess peroxisomes are degraded by autophagic machinery in mammals. *J Biol Chem*, 281(7), 4035–4041.
- Jahreiss, L., Menzies, F., & Rubinsztein, D. (2008). The itinerary of autophagosomes: from peripheral formation to kiss-and-run fusion with lysosomes. *Traffic*, 9, 574–587.
- Jia, G., Cheng, G., Gangahar, D. M., & Agrawal, D. K. (2006). Insulin-like growth factor-1 and TNF-alpha regulate autophagy through c-jun N-terminal kinase and Akt pathways in human atherosclerotic vascular smooth cells. *Immunol. Cell Biol.*, 84, 448–454.
- Jiang, Y., Chen, C., Li, Z., Guo, W., Gegner, J. a, Lin, S., & Han, J. (1996). Characterization of the structure and function of a new mitogen-activated protein kinase (p38beta). *The Journal of biological chemistry*, 271(30), 17920–17926.
- Jiang, Y., Gram, H., Zhao, M., New, L., Gu, J., Feng, L., Di Padova, F., et al. (1997). Characterization of the structure and function of the fourth member of p38 group mitogen-activated protein kinases, p38delta. *The Journal of biological chemistry*, 272(48), 30122–301228.
- Johnson, G. (2003). The p38 MAP kinase signaling pathway in Alzheimer's disease. *Experimental Neurology*, 183(2), 263–268.
- Jung, C., Jun, C., Ro, S., Kim, Y., Otto, N., Cao, J., Kundu, M., et al. (2009). ULK-Atg13-FIP200 complexes mediate mTOR signaling to the autophagy machinery. *Mol. Biol. Cell*, 20, 1992–2003.
- Juo, P., Kuo, C. J., Reynolds, S. E., Konz, R. F., Raingeaud, J., Davis, R. J., Biemann, H. P., et al. (1997). Fas activation of the p38 mitogen-activated protein kinase signalling pathway requires ICE/CED-3 family proteases. *Molecular and cellular biology*, 17(1), 24–35.

- Jäger, S., Bucci, C., Tanida, I., Ueno, T., Kominami, E., Saftig, P., & Eskelinen, E.-L. (2004). Role for Rab7 in maturation of late autophagic vacuoles. *Journal of cell science*, 117(20), 4837–48.
- Kabeya, Y., Mizushima, N., Ueno, T., Yamamoto, A., Kirisako, T., Noda, T., Kominami, E., et al. (2000). LC3, a mammalian homologue of yeast Apg8p, is localized in autophagosome membranes after processing. *The EMBO journal*, 19(21), 5720–5728.
- Kafferlein, M. B. E., & Kieper, D. (1992). In vitro desensitization to lipopolysaccharide suppresses tumor necrosis factor, interleukin-1 and interleukin-6 gene expression in a similar fashion. *Immunology*, 75(2), 264–268.
- Kamada, Y., Funakoshi, T., Shintani, T., Nagano, K., Ohsumi, M., & Ohsumi, Y. (2000). Tor-mediated induction of autophagy via an Apg1 protein kinase complex. *J. Cell Biol.*, 150, 1507–1513.
- Kamada, Y., Yoshino, K., Kondo, C., Kawamata, T., Oshiro, N., Yonezawa, K., & Ohsumi, Y. (2010). Tor directly controls the Atg1 kinase complex to regulate autophagy. *Mol. Cell. Biol.*, 30, 1049–1058.
- Kang, R., Zeh, H. J., Lotze, M. T., & Tang, D. (2011). The Beclin 1 network regulates autophagy and apoptosis. *Cell death and differentiation*, 18(4), 571–80.
- Karantza-Wadsworth, V., Patel, S., Kravchuk, O., Chen, G., Mathew, R., Jin, S., & White, E. (2007). Autophagy mitigates metabolic stress and genome damage in mammary tumorigenesis. *Genes & development*, 21(13), 1621–1635.
- Keil, E., Höcker, R., Schuster, M., Essmann, F., Ueffing, N., Hoffman, B., & Schmitz, I. (2012). Phosphorylation of Atg5 by the Gadd45 β -MEKK4-p38 pathway inhibits autophagy. *Cell Death Differ*, 20(2), 321–322.

- Kihara, A., Kabeya, Y., Ohsumi, Y., & Yoshimori, T. (2001). Beclin-phosphatidylinositol 3-kinase complex functions at the trans-Golgi network. *EMBO Rep.*, 2, 330–335.
- Kihara, A., Noda, T., Ishihara, N., & Ohsumi, Y. (2001). Two distinct Vps34 phosphatidylinositol 3-kinase complexes function in autophagy and carboxypeptidase Y sorting in *Saccharomyces cerevisiae*. *J. Cell Biol.*, 152, 519–530.
- Kim, D., Kim, J., Lee, G., Kim, H., Lim, J., Chae, S., Chae, H., et al. (2010). p38 Mitogen-activated protein kinase is involved in endoplasmic reticulum stress-induced cell death and autophagy in human gingival fibroblasts. *Biol. Pharm. Bull.*, 33, 545–549.
- Kim, I., Rodriguez-Enriquez, S., & Lemasters, J. J. (2007). Selective degradation of mitochondria by mitophagy. *Archives of biochemistry and biophysics*, 462(2), 245–353.
- Kim, J., Kundu, M., Viollet, B., & Guan, K. (2011). AMPK and mTOR regulate autophagy through direct phosphorylation of Ulk1. *Nat. Cell Biol.*, 13, 132–141.
- Kim, John, & Klionsky, D. J. (2000). Autophagy, Cytoplasm-to-Vacuole targeting pathway and pexophagy in Yeast and Mammalian cells. *Annu Rev Biochem*, 69, 303–342.
- Kimura, S., Noda, T., & Yoshimori, T. (2008). Dynein-dependent movement of autophagosomes mediates efficient encounters with lysosomes. *Cell Struct Funct*, 33, 109–122.
- Kinouchi, K., Ichihara, A., Sano, M., Sun-Wada, G.-H., Wada, Y., Kurauchi-Mito, A., Bokuda, K., et al. (2010). The (pro)renin receptor/ATP6AP2 is essential for vacuolar H⁺-ATPase assembly in murine cardiomyocytes. *Circulation research*, 107(1), 30–34.

- Kirkegaard, K., Taylor, M. P., & Jackson, W. T. (2004). Cellular autophagy: surrender, avoidance and subversion by microorganisms. *Nature reviews. Microbiology*, 2(4), 301–314.
- Kirkin, V., Joos, S., & Zörnig, M. (2004). The role of Bcl-2 family members in tumorigenesis. *Biochimica et biophysica acta*, 1644(2-3), 229–49.
- Kirkin, V., McEwan, D. G., Novak, I., & Dikic, I. (2009). A role for ubiquitin in selective autophagy. *Molecular cell*, 34(3), 259–69. doi:10.1016/j.molcel.2009.04.026
- Klionsky, D. J. (1999). Vacuolar import of proteins and organelles from the cytoplasm. *Annu Rev Cell Dev Biol.*, 15, 1–32.
- Klionsky, D. J., Abeliovich, H., Agostinis, P., Agrawal, D. K., Aliev, G., Askew, D. S., Baba, M., et al. (2008). Guidelines for the use and interpretation of assays for monitoring autophagy in higher eukaryotes. *Autophagy*, 4(2), 151–175.
- Klionsky, D. J., Cregg, J. M., Dunn, W. A., Emr, S. D., Sakai, Y., Sandoval, I. V., Sibirny, A., et al. (2003). Unified Nomenclature for Yeast Autophagy-Related genes. *Developmental cell*, 5, 539–545.
- Klionsky, D. J., Cuervo, A. M., & Seglen, P. O. (2007). Methods for monitoring autophagy from yeast to human. *Autophagy*, 3(3), 181–206.
- Kochl, R., Hu, X., Chan, E., & Tooze, S. (2006). Microtubules facilitate autophagosome formation and fusion of autophagosomes with endosomes. *Traffic*, 7, 129–145.
- Koike, M., Shibata, M., Waguri, S., Yoshimura, K., Tanida, I., Kominami, E., Gotow, T., et al. (2005). Participation of autophagy in storage of lysosomes in neurons from mouse models of neuronal ceroid-lipofuscinoses (Batten disease). *The American journal of pathology*, 167(6), 1713–28.
- Kolch, W. (2000). Meaningful relationships: the regulation of the Ras/Raf/MEK/ERK pathway by protein interactions. *The Biochemical journal*, 351, 289–305.

- Kortlever, R., Higgins, P., & Bernardis, R. (2006). Plasminogen activator inhibitor-1 is a critical downstream target of p53 in the induction of replicative senescence. *Nat Cell Biol*, 8, 877–884.
- Kroemer, G., El-Deiry, W., Golstein, P., Peter, M., Vaux, D., Vandenabeele, P., Zhivotovsky, B., et al. (2005). Classification of cell death: recommendations of the Nomenclature Committee on Cell Death. *Cell death and differentiation*, 12, 1463–1470.
- Kumar, S., McDonnell, P. C., Gum, R. J., Hand, a T., Lee, J. C., & Young, P. R. (1997). Novel homologues of CSBP/p38 MAP kinase: activation, substrate specificity and sensitivity to inhibition by pyridinyl imidazoles. *Biochemical and biophysical research communications*, 235(3), 533–8.
- Kummer, J. L., Rao, P. K., & Heidenreich, K. a. (1997). Apoptosis induced by withdrawal of trophic factors is mediated by p38 mitogen-activated protein kinase. *The Journal of biological chemistry*, 272(33), 20490–20494.
- Kundu, M., Lindsten, T., Yang, C.-Y., Wu, J., Zhao, F., Zhang, J., Selak, M. a, et al. (2008). Ulk1 plays a critical role in the autophagic clearance of mitochondria and ribosomes during reticulocyte maturation. *Blood*, 112(4), 1493–502.
- Larsen, K. E., & Sulzer, D. (2002). Autophagy in neurons: a review. *Histology and histopathology*, 17(3), 897–908.
- Lee, J C et al, 1994. (1994). A protein kinase involved in the regulation of inflammatory cytokine biosynthesis. *Nature*, 372, 22–29.
- Levine, B., & Klionsky, D. . (2004). Development by self-digestion: molecular mechanisms and biological functions of autophagy. *Dev cell*, 6(4), 463–477.
- Li, C., Capan, E., Zhao, Y., Zhao, J., Stolz, D., Watkins, S. C., Jin, S., et al. (2006). Autophagy is induced in CD4+ T cells and important for the growth factor-withdrawal cell death. *J. Immunol*, 177, 5163–5168.

- Li, Y., Jiang, B., Ensign, W. Y., Vogt, P. K., & Han, J. (2000). Myogenic differentiation requires signalling through both phosphatidylinositol 3-kinase and p38 MAP kinase. *Cellular signalling*, 12(11-12), 751–7.
- Li, Z., Jiang, Y., Ulevitch, R. J., & Han, J. (1996). The primary structure of p38 gamma: a new member of p38 group of MAP kinases. *Biochemical and biophysical research communications*, 228(2), 334–340.
- Liang, C., Feng, P., Ku, B., & Oh, B. (2007). UVRAG, A new player in autophagy and tumor cell growth. *Archives of biochemistry and biophysics*, 3(1), 69–71.
- Liang, X H, Jackson, S., Seaman, M., Brown, K., Kempkes, B., Hibshoosh, H., & Levine, B. (1999). Induction of autophagy and inhibition of tumorigenesis by beclin 1. *Nature*, 402(6762), 672–6.
- Liang, Xiao Huan, Yu, J., Brown, K., & Function, T. S. (2001). Beclin 1 Contains a Leucine-rich Nuclear Export Signal That Is Required for Its Autophagy and Tumor Suppressor Function. *Cancer Research*, 61(8), 3443–3449.
- Liao, P., Ng, L., Lin, L., Richardson, C., Wang, G., & Lin, C. (2010). Resveratrol arrests cell cycle and induces apoptosis in human hepatocellular carcinoma huh-7 cells. *J. Med. Food*, 13, 1415–1423.
- Liebert, M. A., Death, N. C., Lemasters, J. J., Qian, T., He, L., Kim, J., Elmore, S. P., et al. (2002). Role of Mitochondrial Inner Membrane permeabilization in Necrotic cell death, Apoptosis and Autophagy. *Antioxidants & redox signaling*, 4(5), 769–781.
- Lim, S., Hahm, K., Lee, S., & Oh, S. (2010). Autophagy involvement in cadmium resistance through induction of multidrug resistance-associated protein and counterbalance of endoplasmic reticulum stress WI38 lung epithelial fibroblast cells. *Toxicology*, 276, 18–26.

- Lin, A., Barradas, M., Stone, J., van Aelst, L., & Serrano, M. Lowe, S. (1998). Premature senescence involving p53 and p16 is activated in response to constitutive MEK/MAPK mitogenic signaling. *Genes & development*, *12*, 3008–3019.
- Lin, Y., Kuo, H., Wang, J., & Lin, W. (2012). Regulation of Inflammatory Response by 3-Methyladenine Involves the Coordinative Actions on Akt and Glycogen Synthase Kinase 3 β Rather than Autophagy. *J Immunol.*, *189*(8), 4154–4164.
- Liu, B., Cheng, Y., Zhang, B., Bian, H. ., & Bao, J. . (2009). Polygonatum cyrtoneuma lectin induces apoptosis and autophagy in human melanoma A375 cells through a mitochondria-mediated ROS-p38-p53 pathway. *Cancer Lett.*, *275*, 54–60.
- Lum, J., Bauer, D., Kong, M., Harris, M., Li, C., Lindsten, T., & Thompson, C. (2005). Growth factor regulation of autophagy and cell survival in the absence of apoptosis. *Cell*, *120*, 237–248.
- Lum, J. J., Bauer, D. E., Kong, M., Harris, M. H., Li, C., Lindsten, T., & Thompson, C. B. (2005). Growth factor regulation of autophagy and cell survival in the absence of apoptosis. *Cell*, *120*(2), 237–248.
- Luzio, J. P., Pryor, P. R., & Bright, N. a. (2007). Lysosomes: fusion and function. *Nature reviews. Molecular cell biology*, *8*(8), 622–32.
- Mack, H., Zheng, B., Asara, J., & Thomas, S. (2012). AMPK-dependent phosphorylation of ULK1 regulates ATG9 localization. *Autophagy*, *8*(8), 1197–1214.
- Mahtani, K. R., Brook, M., Dean, J. L. E., Sully, G., Saklatvala, J., & Clark, A. R. (2001). Mitogen-Activated Protein Kinase p38 Controls the Expression and Posttranslational Modification of Tristetraprolin , a Regulator of Tumor Necrosis Factor Alpha mRNA Stability. *Molecular and cellular biology*, *21*(19), 6461–6469.
- Majumder, P., Grisanzio, C., O'Connell, F., Barry, M., Brito, J. ., Xu, Q., Guney, I., et al. (2008). A prostatic intraepithelial neoplasia-dependent p27 Kip1 checkpoint induces

- senescence and inhibits cell proliferation and cancer progression. *Cancer cell*, 14, 146–155.
- Makeeva, N., Myers, J. W., & Welsh, N. (2006). Role of MKK3 and p38 MAPK in cytokine-induced death of insulin-producing cells. *The Biochemical journal*, 393, 129–39.
- Mansour, S., Matten, W., Hermann, A., Candia, J., & Rong, S. (1994). Transformation of mammalian cells by constitutively active MAP kinase kinase. *Science*, 265, 966–970.
- Martin, P., Poggi, M. C., Chambard, J. C., Boulukos, K. E., & Pognonec, P. (2006). Low dose cadmium poisoning results in sustained ERK phosphorylation and caspase activation. *Biochem. Biophys Res. Commun.*, 350, 803–807.
- Matsunaga, K., Noda, T., & Yoshimori, T. (2009). Binding Rubicon to cross the Rubicon. *Autophagy*, 5(6), 876–877.
- Mei, S., Gu, H., Ward, A., Yang, X., Guo, H., He, K., Liu, Z., et al. (2012). p38 mitogen-activated protein kinase (MAPK) promotes cholesterol ester accumulation in macrophages through inhibition of macroautophagy. *J Biol Chem*, 287(15), 11761–11768.
- Mercer, C. a, Kaliappan, A., & Dennis, P. B. (2009). A novel, human Atg13 binding protein, Atg101, interacts with ULK1 and is essential for macroautophagy. *Autophagy*, 5(5), 649–62.
- Michaloglou, C., Vredeveld, L., Soengas, M., Denoyelle, C., Kuilman, T., van der Horst, C., Majoor, D., et al. (2005). BRAFE600-associated senescence-like cell cycle arrest of human naevi. *nature*, 436, 720–724.
- Michaloglou, C., & Vredeveld, L.C.W. Soengas, M. S. (2005). BRAF-associated senescence-like cell cycle arrest of human naevi. *Nature*, 436(7051), 720–724.

- Miyachi, H., Minamino, T., Tateno, K., Kunieda, T., Toko, H., & Komuro, I. (2004). Akt negatively regulates the in vitro lifespan of human endothelial cells via a p53/p21-dependent pathway. *EMBO J*, 23, 212–220.
- Mizushima, N., Noda, T., Yoshimori, T., Tanaka, Y., Ishii, T., George, M. D., Klionsky, D. J., et al. (1998). A protein conjugation system essential for autophagy. *Nature*, 395(6700), 395–8.
- Mizushima, N., (2007). Autophagy: process and function. *Genes & development*, 21(22), 2861–73. doi:10.1101/gad.1599207
- Mizushima, N., Yoshimori, T., & Levine, B. (2010). Methods in mammalian autophagy research. *Cell*, 140(3), 313–26.
- Molnár, A., Theodoras, A. M., Zon, L. I., & Kyriakis, J. M. (1997). Cdc42Hs, but not Rac1, inhibits serum-stimulated cell cycle progression at G1/S through a mechanism requiring p38/RK. *The Journal of biological chemistry*, 272(20), 13229–35.
- Moreau, K., Luo, S., & Rubinsztein, D. (2010). Cytoprotective roles for autophagy. *Curr Opin Cell Biol.*, 22(2), 206–211.
- Morton, J. P., Timpson, P., & Karim, S. A. (2010). Mutant p53 drives metastasis and overcomes growth arrest/senescence in pancreatic cancer. *Proceedings of the National Academy of Sciences of the United States of America*, 107(1), 246–251.
- Moruno-Manchón, J. F., Pérez-Jiménez, E., & Knecht, E. (2013). Glucose induces autophagy under starvation conditions by a p38 MAPK-dependent pathway. *The Biochemical journal*, 449(2), 497–506.
- Nagata, Y., Takahashi, N., Davis, R. J., & Todokoro, K. (1998). Activation of p38 MAP kinase and JNK but not ERK is required for erythropoietin-induced erythroid differentiation. *Blood*, 92(6), 1859–69.

- Newbold, R., & Overell, R. (1983). Fibroblast immortality is a prerequisite for transformation by EJ c-Ha-ras oncogene. *Nature*, *304*, 648–651.
- Nishino, I., Fu, J., Tanji, K., Yamada, T., Shimojo, S., Koori, T., Mora, M., et al. (2000). Primary LAMP-2 deficiency causes X-linked vacuolar cardiomyopathy and myopathy (Danon disease). *Nature*, *406*(6798), 906–10.
- Noda, T., Suzuki, K., & Ohsumi, Y. (2002). Yeast autophagosomes: de novo formation of a membrane structure. *Trends in cell biology*, *12*(5), 231–5.
- Nogueira, V., Park, Y., Chen, C., Xu, P., Chen, M., Tonic, I., Unterman, T., et al. (2008). Akt determines replicative senescence and oxidative or oncogenic premature senescence and sensitizes cells to oxidative apoptosis. *Cancer cell*, *14*, 458–470.
- Nopparat, C., Porter, J. E., Ebadi, M. ., & Govitrapong, P. (2010). The mechanism for the neuroprotective effect of melatonin against methamphetamine-induced autophagy. *J. Pineal Res.*, *49*, 382–389.
- Ogata, M., Hino, S., Saito, A., Morikawa, K., Kondo, S., Kanemoto, S., Murakami, T., et al. (2006). Autophagy is activated for cell survival after endoplasmic reticulum stress. *Mol. Cell. Biol.*, *26*, 9220–9231.
- Ohsumi, Y. (2001). Molecular dissection of autophagy: two ubiquitin-like systems. *Nature reviews. Molecular cell biology*, *2*(3), 211–216.
- Ostenfeld, M., Høyer-Hansen, M Bastholm, L., Fehrenbacher, N., Olsen, O., Groth-Pedersen, L., Puustinen, P., Kirkegaard Sorensen, T Nylandsted, J., et al. (2008). Anti-cancer agent siramesine is a lysosomotropic detergent that induces cytoprotective autophagosome accumulation. *Autophagy*, *4*(4), 487–499.
- Oyama, K., Okawa, T., Nakagawa, H., Takaoka, M., Andl, C., Kim, S., Klein-Szanto, A., et al. (2007). AKT induces senescence in primary esophageal epithelial cells but is permissive for differentiation as revealed in organotypic culture. *Oncogene*, *26*, 2353–2364.

- Paillas, S., Boissière, F., Bibeau, F., Denouel, A., Mollevi, C., Causse, A., Denis, V., et al. (2011). Targeting the p38 MAPK pathway inhibits irinotecan resistance in colon adenocarcinoma. *Cancer research*, 71(3), 1041–9.
- Pankiv, S., Clausen, T. H., Lamark, T., Brech, A., Bruun, J.-A., Outzen, H., Øvervatn, A., et al. (2007). p62/SQSTM1 binds directly to Atg8/LC3 to facilitate degradation of ubiquitinated protein aggregates by autophagy. *The Journal of biological chemistry*, 282(33), 24131–45.
- Parker, C. G., Hunt, J., Diener, K., McGinley, M., Soriano, B., Keesler, G. a, Bray, J., et al. (1998). Identification of stathmin as a novel substrate for p38 delta. *Biochemical and biophysical research communications*, 249(3), 791–6.
- Parrinello, S., Samper, E., Krtolica, A., Goldstein, J., Melov, S., & Campisi, J. (2003). Oxygen sensitivity severely limits the replicative lifespan of murine fibroblasts. *Nature cell biology*, 118, 741–747.
- Pattingre, S., Bauvy, C., & Codogno, P. (2003). Amino acids interfere with the ERK1/2-dependent control of macroautophagy by controlling the activation of Raf-1 in human colon cancer. *J Biol Chem*, 278, 16667 – 16674.
- Perlmutter, D. H. (2002). Liver injury in alpha1 -antitrypsin deficiency: an aggregated protein induces mitochondrial injury. *The Journal of clinical Investigation*, 110(11), 1579–1583.
- Pierrat, B., Correia, S., Mary, J., Toma, M., & Lesslauer, W. (1998). RSK-B , a Novel Ribosomal S6 Kinase Family Member , Is a CREB Kinase under Dominant Control of p38 a Mitogen-activated Protein Kinase (p38 a MAPK). *The Journal of biological chemistry*, 273(45), 29661–29671.
- Pimkina, J., Humbey, O., Zilfou, J. T., Jarnik, M., & Murphy, M. E. (2009). ARF induces autophagy by virtue of interaction with Bcl-xl. *The Journal of biological chemistry*, 284(5), 2803–10.

- Pivtoraiko, V. N., Stone, S. L., Roth, K. A., & Shacka, J. J. (2009). Oxidative Stress and Autophagy in the Regulation of Lysosome-Dependent Neuron Death. *Antioxidants & Redox signaling*, *11*(3), 481–496.
- Plowey, E. D., Cherra, S.J., 3rd, Liu, Y. J., & Chu, C. T. (2008). Role of autophagy in G2019S-LRRK2-associated neurite shortening in differentiated SH-SY5Y cells. *J. Neurochem.*, *105*, 1048–1056.
- Pyo, J., Jang, M., Kwon, Y., Lee, H., Jun, J., Woo, H., Cho, D., et al. (2005). Essential roles of Atg5 and FADD in autophagic cell death: dissection of autophagic cell death into vacuole formation and cell death. *J Biol Chem*, *280*, 20722–20729.
- Qin, Z.-H., Wang, Y., Kegel, K. B., Kazantsev, A., Apostol, B. L., Thompson, L. M., Yoder, J., et al. (2003). Autophagy regulates the processing of amino terminal huntingtin fragments. *Human molecular genetics*, *12*(24), 3231–44.
- Raingaud, J, Gupta, S. (1995). Pro inflammatory cytokines and environmental stress cause p38 mitogen activated protein kinase activation by dual phosphorylation on tyrosine and threonine. *The Journal of biological chemistry*, *270*(31), 7420–7426.
- Ralston, S. H. (2008). Pathogenesis of Paget's disease of bone. *Bone*, *43*(5), 819–25.
- Ravikumar, B, Acevedo-Arozena, A Imarisio, S., Berger, Z., Vacher, C., & O'kane, CJ, Brown, SD Rubinsztein, D. (2005). Dynein mutations impair autophagic clearance of aggregate-prone proteins. *Nature genetics*, *37*, 771–776.
- Ravikumar, Brinda, Duden, R., & Rubinsztein, D. C. (2002). Aggregate-prone proteins with polyglutamine and polyalanine expansions are degraded by autophagy. *Human molecular genetics*, *11*(9), 1107–1117.
- Reef, S., Zalckvar, E., Shifman, O., Bialik, S., Sabanay, H., Oren, M., & Kimchi, A. (2006). A short mitochondrial form of p19ARF induces autophagy and caspase-independent cell death. *Molecular cell*, *22*(4), 463–75.

- Reggiori, F., & Klionsky, D. J. (2002). Autophagy in the Eukaryotic Cell. *Eukaryotic Cell*, 1(1), 10–21.
- Rouse, J., Cohen, P., Trigon, S., Morange, M., Alonso-Llamazares, a, Zamanillo, D., Hunt, T., et al. (1994). A novel kinase cascade triggered by stress and heat shock that stimulates MAPKAP kinase-2 and phosphorylation of the small heat shock proteins. *Cell*, 78(6), 1027–37.
- Saftig, P., Beertsen, W., & Eskelinen, E.L. (2008). LAMP2.A control step for phagosome and autophagosome maturation. *Autophagy*, 4(4), 510–512.
- Sager, R. (1991). Senescence as a mode of tumor suppression. *Environmental Health Perspectives*, 93, 59–62.
- Salminen, A., Kaarniranta, K., & Kauppinen, A. (2012). Beclin 1 interactome controls the crosstalk between apoptosis, autophagy and inflammasome activation: Impact on the aging process. *Ageing Res Rev*.
- Sarkisian, C. J., Keister, B. A., Stairs, D. B., Boxer, R. . ., Moody, S. E., & Chodosh, L. . (2007). Dose-dependent oncogeneinduced senescence in vivo and its evasion during mammary tumorigenesis. *Nature cell biology*, 9(5), 493– 505.
- Scott, S. V., & Klionsky, D. J. (1998). Delivery of proteins and organelles to the vacuole from the cytoplasm. *Current opinion in cell biology*, 10, 523–529.
- Serrano, M., Lin, A., McCurrach, M., Beach, D., & Lowe, S. (1997a). Oncogenic ras provokes premature cell senescence associated with accumulation of p53 and p16INK4a. *Cell*, 88, 593–602.
- Serrano, M., Lin, A. W., McCurrach, M. E., Beach, D., & Lowe, S. W. (1997b). Oncogenic ras provokes premature cell senescence associated with accumulation of p53 and p16INK4a. *Cell*, 88(5), 593–602.
- Shahpasand, K., Uemura, I., Saito, T., Asano, T., Hata, K., Shibata, K., Toyoshima, Y., et al. (2012). Regulation of mitochondrial transport and inter-microtubule spacing by

- tau phosphorylation at the sites hyperphosphorylated in Alzheimer's disease. *The Journal of neuroscience*: the official journal of the Society for Neuroscience, 32(7), 2430–41.
- Sharpless, N., & DePinho, R. (2004). Telomeres, stem cells, senescence, and cancer. *Journal of Clinical Investigation*, 113(2), 160–168.
- Shi, M., Zhang, T., Sun, L., Luo, Y., & Zhang, Y. (2012). Calpain, Atg5 and Bak play important roles in the crosstalk between apoptosis and autophagy induced by influx of extracellular calcium. *apoptosis*.
- Shibata, M., Lu, T., Furuya, T., Degtarev, A., Mizushima, N., Yoshimori, T., MacDonald, M., et al. (2006). Regulation of intracellular accumulation of mutant Huntingtin by Beclin 1. *The Journal of biological chemistry*, 281(20), 14474–85.
- Simonsen, A., & Tooze, S. a. (2009). Coordination of membrane events during autophagy by multiple class III PI3-kinase complexes. *The Journal of cell biology*, 186(6), 773–82.
- Sitte, N., Merker, K., Von Zglinicki, T., Grune, T., & Davies, K. (2000). Protein oxidation and degradation during cellular senescence of human BJ fibroblasts: part I--effects of proliferative senescence. *FASEB J.*, 14(15), 2495–2502.
- Sivaprasad, U., & Basu, A. (2008). Inhibition of ERK attenuates autophagy and potentiates tumour necrosis factor-alpha-induced cell death in MCF-7 cells. *J. Cell. Mol. Med.*, 12, 1265–1271.
- Spangenberg, C., Lausch, E., Trost, T., Prawitt, D., May, A., Keppler, R., Fees, S., et al. (2006). ERBB2-mediated transcriptional up-regulation of the alpha5beta1 integrin fibronectin receptor promotes tumor cell survival under adverse conditions. *Cancer Res*, 66(7), 3715–3725.
- Stokoe, D., P, K. E., Campbell, D. G., Cohen, P., & Oaestep, M. (1992). Identification of MAPKAP kinase 2 as a major enzyme responsible for the phosphorylation of the small mammalian heat shock proteins. *FEBS*, 313(3), 307–313.

- Sun, P., Yoshizuka, N., New, L., & Al, E. (2007). PRAK is essential for rasinduced senescence and tumor suppression. *Cell*, 128(2), 295–308.
- Suzuki, K., Kirisako, T., Kamada, Y., Mizushima, N., Noda, T., & Ohsumi, Y. (2001). The pre-autophagosomal structure organized by concerted functions of APG genes is essential for autophagosome formation. *The EMBO journal*, 20(21), 5971–81.
- Sweeney, G., Somwar, R., Ramlal, T., Volchuk, a, Ueyama, a, & Klip, a. (1999). An inhibitor of p38 mitogen-activated protein kinase prevents insulin-stimulated glucose transport but not glucose transporter translocation in 3T3-L1 adipocytes and L6 myotubes. *The Journal of biological chemistry*, 274(15), 10071–8.
- Tallóczy, Z., Virgin, H. W., & Levine, B. (2006). PKR-Dependent Autophagic Degradation of Herpes Simplex Virus Type 1. *Archives of biochemistry and biophysics*, 2(1), 24–29.
- Tan, Y., Rouse, J., Zhang, A., Cariati, S., Cohen, P., & Comb, M. J. (1996). FGF and stress regulate CREB and ATF-1 via a pathway involving p38 MAP kinase and MAPKAP kinase-2. *The EMBO journal*, 15(17), 4629–4642.
- Tanaka, Y., Guhde, G., Suter, A., Eskelinen, E. L., Hartmann, D., Lüllmann-Rauch, R., Janssen, P. M., et al. (2000). Accumulation of autophagic vacuoles and cardiomyopathy in LAMP-2-deficient mice. *Nature*, 406(6798), 902–906.
- Tang, G., Yue, Z., Talloczy, Z., Hagemann, T., Cho, W., Messing, A., Sulzer, D., et al. (2008). Autophagy induced by Alexander Disease-mutant GFAP accumulation is regulated by p38/ MAPK and mTOR signaling pathways. *Hum Mol Genet*, 17, 1540 – 1555.
- Tanida, I., Tanida-Miyake, E., Ueno, T., & Kominami, E. (2001). The human homolog of *Saccharomyces cerevisiae* Apg7p is a Protein-activating enzyme for multiple substrates including human Apg12p, GATE-16, GABARAP, and MAP-LC3. *The Journal of biological chemistry*, 276(3), 1701–6.

- Tatti, M., Motta, M., Di Bartolomeo, S., Scarpa, S., Cianfanelli, V., Cecconi, F., & Salvioli, R. (2012). Reduced cathepsins B and D cause impaired autophagic degradation that can be almost completely restored by overexpression of these two proteases in Sap C-deficient fibroblasts. *Hum Mol Genet*, *21*(23), 5159–5173.
- Thomas, G., Haavik, J., & Cohen, P. (1997). Participation of a stress-activated protein kinase cascade in the activation of tyrosine hydroxylase in chromaffin cells. *European journal of biochemistry / FEBS*, *247*(3), 1180–9.
- Thumm, M. (2002). Hitchhikers guide to the vacuole-mechanisms of cargo sequestration in the Cvt and autophagic pathways. *Molecular cell*, *10*(6), 1257–1258.
- Thyagarajan, A., Jedinak, A., Nguyen, H., Terry, C., Baldrige, L., Jiang, J., & Sliva, D. (2010). Triterpenes from Ganoderma Lucidum induce autophagy in colon cancer through the inhibition of p38 mitogen-activated kinase (p38 MAPK). *Nutr. Cancer*, *62*, 630–640.
- Tolkovsky, A. M., Xue, L., Fletcher, G. C., & Borutaite, V. (2002). Mitochondrial disappearance from cells: a clue to the role of autophagy in programmed cell death and disease? *Biochimie*, *84*(2-3), 233–240.
- Tresini, M., Mawal-Dewan, M., Cristofalo, V., & Sell, C. (1998). A phosphatidylinositol 3-kinase inhibitor induces a senescent-like growth arrest in human diploid fibroblasts. *cancer Res*, *58*, 1–4.
- Trost, T., Lausch, E., Fees, S., Schmitt, S., Enklaar, T., Reutzel, D., Brixel, L., et al. (2005). Premature senescence is a primary fail-safe mechanism of ERBB2-driven tumorigenesis in breast carcinoma cells. *Cancer Res*, *65*(3), 840–849.
- Tsujiimoto, Y., & Shimizu, S. (2005). Another way to die: autophagic programmed cell death. *Cell death and differentiation*, *12*, 1528–1534.

- Tsukada, M., & Ohsumi, Y. (1993). Isolation and characterization of autophagy-defective mutants of *Saccharomyces cerevisiae*. *FEBS lett*, 333(1-2), 169–174.
- Tu, Y., Fan, X., Yang, X., Zhang, C., & Liang, H. (2012). Evodiamine activates autophagy as a cytoprotective response in murine Lewis lung carcinoma cells. *Oncol Rep.*, 29(2), 481–490.
- Töröcsik, B., & Szeberényi, J. (2000). Anisomycin uses multiple mechanisms to stimulate mitogen-activated protein kinases and gene expression and to inhibit neuronal differentiation in PC12 pheochromocytoma cells. *Eur J Neurosci.*, 12(2), 527–532.
- Wang, S. H., Shih, Y. L., Lee, C. C., Chen, W. L., Lin, C. J., Lin, Y. S., Wu, K. H., et al. (2009). The role of endoplasmic reticulum in cadmium-induced mesangial cell apoptosis. *Chem. Biol. Interact*, 181, 45–51.
- Wang, W., Chen, J. X., Liao, R., Deng, Q., Zhou, J. J., Huang, S., Sun, P., et al. (2002). Sequential Activation of the MEK–Extracellular Signal-Regulated Kinase and MKK3/6 – p38 Mitogen-Activated Protein Kinase Pathways Mediates Oncogenic ras-Induced Premature Senescence. *Molecular and cellular biology*, 22(10), 3389–3403.
- Wang, X., McGowan, C. H., Zhao, M., He, L., Downey, J. S., Fearn, C., Wang, Y., et al. (2000). Involvement of the MKK6-p38gamma cascade in gamma-radiation-induced cell cycle arrest. *Molecular and cellular biology*, 20(13), 4543–52.
- Wang, Y., Huang, S., Sah, V. P., Ross, J., Brown, J. H., Han, J., & Chien, K. R. (1998). Cardiac muscle cell hypertrophy and apoptosis induced by distinct members of the p38 mitogen-activated protein kinase family. *The Journal of biological chemistry*, 273(4), 2161–8.
- Wang, H., Zhang, D., Tan, Y., & Li, T. (2012). Autophagy in endothelial progenitor cells is cytoprotective in hypoxic conditions. *Am J Physiol Cell Physiol*.

- Waskiewicz, A.J., Flynn, a, Proud, C. G., & Cooper, J. A. (1997). Mitogen-activated protein kinases activate the serine/threonine kinases Mnk1 and Mnk2. *The EMBO journal*, 16(8), 1909–20.
- Webb, J. L., Ravikumar, B., Atkins, J., Skepper, J. N., & Rubinsztein, D. C. (2003). Alpha-Synuclein is degraded by both autophagy and the proteasome. *The Journal of biological chemistry*, 278(27), 25009–13.
- Webb, J. L., Ravikumar, B., & Rubinsztein, D. C. (2004). Microtubule disruption inhibits autophagosome-lysosome fusion: implications for studying the roles of aggresomes in polyglutamine diseases. *The international journal of biochemistry & cell biology*, 36(12), 2541–2550.
- Webber, J., & Tooze, S. (2010). Coordinated regulation of autophagy by p38alpha MAPK through mAtg9 and p38IP. *EMBO J.*, 29, 27–40.
- Wei, S., Wei, W., & Sedivy, J. (1999). Expression of catalytically active telomerase does not prevent premature senescence caused by overexpression of oncogenic ha-Ras in normal human fibroblasts. *cancer Res*, 59, 1539–1543.
- Wright, W., & Shay, J. (2001). “Cellular senescence as a tumor-protection mechanism: the essential role of counting. *Current Opinion in Genetics and Development*, 11(1), 98–103.
- Xia, Z., Dickens, M., Raingeaud, J., Davis, R. J., & Greenberg, M. E. (1995). Opposing effects of ERK and JNK-p38 MAP kinases on apoptosis. *Science*, 270(5240), 1326–31.
- Yang, L. Y., Wu, K. H., Chiu, W. T., Wang, S. H., & Shih, C. M. (2009). The cadmium-induced death of mesangial cells results in nephrotoxicity. *Autophagy*, 5, 571–572.
- Yee, A. S., Paulson, E. K., McDevitt, M. a, Rieger-Christ, K., Summerhayes, I., Berasi, S. P., Kim, J., et al. (2004). The HBP1 transcriptional repressor and the p38 MAP

- kinase: unlikely partners in G1 regulation and tumor suppression. *Gene*, 336(1), 1–13.
- Yoshimori, T. (2004). Autophagy: a regulated bulk degradation process inside cells. *Biochemical and Biophysical Research Communications*, 313(2), 453–458.
- Yoshimori, T. (2006). Autophagy vs. Group A Streptococcus. *Autophagy*, 2(3), 154–155.
- Younce, C., & Kolattukudy, P. (2010). MCP-1 causes cardiomyoblast death via autophagy resulting from ER stress caused by oxidative stress generated by inducing a novel zinc-finger protein, MCPIP. *Biochem. J.*, 426, 43–53.
- Young, A., Narita, M., Ferreira, M., Kirschner, K., Sadaie, M., Darot, J., Tavaré, S., et al. (2009). Autophagy mediates the mitotic senescence transition. *Genes & development*, 23, 798–803.
- Young, A. P., Schisio, S., & Minamishima, Y. A. (2008). VHL loss actuates a HIF-independent senescence programme mediated by Rb and p400. *Nature cell biology*, 10(3), 361–369.
- Yu, L., McPhee, C., Zheng, L., Mardones, G., Rong, Y., Peng, J., Mi, N., et al. (2010). Termination of autophagy and reformation of lysosomes regulated by mTOR. *Nature*, 465, 942–946.
- Yu, QC, Marzella, L. (1986). Modification of lysosomal proteolysis in mouse liver with taxol. *Am J Pathol*, 122, 553–561.
- Zheng, L., Roeder, R. G., & Luo, Y. (2003). S phase activation of the histone H2B promoter by OCA-S, a coactivator complex that contains GAPDH as a key component. *Cell*, 114(2), 255–266.
- Zhong, Y., Wang, Q. J., Li, X., Yan, Y., Backer, J. M., Chait, B. T., Heintz, N., et al. (2009). Distinct regulation of autophagic activity by Atg14L and Rubicon associated

with Beclin1-phosphatidylinositol-3-kinase complex. *Nature cell biology*, 11(4), 468–476.

Zhu, J., Woods, D., McMahon, M., & Bishop, J. M. (1998). Senescence of human fibroblasts induced by oncogenic Raf. *Genes & Development*, 12(19), 2997–3007.

Zhu, JH, Guo, F., Shelburne, J., Watkins, S., & Chu, C. (2003). Localization of phosphorylated ERK/MAP kinases to mitochondria and autophagosomes in Lewy body diseases. *Brain Pathol*, 13, 473 – 481.

vom Dahl, S., Dombrowski, F., Schmitt, M., Schliess, F., Pfeifer, U., & Häussinger, D. (2001). Cell hydration controls autophagosome formation in rat liver in a microtubule-dependent way downstream from p38MAPK activation. *The Biochemical journal*, 354(Pt 1), 31–6.

Declaration of authorship

I hereby declare that this thesis is my own work and that it contains neither material previously published or written by another person nor any contribution made to the research by others except where due acknowledgement is made in the thesis.

25.01.2013, Dortmund

Jakia Amin

Acknowledgements

Thanks to Omnipotent for enabling me to execute a project, which seemed very grueling at times, especially towards the beginning. I would like to express my immense gratitude to all the people who had assisted me in solving numerous problems during the course of the assignment. By doing so, they have initiated the completion of my endeavor. I am much indebted to my venerable supervisor Prof. Dr. med. Jan G. Hengstler, Department of systems toxicology, IfADo-Leibniz Research Centre for Working Environment and Human Factors. I would like to express my profound gratitude with deep pleasure for his continuous encouragement, valuable suggestion, supervision and cooperation to enable me to complete the research. I also gratefully acknowledge the advice and encouragement of my co-supervisor Dr. Cristina Cadenas, Department of systems toxicology, IfADo-Leibniz Research Centre for Working Environment and Human Factors, for her guidance, cooperation and encouragement during the course of the investigation as well as my adaptation to a new environment in a new country. Further, I would like to express my gratitude to Prof. Dr. Frank Wehner for accepting being a referee of my work.

Finally, I am greatly thankful to my family, friends, colleagues and well-wishers for their help, encouragement and cooperation throughout my study period.

Curriculum Vitae of JAKIA AMIN



Personal details:

Name	Jakia Amin
Present Address	Heroldstarsse-44, D-44145, Dortmund, Germany Skype name: jakiaamin
Permanent Address	House-16, Flat-6B, Block-A, Road-2, Banasree, Dhaka-1219, Bangladesh.
Date of Birth	04 March 1979
Nationality	Bangladeshi
Occupation	Doctoral researcher, IfADo, Dortmund University, Germany.

Educational Qualification:

Degree	Group /Subject	Institute / University	Year	Division/ Class
S.S.C. (Primary school)	Science	Dhaka Board (Bangladesh)	1984 - 1994 (10 years)	1 st Division
H.S.C. (Higher school)	Science	Dhaka Board (Bangladesh)	1994 - 1996 (2 years)	1 st Division
Bachelor (B.Sc.) (4-years Honours)	Microbiology	University of Dhaka (Bangladesh)	1996 - 2000 (4 years)	Second class
Master (M.S.)	Microbiology	University of Dhaka (Bangladesh)	2000 - 2001 (1 year)	First class
Master	Applied Medical Engineering Science	Yamaguchi University (Japan)	2006 - 2007 (1 year 6 months)	S grade (excellent) in research. (90-100% marks)

Publications:

1. Patricio Godoy, Markus Schug, Alexander Bauer, Johanna Stewart, Essam Bedawy, Seddik El-kariem, **Jakia Amin**, Rosemarie Marchan, Wiebke Schormann, Lindsey Maccoux, Iris von Recklinghausen, Raymond Reif, Jan G Hengstler. Dexamethasone dependent versus independent markers of EMT in primary hepatocyte. Journal of Biological Chemistry 2010 Jan; 391(1):73-83.
2. Saeid Abroun, Ken-ichiro Otsuyama, Karim Shamsasenjan, Khademul Islam, **Jakia Amin**, Michio M Kawano. Galectin-1 supports the survival of CD45RA(-) primary myeloma cells in vitro. Br J Haematol. 2008 Sep;142(5):754-65.
3. Shangqin Liu, Ken-ichiro Otsuyama, Zi Ma, Saeid Abroun, Karim Shamsasenjan, **Jakia Amin**, Hideki Asaoku and Michio M. Kawano. 2007. Induction of multilineage markers in human myeloma cells and their down-regulation by interleukin 6. International Journal of Hematology. Vol. 85: 49-58.
4. Ken-ichiro Otsuyama, Zi Ma, Saeid Abroun, **Jakia Amin**, Karim Shamsasenjan, Hideki Asaoku and Michio M. Kawano. 2007. PPARbeta-mediated growth suppression of baicalein and dexamethasone in human myeloma cells. Leukemia. Vol. No. 21(1):187-190.
5. **Jakia Amin**, ABMM Khademul Islam and Md. Majibur Rahman. 2004. Prevalence and antibiotic resistance of pathogenic microorganisms of poultry products and associated manpower. Bangladesh Journal of Microbiology. Volume 21, no. 2; page: 101-103.

Work Experience:

1. **Researchers:** 1/2 TVL E13 position for doctoral research (October 2008 – to date) in IfADo, Dortmund University Germany.
2. **Research Assistant (part time)** (1st October 2005 to 31st March 2006): Worked as a research assistant in the Laboratory of Cellular Signal Analysis, Department of Bio-Signal Analysis, Graduate School of Medicine, Yamaguchi University.
3. **Teaching Assistant (part time)** (October 2005 to September 2007): Worked as part time teaching assistant in the Laboratory of Cellular Signal Analysis, Department of Bio-Signal Analysis, Graduate School of Medicine, Yamaguchi University.

Academic Awards:

1. Japanese Government Monbusho Scholarship for Master degree in Japan.
2. Government Scholarship for the academic feat throughout the Masters course at Dhaka University.
3. Bangladesh Government Primary School scholarship (Talent pool Grade).
4. Bangladesh Government High School scholarship (Talent pool Grade).

Training/Workshop/Seminar:

Molecular Ecological Techniques (4/12/04 to 8/12/04): Participated in training program of Molecular Ecological Techniques jointly organized by University of Bergen, Norway and Department of Microbiology, University of Dhaka, Bangladesh. (PCR DGGE, FISH, Ribotyping, Southern Blot, Genomic & plasmic DNA extraction).

Meetings with Nobel Laureates: (1/7/07 to 6/7/07). Participated in 57th Meetings of Nobel Laureates at Lindau, Germany. (Participants had been chosen based on a world-wide competition among young scientist).

Technical Skills:

Immunization of mice, mice liver isolation, cell culture, Immunoblotting/Western blotting, Immune precipitation (IP), Electrophoretic Mobility Shift Assay (EMSA), Cell transfection, cell immune staining, DAPI, Laser confocal microscopy, Fluorescent microscopy, Flowcytometry, FACS (fluoresceine-activated cell sorter), Real time PCR, Gel electrophoresis, Gel Immunodiffusion, Hemagglutination, Ribotyping, Microbiological techniques, enzyme assay, plasmid profiling, FISH, ELISA.

Jakia Amin